Dimming of metal halide lamps

van Casteren, D.H.J.

Award date:
1999

TU/e Technische Universiteit Eindhoven
/Sectie Elektromechanica en Vermogenselektronica

Afstudeerverslag

DIMMING OF METAL HALIDE LAMPS

EMV 99-13 D.H.J. van Casteren

Hoogleraar : Prof.dr.ir. A.J.A. Vandenput

Mentoren : Ir. M.A.M. Hendrix, Dr. J.L. Duarte,
Ir. W.D. Couwenberg (Philips Lighting B.V.)

Eindhoven : 31 augustus 1999

Samenvatting

Er bestaat een toenemende belangstelling om hoge druk gasontladingslampen lampen te dimmen, met als doel de resulterende energie besparing. Indien een HID lamp met een elektronische ballast in een vermogens gebied tussen de 50% en 100% wordt bedreven, worden elektrische instabiliteiten waargenomen. Soms hebben de optredende instabiliteiten het doven van de lamp tot gevolg. In dit rapport een onderzoek naar deze instabiliteiten.

De toegepaste HID lamp is een compacte hoge druk gasontladingslamp met metaalhalogeen componenten in de ontladingbuis, het nominaal elektrische vermogen bedraagt 73W. De metaalhalogeen componenten bepalen de kleur eigenschappen en verbeteren het licht rendement in vergelijking met een klassieke hoge druk kwik lamp. De start fase is onder te verdelen in verschillende ontladingstoestanden. Na een korte periode (enkele minuten) komt een stabiele toestand tot stand met een bijbehorende temperatuur verdeling. Om het elektrische gedrag van de lamp te bestuderen in de stabiele toestand, worden de fysische processen in de ontladingsbuis onderverdeeld in plasma en elektrode effecten.

Om een hoge druk gasontladingslamp te bedrijven zijn er verschillende mogelijkheden ondermeer: DC, LF, HF, en puls sturing. Een stabiele methode is laag frequent blok golf sturing. Deze methode is toegepast in de elektronische ballast, voor aansturing van de HID lamp. Echter in gedimde toestand kan de lamp ballast combinatie instabiel worden met het doven van de lamp als gevolg. Onderzoek naar de instabiliteiten, in gedimde toestand, laten twee hoofd problemen zien: plasma instabiliteiten en elektrode problemen.

De plasma instabiliteiten worden veroorzaakt door de interactie tussen de lamp en de circuit capaciteit, dit kan worden gemodelleerd met een tweede orde systeem. Nadere onderzoek wijst uit dat na een stapvormige vermogens reducering de stabiliteit marge verminderd voor een HID lamp. Dit resulteert in grote vermogens schommelingen, welke het doven van de lamp tot gevolg kunnen hebben.

De elektrode problemen zijn gerelateerd aan de elektrode temperatuur, omdat dit de wijze van functioneren bepaald. Voor nominaal vermogen kan worden verondersteld dat de elektrodes een geschikte temperatuur bezitten voor thermische emissie. Indien het vermogen van de lamp wordt gereduceerd kan de grens van correct functionerende elektroden worden bereikt. Als de grens is bereikt wordt de situatie instabiel en dooft de lamp.

Voor nader onderzoek is het elektrisch gedrag van de lamp is geïdentificeerd, om een computer simulatie model op te bouwen. Gekozen is voor een grijze doos model, om de identificatie procedure te kunnen splitsen in: statisch, snelle dynamiek en trage dynamiek. De voordelen van deze methode is een sterke reductie van de benodigde meet gegevens voor de identificatie, en een grotere nauwkeurigheid over een uitgestrekter lamp vermogens gebied in vergelijking met zwarte doos modellering. De belangrijkste componenten van het elektronische ballast circuit zijn ook opgenomen in het simulatie model. Om de lamp ballast interactie te kunnen bestuderen.

Een nieuwe regellus is ontworpen en de prestaties zijn vergeleken met de originele regellus. Om het lamp gedrag te bestuderen in gedimde toestand is een extra terugkoppeling noodzakelijk. Vier signalen zijn voorgesteld, elk om een bepaald deel van het lamp gedrag te bestuderen. Het doel van deze terugkoppeling is om het momentane minimale dim niveau te bepalen. Dit is in principe afhankelijk van de toegepaste type lamp en leeftijd.

Summary

There is a growing interest in the possibilities for dimming high intensity discharge (HID) lamps. Driving force is that considerable energy savings could result. When operating a HID burner on a electronic ballast, within a power range between 50% and 100%, electrical instabilities are observed. In some cases, these instabilities cause extinguishing of the burner. In this rapport an investigation is done towards the observed instabilities.

The used HID burner is a compact high pressure metal halide lamp, with a nominal input power of 73 W. The metal halides in the arc define the colour of the lamp and improve the luminous efficacy and colour rendering compared with a classical high-pressure mercury lamp. The starting process of a HID lamp is a sequence of different stages, each presenting a distinct discharge condition. After a brief period (minutes) a steady state is reached and stable temperature distribution is established. To study the electrical behaviour of the lamp in steady state, the physical processes in de arc tube can be divided into two main systems: the plasma effects and the effects in the electrode region.

To drive a HID lamp there are several possibilities like DC, LF, HF, and pulse mode operation. A very stable way is LF square wave operation. This method is applied in the used electronic gear, to drive the HID lamp. But, in reduced power mode, the system (lamp + ballast) can become instable and the lamp extinguishes. Investigation of the burner ballast circuit stability, in reduced power mode, shows two main problems: plasma instabilities and electrode problems.

The plasma instabilities are caused by the interaction between the burner and the circuit capacitance, which be modelled with a second order system. Further investigation show for the HID lamp a decreasing stability margin for a step down in power, resulting in large power fluctuations, which cause extinguishing of the lamp.

Electrode problems are related to the electrode operating temperature, because it defines the mode of operation. During normal power operation we can assume that the electrodes have an appropriate temperature for thermionic emission. When the electrical input power of the lamp is reduced, the border of proper electrode function can be reached. If the border is reached the situation becomes unstable and the lamp extinguishes.

For a detailed investigation, the electrical lamp behaviour is identified to build up a computer simulation model. A grey-box lamp model is chosen to split up the identification in three separated stages namely: Steady state, fast dynamics and slow dynamics. The benefit of this method are a strong reduction of the data sets needed for identification. Futher more, the approach yields better accuracy over a larger range of lamp operation than black-box modelling. The most important components of the electronic ballast circuit are also implemented in the simulation model, to investigate the lamp-ballast interaction.

A new control loop is designed, with a larger stability margin. The performances of this loop are compared with the original control loop. To observe the behaviour of the burner, especially in reduced power mode, an extra feedback signals are needed. Four possible signals are presented, each observes a special part of the lamp behaviour. The target of this extra feedback path is to define the minimum dimming level on the moment of operation. This depends principally on the used type of lamp and the age of the lamp.

Contents

1. Introduction

The metal halide lamp has become very popular as a practical light source for general and specific applications. Its application range has been greatly expanded, especially in the last ten years. This growth can be attributed to its high efficacy (measured in lumens per watt) as a general purpose light source. It is now widely used for interior and exterior lighting of large scale facilities. Another reason for its increased use is its applicability to interior retail applications through the creation of compact low-power lamps with superior colour rendering properties. As a result, metal halide lamps have been able to replace incandescent lamps, formerly the only option for many shop lighting applications. (The used light related terms are explained in appendix 1).

During the last years the electronic ballasting of lamps has been fairly well established. For fluorescent lamps, millions of electronic ballasts are already installed. Their number is growing rapidly, since they are now being combined with lamps in order to form compact fluorescent lamps (CFL), suitable for replacement of incandescent lamps. The higher price of the ballast is offset by the increased efficiency and reduced energy consumption.

High pressure discharge lamps have not so far participated in this progress, although the anticipated advantages of an electronic ballasts are just the same as for fluorescent lamps, with the exception of the 10% efficiency gain. The reason for this delay is the different behaviour of metal halide lamps at high frequency. It is well known that instabilities of the arc over a wide frequency range exclude ballasts of simple design such as those used for fluorescent lamps. Considerable work has been published to explain and describe the phenomena or to find methods for designing resonance free discharges, and to find methods and circuitry on the ballast side.

Electronic ballasts lead to the possible advantages:
- A longer lamp life by improving ignition and lamp power control; consequently the lamp efficiency will decrease less in time.
- Higher system efficiency is due to lowered ballast losses for power levels below 150W.
- Functional advantages such as lamp dimming and failure monitoring.
- System is compact and light weight.

Energy saving ballasts and dimming systems have been used in fluorescent lamps for some time. Until now, almost all high intensity discharge (HID) lamps have been operated at rated power. But there is a growing interest in dimming possibilities for high intensity discharge (HID) lamps. Driving force is that considerable energy savings could result.

When operating a CDM 70W burner on a MHC070 electronic ballast within a power range between 50% and 100%, electrical instabilities are observed. In some cases, these instabilities cause extinguishing of the burner. In this report an investigation towards the observed instabilities is presented.

In the first three chapters a short introduction of high intensity discharge lamps and electronic ballast circuits is given, focussing on the Philips CDM 070W burner and the MHC070 electronic gear. In Chapter 4 the phenomena related to the lamp extinguishing during dimming are investigated, together with the origins of the problems. For a detailed investigation a powerful tool is needed. So in Chapter 5 a lamp model is build up to make a full simulation of the lamp-ballast interaction possible. In Chapter 6 the lamp-ballast interaction is simulated, the results being validated by practical measurements. Finally, an improvement of the electronic ballast is suggested in order to prevent the lamp with the extinguishing during specific circumstances.

2. Characterisation of HID lamps

2.1 The high pressure gas discharge lamp

A high pressure gas discharge lamp transforms electric energy into heat and electromagnetic radiation. A considerable part of the radiation is at visible wavelengths. This rapport is focused on compact low wattage metal halide lamps like the Philips CDM-T 70W. A detailed view of this lamp is shown in figure 2.1, with a description of the most important elements of the lamp construction. The CDM 70W is a high-pressure metal halide lamp with a nominal input power of 73W.

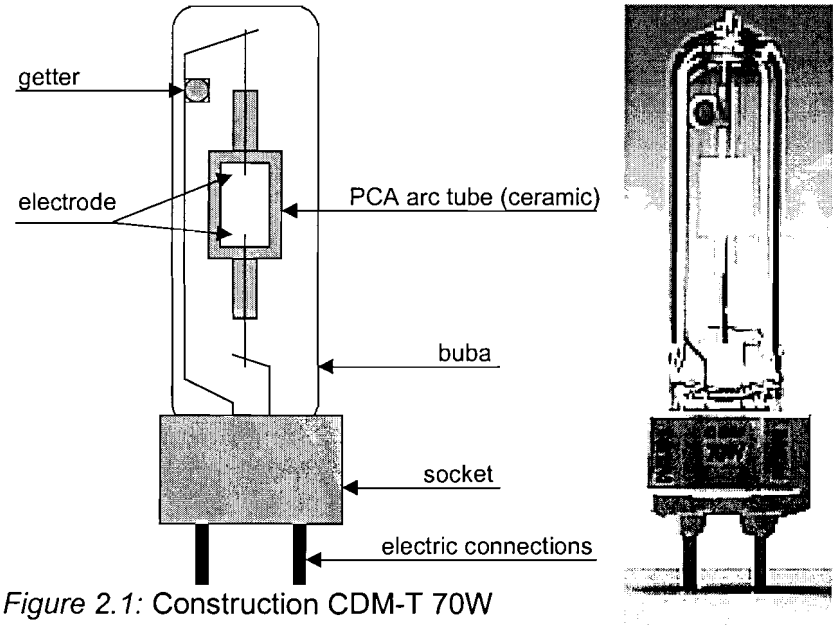

Figure 2.1: Construction CDM-T 70W

The most important part of the high pressure lamp is the arc tube. The arc tube is the enclosure where light is produced, can be pictured as a closed cylindrical container with two tungsten electrodes, one at each end. The tube is made of glass, quartz or in this case a ceramic material PCA (Poly Cristalline Aluminiumoxide Al_2O_3). Inside there is a chemical mixture, which normally contains mercury, metal halides plus an inert (start) gas. The start gas (xenon) has an important function during starting: it's the only gas component in cold condition. Mercury is a buffer gas, it's an element for the regulation of the arc voltage and heat. The nominal lamp voltage of a metal halide lamp is a result of the mercury dose and the electrode distance. The mercury doesn't serve as a generator of light because the excitation levels of the metal halides are much lower than those of mercury. The metal halides in the arc define the colour of the lamp and improve the luminous efficacy and colour rendering compared with a classical high-pressure mercury lamp.

Metal halides
Metal halides are compounds of metals and halogens. The metal halide compounds start melting and evaporating at a certain temperature of the wall of the discharge tube. The vapour is carried into the hot region of the arc by diffusion and convection, where the molecules dissociate into metal and halide ions. Radiation is emitted by the excited metal ions or atoms in the discharge area. The ions or atoms combine to a less-aggressive metal halide compound again when they diffuse away from the hot discharge area to the lower temperature outside areas near the wall of the discharge tube.

Other construction components

The arc tube is encapsulated in an outer bulb called the buba. To free the buba from any impurities a getter is implemented. To fit the lamp easily into a fitting a socket with the electric connections is build on.

2.2 Lamp starting and run-up

The starting process has been defined as a sequence of phases, each representing a distinct discharge condition, as shown in figure 2.2.

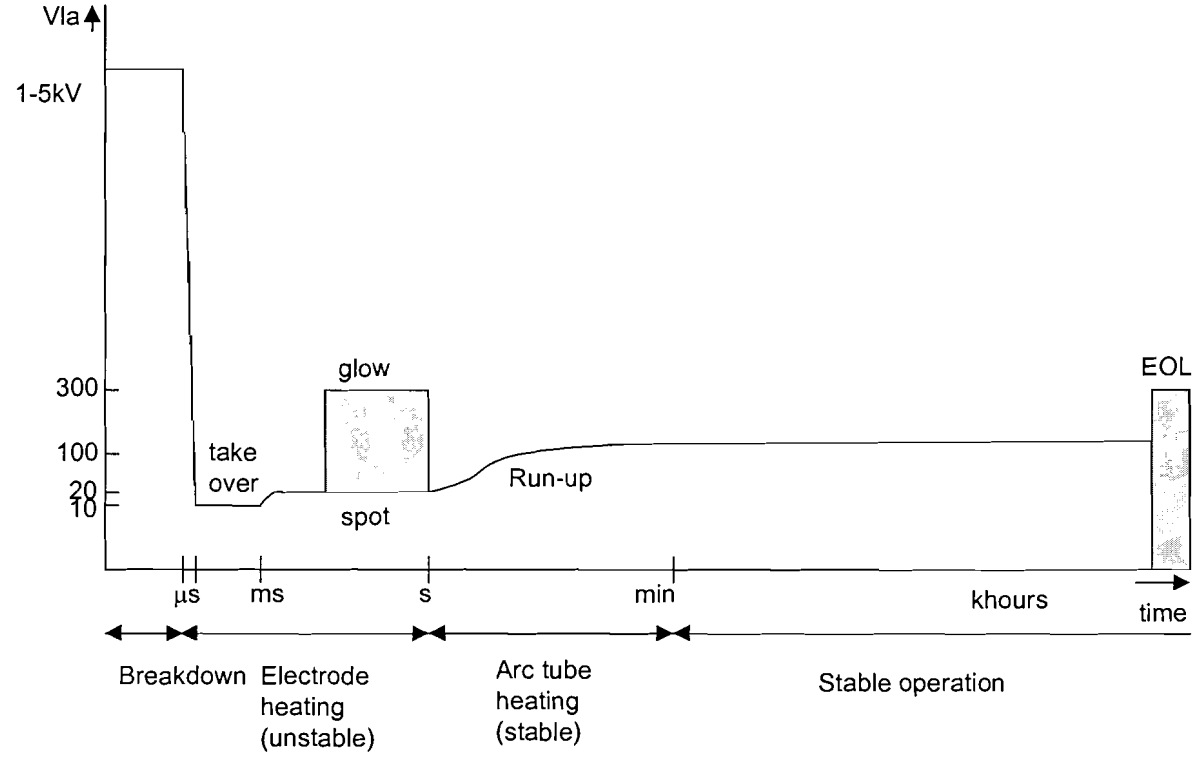

Figure 2.2: Phases of lamp operation

Breakdown
Before the lamp is started the gas behaves as an insulator. To initiate the starting process, the gas between the electrodes must be ionised to a sufficiently conductive state by electrical breakdown, this occurs after a statistical time. Generation of the high-field condition sufficient for breakdown is typically achieved through application of a high voltage pulse to the lamp (several kV). After breakdown has occurred the conducting channel between the electrodes has to be sustained by the circuit. In other words the power input into the discharge has to be sufficient to prevent the discharge from extinguishing. This stage is called the take-over phase.

Electrode heating
In this phase the electrodes are heated. The temperature of the electrode increases and eventually gets high enough to emit the electrons thermionically. The time necessary to get to such high temperature is in order of some seconds. The lamp behaves very irregular and jumps discontinuous between different voltage levels suddenly, the resulting impedance is very unstable. During the glow phase a low voltage phase can occur, the so-called spot mode phase. In this phase the electrode has not reached it full operating temperature, but a local hot spot is created. Sometimes high frequency oscillations (up to a few MHz) are observed which are related to this type of spot mode.

Arc tube heating
In the beginning of this phase the lamp voltage is low due to the low burner temperature and thus low gas pressures, but the electrodes have reached their working temperature. Further heating of the burner to its end temperature takes place, called run-up, typical time scale several minutes. In this period the resistance of the lamp continuously increases from a low value to an essential higher nominal value. Therefore, the ballast should act as a nearly constant current source providing sufficient increasing power for the lamp.

Steady state operation
After a brief period (minutes) a steady state is reached and stable temperature distribution is established. This is the region where the lamp has its optimum light performance. The electric behaviour in full and reduced power mode are the most important lamp properties for this investigation. In the following sections a quick overview of this important electric lamp behaviour is given.

End of life EOL
End of life lamp behaviour has proven a difficult phase to handle. The way lamps reach EOL can be different for an electronic ballast compared to a magnetic ballast. End of life behaviour of the burner can even damage the ballast.

2.3 Main processes determining the electric behaviour of the lamp

To study the electrical behaviour of the lamp the physical processes in de arc tube can be divided into two main systems. First all plasma effects can be lumped together in one resistor. Also the effects in the electrode region (which is the interference between the gas and the electrode) can be lumped together in one resistor. This results in two resistors, one for every electrode. Finally the equivalent electric circuit can build up as a series circuit with three resistors as showed in figure 2.3.

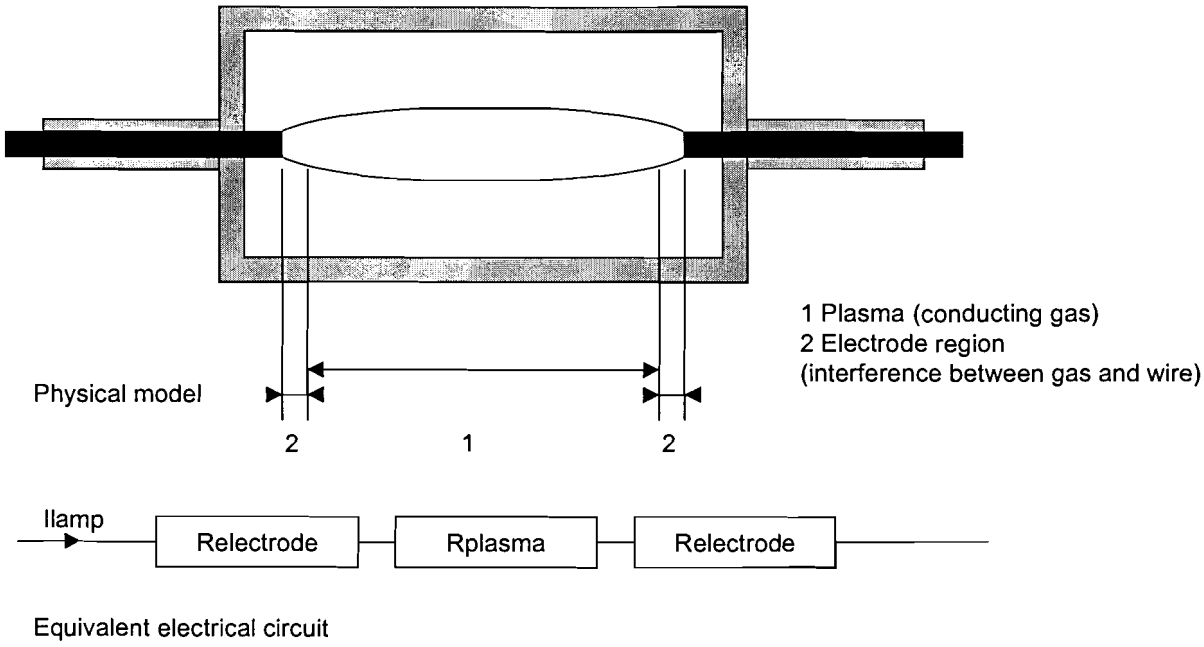

Figure 2.3: Electric behaviour of a HID lamp

For full power operation the electrode effects are relatively small and we can assume a symmetrical situation. Then all the electrode effects can be represented with one resistor.

Resulting in a final equivalent circuit containing two resistors.

2.4 Time scales in lamp operation

There are three important time scales involved in the operation of the lamp.

1 Plasma time scale: Phenomena within the plasma, at the electrode surface (other than corrosion/ erosion) and in the electric circuit, take place within micro- or milliseconds.

2 Thermal wall time scale: After a change of some condition, the system normally reaches a thermal steady state in the order of seconds or minutes.

3 Chemical time scale: Corrosion or loss processes affecting properties of the lamp and finally limiting its useful life, take place over hundreds or thousands of hours. For example: HPS (High Pressure Sodium) lamps in particular, have a excessive rise in lamp voltage during their life time. Therefore, a ballast should keep the lamp power within an acceptable power range.

2.5 Electrical behaviour versus time

If the lamp is forced to change with a certain current value (ΔI) the lamp can respond in three different ways as is shown in fig 2.4.

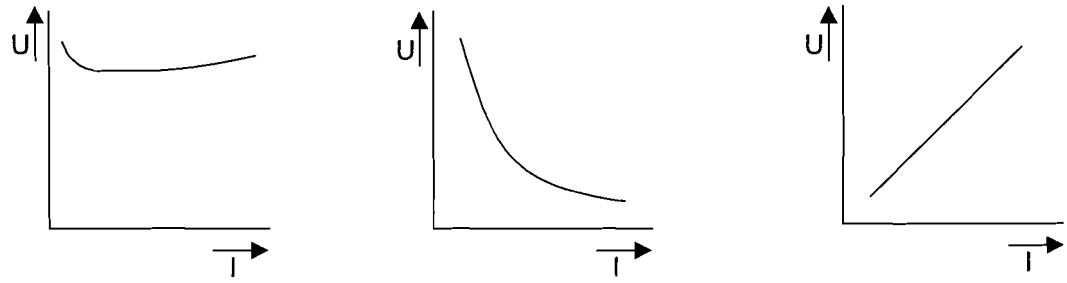

Figure 2.4: Electric behaviour versus time

Steady state behaviour: If the current is changed very slowly, (i.e. within a minute), and with a certain value (ΔI) the lamp voltage changes only with a small value. In this case the lamp acts like a non-ideal bi-directional zener diode. For normal power operation the HID lamp has a slight resistive behaviour but for a reduced power mode we see a negative resistive behaviour. Remark: In this respect a HID lamp differs in comparison to a low pressure gas discharge lamp. If a power control unit is implemented in the ballast it should keep the lamp power constant when the lamp voltage changes.
Furthermore, if the change is fast (msec. time scale), a decreased lamp voltage is produced by increased lamp current and visa versa. The lamp act like a negative resistor. Therefore, if a lamp is connected directly to a voltage source, a highly unusable state results. Any small current fluctuation can cause extinction or very fast current increase, which can damage the lamp resulting in a practically short circuited voltage source. Evidently, a ballast should act like a current source allowing the lamp to determine its voltage.
If the current supplied to the lamp is changed very fast (on a μs time scale), the lamp act like a resistor, because the state of the plasma can't change quickly. This is shown very clear on a high frequency ballast, where the voltage and the current are identically shaped.

Lamp re-ignition
When a lamp is operated on a low frequency alternating sinus or a non ideal square wave current, the lamp must re-ignite after every change in current polarity. During the polarity

change the current level is low and even momentarily zero, which results in a decrease in the plasma temperature with as consequence an increase of the lamp resistance. This results in a re-ignition peak in the voltage when the current begin to flow after the polarity change. To minimise the voltage peak the current commutation must be as fast as possible (di/dt).

3. Ballast for high pressure lamps

3.1 An overview of ballast topologies for high pressure lamps

DC
To operate a high pressure lamp on a direct current is very attractive from an electronic ballast point of view because the low cost and the small size of this type of ballast. But there are disadvantages, like cataphoretic effects and demixing of the gas-filling, making the lamp unsuited for lighting purposes. Therefore, the polarity of the lamp should be periodically changed by the ballast (i.e. every 10ms) providing an axially homogeneous discharge. An approximately zero DC component is recommended. Obviously the situation is different for special HID lamps designed for DC operation.

LF sinusoidal wave (copper iron ballast)
Driving a high pressure lamp on a copper iron ballast is the classical way, but there are disadvantages like light flickering on a 50Hz mains frequency. Standard there is no power control to eliminate power changes caused by voltage changes of the mains or voltage changes of the burner over life. But still used for high power applications because the low losses of EM (Electro Magnetic) ballasts.

HF
Operation of high pressure discharge lamps at frequencies in the several tens of kHz range has been a matter of great interest for the potential reduction of the size, weight and power consumption of electronic ballasts and for other potential functions like dimming. For fluorescent lamps, full-electronic ballasts for high frequency operation on the order of several tens of kHz have already been developed and put into practical use. However this has yet to happen for high intensity discharge lamps (HID) lamps. Acoustical resonances have been observed in HID lamps operated at high frequency. Such acoustic resonances cause various problems such as arc instability, light output fluctuations, and colour temperature and colour point variations. They also increase the lamp voltage, which may cause arc extinction or, in the worst case, cracked arc tubes.
From a theoretical point of view, the acoustic resonance phenomenon is a relatively well understood. By exciting a high-intensity discharge lamp at its eigen frequencies the discharge path will perturb. Lamp eigen frequencies depend on arc vessel geometry and gas filling, i.e. gas thermodynamic state variables (pressure, temperature and density); and both vary with manufacturing tolerances, while the thermodynamic state variables will change with lamp age as well.
Stable operation of lamps is possible at frequency ranges between 500Hz and 20kHz but these are of no practical value because of acoustical noise of the generator and the lamp. Frequency ranges exists between 10 and 150 kHz in which a stable operation with constant frequency seems to be possible. But they are either too narrow or to sensitive to changes in lamp parameters. Additional influences come from changes during lamp life, such as increasing electrode gap or pressure increase because of arc tube blackening.
Above 150 kHz the excitation of resonances normally becomes less sever, and operation of the lamps becomes independent of frequency and lamp parameters, provided that the lamps are not too small. Lamps with small arc tubes may not be stable below 280 kHz.
There are clear indications that modulation of frequency, or more generally of phase angle, of the driving generator suppress the onset of instabilities.

VHF
Very high frequency operation above the acoustic resonance frequency range (>1MHz). This is a stable way of operation but in this frequency range there are problems with radio interference, EMC and increasing losses in the power electronic components caused by the

high switching frequency.

Pulse operation
This is interesting for particular types of high pressure lamps like HPS (High Pressure Sodium). By changing the pulses the colour of the light changes also. Pulse operation is an effective means to raise the correlated colour temperature of a HPS lamp by means of transient increase of the plasma temperature of the discharge [1].

LF square wave
Apart from the already mentioned methods, DC operation of the lamps could be a quite suitable basis for electronic ballasts. Symmetry of the discharge can be achieved by periodical reversing the polarity, resulting in a low frequency square wave.

3.2 LF square wave three stage converter

Figure 3.1 illustrates the different stages in the MHC070 electronic gear [19] is also shown in appendix 5.

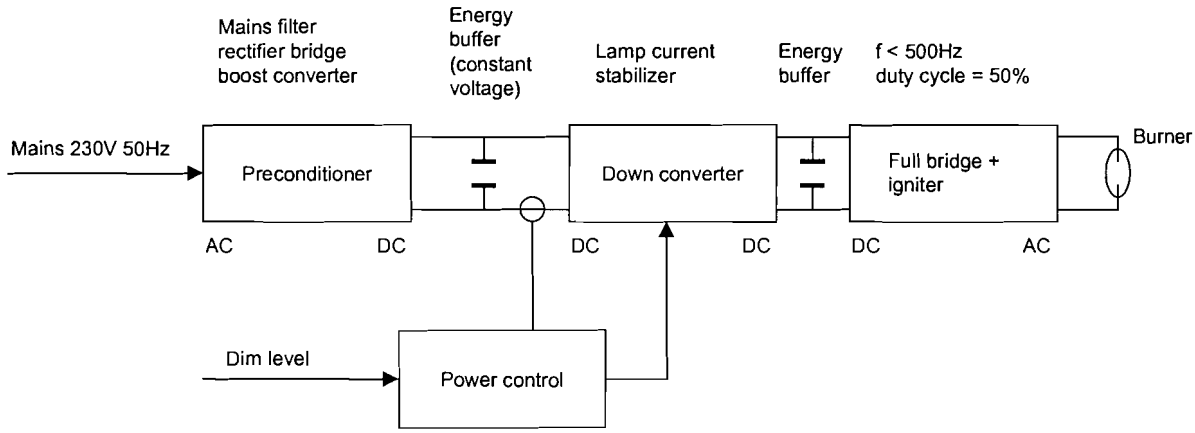

Figure 3.1: Three stage square wave ballast structure

Pre conditioner
The first step in the converter is the AC - DC conversion. But the conventional solution with a diode bridge in combination with a large capacitor may cause severe pollution of the power distribution system. An appropriate principle to solve this problem is to use a switched mode power circuit. The alternating voltage of the system is rectified by a diode bridge but not buffered by a large capacitance. The input voltage of the SMPS is a full wave rectified sine wave. When the input current of the converter is proportional to the input voltage then the waveform of the current will be sinusoidal and ideally all distortion disappears. There will be no phase difference either. However, current at the operating frequency and its harmonics will flow into the distribution system. It has to be attenuated to the desired level by filtering. The pre-conditioner is implemented as an up-converter. Note that the output voltage of this type of converter is always higher than the input voltage. In this circuit concept the output voltage of the pre-conditioner is set to 400V. The control loop build in the pre-conditioner circuit holds the output voltage constant within a wide range of input voltages.

Down converter
The next stage in lamp ballast topology is the down converter. The down converter in the MHC 070 ballast circuit with current control operates in critical discontinuous mode. New topologies will work in continuous / critical discontinuous / discontinuous mode depending on the current required. During the run-up transition the down converter delivers the required

large current in continuous mode. The normal operation mode is critical discontinuous with a frequency clamp to avoid too high frequencies when the lamp current is low. If the frequency clamp becomes active the mode of operation is discontinuous.

The most important control system of the lamp driver is the control of the down converter because the lamp behaviour interacts with the down converter. So for the different stages in lamp operation during start-up, but also with normal power or reduced power operation, the down converter in co-operation with control must have the adaptability to provide a stable lamp operation. The lamp needs during the warm-up time a constant lamp current (current limitation), and a constant power during normal operation (equal to the nominal lamp power in the required lamp voltage range). The ballast curve is showed in figure 3.2. The current / power must be controlled because the lamp has a negative resistance behaviour.

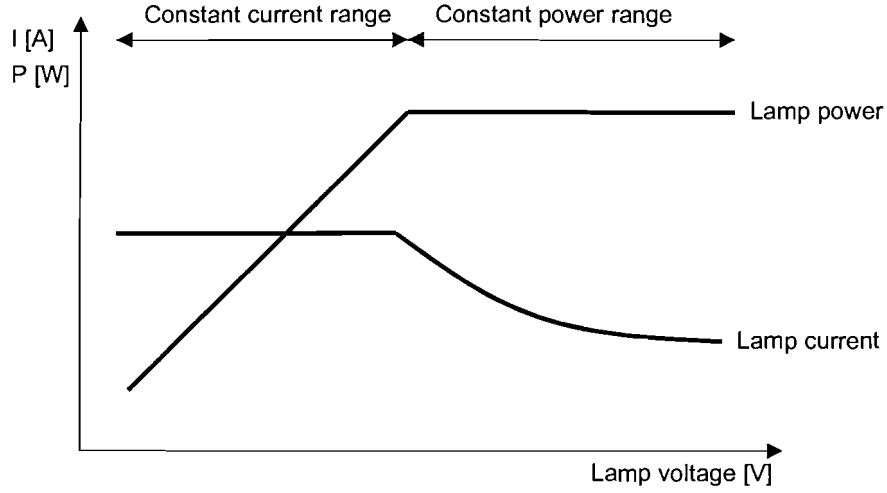

Figure 3.2: Ballast curve

Commutator
For the best performance a compact metal halide lamp must be driven on alternating current. The commutator transforms the DC current delivered by the down-converter into a low frequency square wave current. The topology of the commutator is simple. It's a full bridge controlled by a stand alone integrated circuit. The commutation frequency is set to 130 Hz with a duty cycle of 50% to prevent a direct current through the lamp and to avoid visible flickering.

Igniter
The commutator supplies the lamp through the series igniter coil. This type of igniter is self running. When the no load voltage becomes high the igniter start to fire. When the lamp ignites the voltage drops and the igniter stops immediately. The igniter produce 3 to 5kV peaks. In figure 3.3 the full bridge with the igniter circuit is shown.

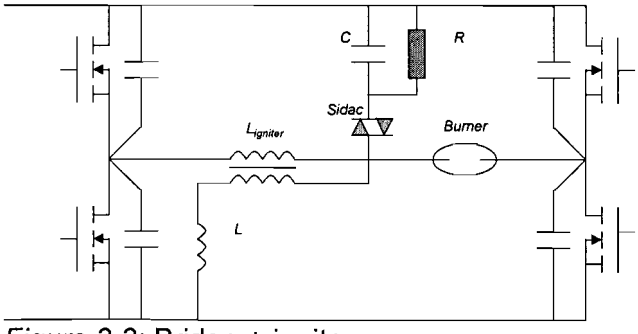

Figure 3.3: Bridge + igniter

4. Dimming metal halide lamps

Energy saving ballasts and dimming systems have been used in fluorescent lamps for some time. Until now, almost all high intensity discharge (HID) lamps have been operated at rated wattage. In the application of a reduced power system, the HID lamps will spend most of their live working at reduced wattage. Will these conditions change the lamp properties in any way? The effect of using power reduction systems on HID lamps has not been studied closely.

The combination of HID lamps and ballast dimming systems can result in significant energy savings over conventional, constant powered systems. The main issues that arise regarding the use of metal halide lamps on dimming systems are:
1. colour shift;
2. lamp life;
3. flickering of the light in dimmed mode especially when the lamp ages;
4. stability when the lamp operates in dimmed mode.
5. lamp efficacy in dimmed mode.

Among these points:

Colour shift
Metal halide lamp operation at power levels other than the design power influences the distribution of the halides in the arc stream, thus affecting the lumen output and characteristic colour temperature of the emitted light. Lamps operating at low power contain lower quantities of the halides in the arc stream than at full power. The reduced emission of light at particular wavelengths affects the total lumen output, which is a quantity calculated directly from the spectral intensities. For a CDM lamp operating on a reduced power level, the green lines in the colour spectrum become dominating. A dimmed quartz metal halide lamp has a larger colour shift, by this type of lamp the blue lines in the colour spectrum become dominant.

Lamp life
A decrease in lamp power results lower electrode temperatures. This could lead to generation of re-ignition spikes in the voltage waveform and additional arc tube darkening due to electrode sputtering. This effect on lamp maintenance is expected to be offset by lowering the arc temperature. Since the lamp voltage remains nearly constant with reduced power, the mercury remains unsaturated, inhibiting diffusion of tungsten to the wall. On the other hand, wall and seal temperatures are reduced at low power levels, reducing degradation of the lamp through chemical reaction [2]. Remark: There are exceptions.

It is necessary to ensure that the outer jacket getter will work efficiently at reduced power levels. Attaining the proper operating temperature of the getter is crucial to lamp survival. If the impurities contained within the outer jacket are not absorbed by the getter, they will diffuse into the arc tube and may drastically shorten lamp life. But measurements showed that in reduced power mode getter temperature decrease is very small, so this seems not to be a large problem [2].

Efficacy
HID burners shows for a decreasing power level a decreased lamp efficiency [20,22].

4.1 Dimming systems.

Two dimming systems are used commonly: bi-level and continuous. Bi-level dimming systems in the USA typical consists of a copper iron ballast that has a capacitive element in

series with the lamp. The impedance of the ballast is changed by switching a second capacitor in series or in parallel with the first capacitor. In Europe the bi-level systems common consist of a switched inductive element. Some typical continuous copper iron ballast dimming circuits work by changing the primary voltage to the whole system with a variable voltage transformer (or phase-cut), or by electronically switching a series/parallel ballast component such as an inductor [3]. This type of system is only useful for sodium lamps because for a reduced power level the time with low current (current off time) becomes long, and only sodium lamps with their very friendly electrical behaviour are stable during this way of operation. Other lamp types like metal halide, especially CDM, have problems with this type of operation and will extinguish or cause light flickering especially when the lamp ages. Conclusion: Driving this last mentioned type of lamp on reduced power levels is only possible with a full electronic ballast. Fast commutation and good control facilities are required.

Dimming should be done smoothly and without abrupt changes in light levels when transitioning from one light level to another. In the event of a power failure the ballast should restart the lamp at full light output and then dim back down to its previously set level.

If lamps are turned on at low power wattage, lower current and voltage will increase the ignition time during which glow discharge and vapour arc mode are present. Excessively long ignition time has to be avoided as the corrosion of the emitter material during this period results in blackening of the wall of the arc tube. This arc tube blackening causes an increase in lamp voltage and a decrease in lumen output [2]. Conclusion: A dimming system must always start at full power.

4.2 Dimming CDM lamps

For metal halide lamps there are two major issues connected with lamp operation at reduced power. The first one is the dependence of the luminous flux and the spectral distribution of the emitted light on the lamp power level. A second important issue concerns the possible consequences of MH lamp (quartz) performance over life. Early studies [2,3] have reported on results obtained for specific types of quartz metal halide lamps. Recently, HID explorations have led to the introduction of a new generation of metal halide lamps in ceramic envelope (DGA) with light technical properties superior of those of the traditional quartz metal halide lamps [5].
It has been found that in most of the cases the variation of the light technical properties only depends on the lamp power level and that the dimming method applied has no significant influence on this relation. It is also found that both the decrease in luminous flux and the change in colour temperature and colour rendering are considerable less for the ceramic types of lamps. The explanation for this reduced sensitivity for the reduction of the lamp power can be found in the fact that the metal halide vapour pressures are considerable higher in the ceramic lamps compared with the quartz types.
Regarding the other aspects of dimmed operation, indicate that concerns and limitations for ceramic and quartz metal halide lamps are similar. Lamp operation at low power can lead to extra blackening as a result of excessive evaporation or sputtering from the electrodes. It also appears that, for dimming systems operating at 50/60Hz, beyond a certain point improper electrode functioning can provoke visible flickering at the mains frequency [4].

4.3 Problem definition: Lamp extinguishing during dimming

There are three main problems causing extinguishing of the lamps during low power operation, or stepping down to a low power level, which are:

1. plasma instabilities;
2. electrode problems (re-ignition problems);
3. re-ignition voltage versus open voltage down converter.

4.4 Plasma instabilities

When the lamp is forced by a small current step, the burner voltage response is given in the time domain in figure 4.1. From this, the response can be translated to the Laplace domain leading to the transfer function H(s) of the burner (only small signal and plasma effects). Next, the parallel capacitor is incorporated in the scheme and the resulting impedance Z(s) is calculated. From the expression for Z(s) the stability criterion follows using the Routh-Hurwitz stability criterion for polynomials in the Laplace domain.

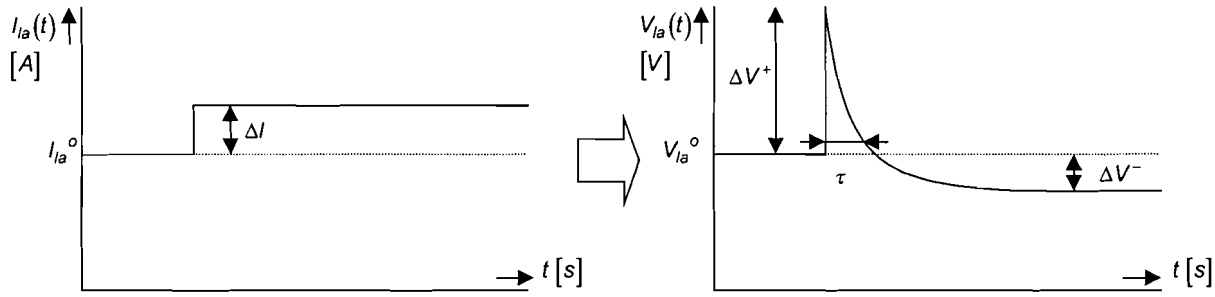

Figure 4.1: Lamp current and lamp voltage reaction

The following definitions are of importance for the derivation:

$$R_{la} = \frac{V_{la}{}^{o}}{I_{la}{}^{o}} = \frac{\Delta V^{+}}{\Delta I} \tag{1}$$

where R_{la} is the nominal lamp-impedance. Since the plasma conductivity can not change instantaneously, an increase in current also means a proportional increase in lamp voltage, resistive behaviour. However, within some milliseconds the lamp voltage decreases as the plasma temperature changes. In the following we suppose this voltage to decrease according to an exponential curve, with time constant τ. Note that since ΔV^{-} in figure 4.1 is negative we define the negative resistance as follows:

$$r = \frac{\Delta V^{-}}{\Delta I} \tag{2}$$

On a time scale of seconds to minutes, the lamp voltage increases again to some volts higher than prior to the current step. But this slow voltage change is neglected because only the millisecond time scale is of interest for this instability research.

Referring to figure 4.1 and describing the time response of the burner as

$$V_{la}(t) = V_{la}{}^{o} + V(t) \tag{3}$$

Now we can find the following expression for V(t):

$$\begin{aligned} V(t) &= 0 && t < 0 \\ V(t) &= \Delta V^{+} - \left(\Delta V^{+} - \Delta V^{-}\right)\left(1 - e^{-\frac{t}{\tau}}\right) && t \geq 0 \end{aligned} \tag{4}$$

With the definitions of R_{la} (1) and (2) and re-arranging this can be written as

$$\begin{aligned} V(t) &= 0 && t < 0 \\ V(t) &= \Delta I \cdot r + \Delta I({R_{la}}^{o} - r)e^{-\frac{t}{\tau}} && t \geq 0 \end{aligned} \tag{5}$$

The Laplace transform of this expression is straightforward

$$V(s) = \frac{\Delta I \cdot r}{s} + \frac{\Delta I({R_{la}}^{o} - r)}{s + \frac{1}{\tau}} \tag{6}$$

The response for a step change in the current is found to be

$$\begin{aligned} i(t) &= 0 && t < 0 \\ i(t) &= \Delta I && t \geq 0 \\ I(s) &= \frac{\Delta I}{s} \end{aligned} \tag{7}$$

Therefore, the transfer function describing the burner response H(s) is then

$$H(s) = \frac{V(s)}{I(s)} = \frac{s{R_{la}}^{o} + \frac{r}{\tau}}{s + \frac{1}{\tau}} \tag{8}$$

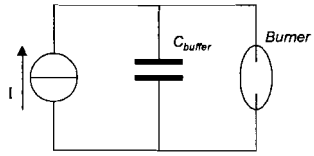

Figure 4.2: Lamp interaction with buffer capacitor

Assuming a capacitor C parallel to the burner (figure 4.2), the resulting impedance Z(s) can be found from

$$\frac{1}{Z(s)} = \frac{1}{H(s)} + sC \tag{9}$$

$$Z(s) = \frac{s{R_{la}}^{o} + \frac{r}{\tau}}{s^2{R_{la}}^{o}C + s\left(1 + \frac{rC}{\tau}\right) + \frac{1}{\tau}} \tag{10}$$

Stability requires the real part of the two poles to be smaller then 0. An easy test for stability is the Routh-Hurwitz criterion. For a second order polynomial, this criterion states that all coefficients of the dominator be positive. Obviously this is the case for $R_{la}C$ and $1/\tau$, so the

criterion for stability in this case becomes (remember r<0):

$$1 + \frac{rC}{\tau} > 0 \Rightarrow \frac{|r|C}{\tau} < 1 \Rightarrow \textit{stability border} \Rightarrow C = \frac{\tau}{|r|} \tag{11}$$

Thus, given the lamp-parameters r and τ, and to avoid instability, a maximum value of the parallel capacitor is can be calculated. End of stability criterion derived by [16].

In the practical circuit situation, the influence of the series igniter coil can not be neglected so a more realistic interaction circuit is given in figure 4.3.

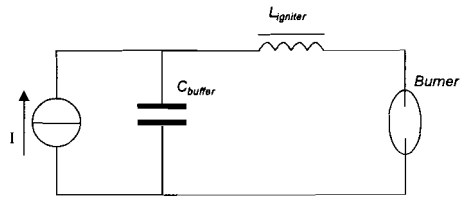

Figure 4.3: Burner + C_{buffer} + $L_{igniter}$

The resulting transfer function G(s) is given by

$$\frac{1}{G(s)} = \frac{1}{H(s) + sL} + sC \tag{12}$$

$$G(s) = \frac{s^2 L + s\left(\frac{L}{\tau} + R_{la}{}^{o}\right) + \frac{r}{\tau}}{s^3(CL) + s^2\left(\frac{CL}{\tau} + R_{la}{}^{o}C\right) + s\left(\frac{Cr}{\tau} + 1\right) + \frac{1}{\tau}} \tag{13}$$

4.5 Simulations of the steady state burner interaction

In figure 4.4 the measurement set-up to derive the small signal lamp parameters is shown. The ballast resistor is split in two parts, one of which can be short-circuit by means of an electronic switch driven by a pulse generator. The resulting instantaneous decrease in total ballast resistance gives the small current step in the lamp current. The lamp voltage and current are measured with a scope which is triggered by the current step.

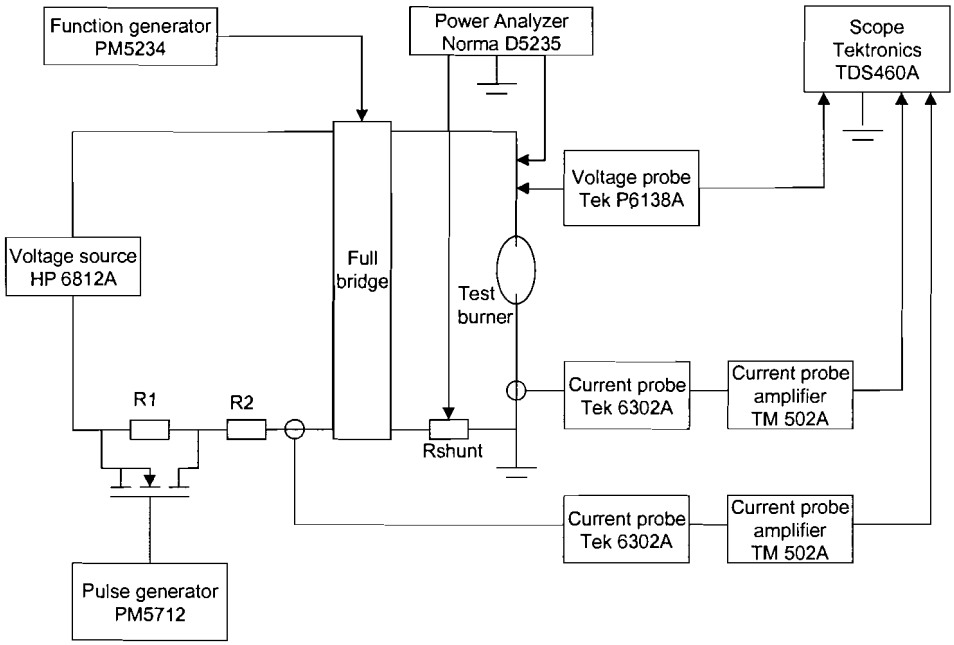

Figure 4.4: Measurement set-up

The steady state behaviour is measured for full power. Note: Steady state means that the small signal measurement is taken after the burner has reached a thermal equilibrium, which takes approximately 2 min. after a disturbance. The result of steady state measurement with a CDM-T 70W/830 burner operating on the rated power level of 73W is given in table 4.1. Also given in this table are the practical values used for the buffer capacitor and igniter coil in an electronic ballast circuit.

Table 4.1

R_{la}	110Ω
r	-9.65Ω
τ	85μsec.
C	1μF
L	3.8mH

In the simulations first the results with the transfer function Z(s) (without the $L_{igniter}$ coil) are presented. Further the results with transfer function G(s) (with the igniter coil) are shown.

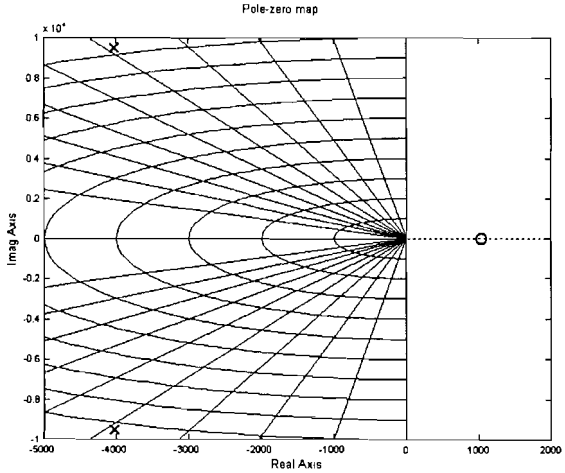

Figure 4.5(a): Pole zero plot (lamp+C)

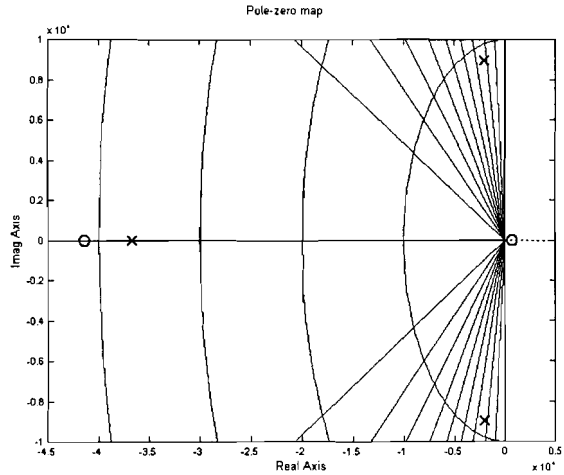

Figure 4.5(b): Pole zero plot (lamp+C+L)

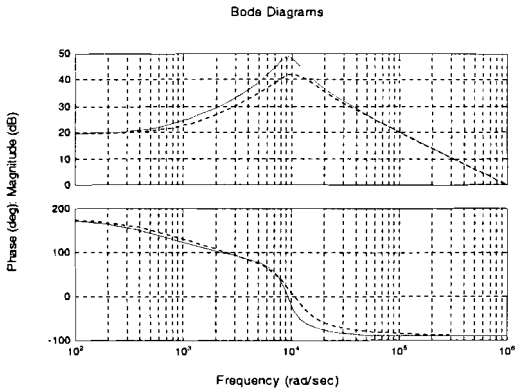

Figure 4.5(c): Bode diagrams

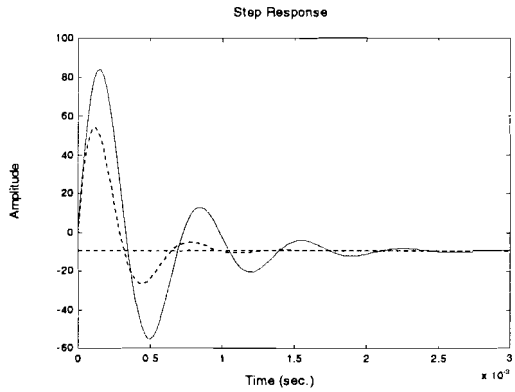

Figure 4.5(d): Step response

The simulation results shown in a pole zero plot (figure 4.5(a)) for the lamp capacitor interaction a complex pole pair on the LHP and a zero on the RHP. In the pole zero plots the lines of constant damping ratio (ζ) and natural frequency (ω_n) are drawn. In the second pole zero plot figure 4.5(b), the situation with the igniter coil is presented, an extra pole and zero appears in the LHP. The dominant complex pole pair is shifted a little towards the imaginary axis, this resulting in a decrease in the damping ratio of the system. This effect is also visible in table 4.2 with the system pole parameters. The bode diagram figure 4.5(c) and the step response figure 4.5(d) shows us the behaviour for both systems. The dotted line for the lamp+C combination and the continuous line for the lamp+C+L combination. In the step response plot it become clear that the addition of the igniter coil in the interaction circuit decreases the damping ratio of the system, and the amplitude of the fluctuations becomes larger.

Table 4.2

Natural frequency and damping factor of system poles. (burner + C)		
Eigenvalue	Damping	Frequency (rad/s)
-4.03e+003 + 9.52e+003i	3.90e-001	1.03e+004
-4.03e+003 – 9.52e+003i	3.90e-001	1.03e+004
Natural frequency and damping factor of system poles. (burner + C + L)		
Eigenvalue	Damping	Frequency (rad/s)
-2.03e+003 + 8.96e+003i	2.21e-001	9.19e+003
-2.03e+003 – 8.96e+003i	2.21e-001	9.19e+003
-3.67e+004	1.00e+000	3.67e+004

4.6 Plasma dynamical behaviour

In this investigation not only steady state operation on full power is important also reduced power mode behaviour and changes between full and reduced power are a matter of interest. So, first the small signal lamp properties are measured for several (steady state) power levels. Second, the small signal lamp properties are measured after a large step change in the lamp power level, to investigate the lamp stability when the lamp operation point changes from full power to reduced power and visa versa.

The results of measurements with a CDM-T 70W/830 burner are displayed in figure (4.6). The steady state behaviour shows for a decreasing power level an increase in the critical capacitor value, when the power level is lowered further the critical capacitor value decreases. The dynamical approach is split up into two figures one for a power decrease operating in full power steady state, and second for a power increase operating in a reduced power level (steady state). The results of the measurements shows for a power decrease a

decreasing critical capacitor value. When the power step down is larger this results also in a larger decrease of the critical capacitor value. This is an important result because when the lamp power is lowered by a step the stability margin become smaller and large power fluctuations can occur. For the situation when the power level rise in a step the measurements shows an increase in the critical capacitor value. The stability margin becomes larger, and plasma instabilities are absolutely no problem during this transient in power.

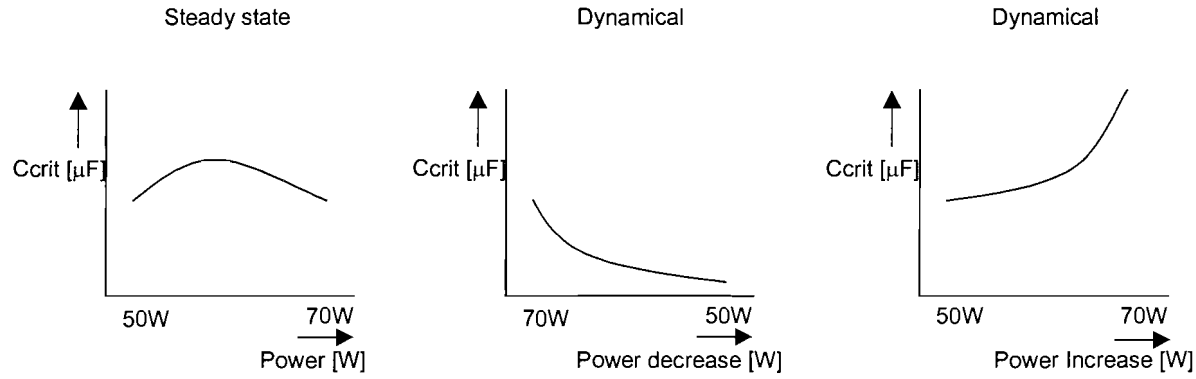

Figure 4.6: Behaviour CDM burner steady state + dynamical

The small signal analysis results of the plasma behaviour are also presented in the table (4.3) for a CDM burner and a MHW burner, for extensive information see appendix 2.

Table 4.3

CDM-T 70W (DGA)				
	Power [W]	τ [µsec.]	-r [V/A]	C_{crit} [µF]
Steady state	70	85	9,65	8,8
	50	155	18,02	8,6
Dynamic	70 – 50	122	21,07	5,79
	50 – 70	125	6,23	20
MHW 70W (quartz)				
	Power [W]	τ [µsec.]	-r [V/A]	C_{crit} [µF]
Steady state	70	190	4,6	41,3
	50	240	14	17
Dynamic	70 – 50	190	4,28	44,4
	50 – 70	180	3,79	47,5

Lamp dynamics simulation

The dynamical description is important to know how a HID lamp behaves before a steady state is reached. Immediately after a large power step (large signal change) the small signal behaviour is examined. This is interesting for stability analysis after a large change in power.

The results of the measurements are applied in the transfer function G(s) (formula 13). The simulations are done with two types of lamps first a CDM burner (DGA arc tube) and second a MHW burner (quartz arc tube), to see the characteristic differences in dynamical behaviour. The simulation plots and tables shows three different situations, as follows:

1. Normal operation P_{la}=70W with C=1µF
2. Dynamical power step down from 70W to 50W with C=1µF
3. Dynamical power step down from 70W to 50W with C=0.3µF

Note: In these simulations the buffer capacitor and the igniter coil are incorporated $L_{igniter}$ = 3.8mH is valid for all situations.

Simulation with the CDM 70W (DGA) burner

Note: In practical situation this type of lamp has a problem with a immediate step down in power, most of the times the lamps extinguish.

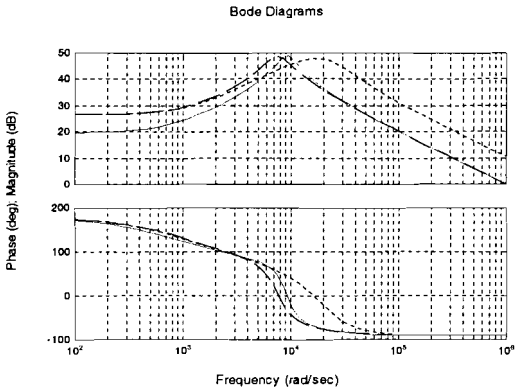

Figure 4.7(a): Bode plot (CDM)

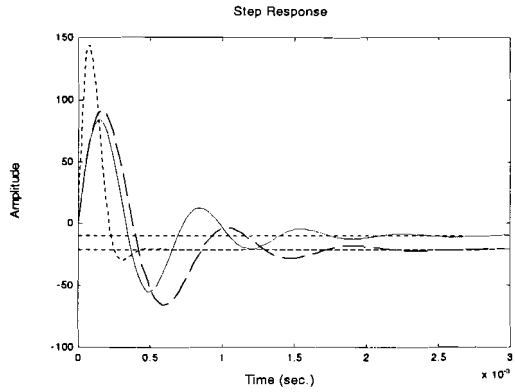

Figure 4.7(b): Step response

First the steady state behaviour for full power is showed in figure 4.7(a and b), the continuous line being the reference lamp behaviour. The lines of the dynamical approach can be recognised by a dashed line for C=1μF and dotted line for C=0.3μF in the simulation plots. Now a dynamical power step down from 70W to 50W in combination with a 1μF capacitor can be compared with the full power situation. The damping of the complex pole pair increases a little in spite of the calculated decreased critical capacitor value. But the amplitude of the first swing becomes larger as result of the increased negative resistive behaviour of the burner. And especially the increase of the negative overshoot is very important in reduced power mode in relation to lamp extinguishing, so it must be as small as possible. In the situation with the reduced size buffer capacitor C=0.3μF the damping of the complex system poles increases and the real pole become dominant (table 4.4). The negative overshoot become small and the damping increased. But the positive overshoot becomes large with the small parallel capacitor.

Table 4.4.

Simulation Philips CDM burner (DGA)				
Lamp situation	$C_{parallel}$	Resulting system poles		
		Eigenvalue	Damping	Freq. (rad/s)
Steady P_{la} = 70W	1μF	-2.03e+003 + 8.96e+003i	2.21e-001	9.19e+003
		-2.03e+003 - 8.96e+003i	2.21e-001	9.19e+003
		-3.67e+004	1.00e+000	3.67e+004
Dynamical P_{la} = 70 – 50W	1μF	-2.11e+003 + 7.21e+003i	2.81e-001	7.52e+003
		-2.11e+003 - 7.21e+003i	2.81e-001	7.52e+003
		-3.82e+004	1.00e+000	3.82e+004
Dynamical P_{la} = 70 – 50W	0.3μF	-1.84e+004	1.00e+000	1.84e+004
		-1.20e+004 + 1.57e+004i	6.07e-001	1.97e+004
		-1.20e+004 - 1.57e+004i	6.07e-001	1.97e+004

Results simulations with MHW 70W burner (quartz)

Note: In practical measurements the MH lamp does not extinguish during a step down in power.

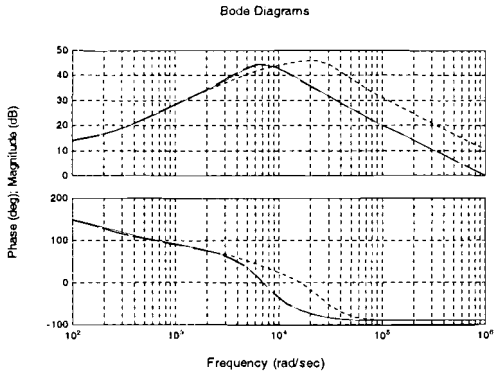

Figure 4.8(a): Bode plot (MHW)

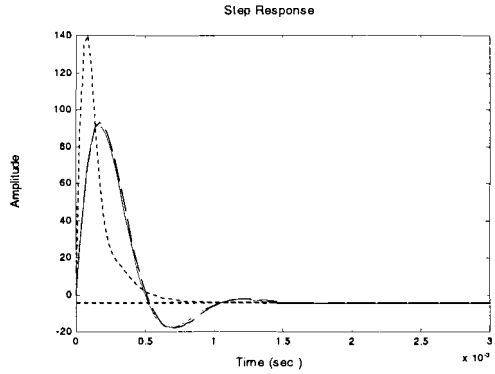

Figure 4.8(b): Step response

Again in the bode and the step response plot (figure 4.8) the full power line is continuous, the dynamical line with C=1μF is dashed, and with C=0.3μF is dotted. For the MH burner in full power steady state (P_{la} =70W) the situation is as follows: The complex pole pair is dominant and has a damping ratio about 0.534 (see also table 4.5). For the power transient (70W-50W) with C=1μF there isn't a great change in the system poles. For the dynamical situation with the smaller capacitor the situation in the s-domain change, the real pole become dominant, and resulting total system damping increased. Reducing the size of the capacitor is not needed to archive stability.

Table 4.5

Simulation Philips MHW burner (quartz)				
Lamp situation	$C_{parallel}$	Resulting system poles		
		Eigenvalue	Damping	Freq. (rad/s)
Steady P_{la} = 70W	1μF	-3.86e+003 + 6.11e+003i	5.34e-001	7.23e+003
		-3.86e+003 - 6.11e+003i	5.34e-001	7.23e+003
		-2.65e+004	1.00e+000	2.65e+004
Dynamical P_{la} = 70 – 50W	1μF	-3.70e+003 + 5.96e+003i	5.27e-001	7.02e+003
		-3.70e+003 - 5.96e+003i	5.27e-001	7.02e+003
		-2.81e+004	1.00e+000	2.81e+004
Dynamical P_{la} = 70 – 50W	0.3μF	-6.84e+003	1.00e+000	6.84e+003
		-1.43e+004 + 2.17e+004i	5.52e-001	2.60e+004
		-1.43e+004 - 2.17e+004i	5.52e-001	2.60e+004

Discussion results

With the transfer function simulations, it is possible to predict the large fluctuations after a power step. For normal operation the situation with CDM burner is under-damped but a negative power swing doesn't matter much in full power operation. But, after a power step down the commutations result in large power fluctuations and now in a negative swing the absolute power level becomes very low and the lamp extinguishes. With the reduced capacitor the damping increases and the negative overshoot becomes smaller. A damping ratio of 0.5 seems to be a practical border value for the dominant complex poles. As shown in the results with the MHW burner the damping ratio is for all situations above 0.5. The remaining fluctuations in the power will be reduced in practice with the power control loop.

The calculated dynamical critical capacitor behaviour shows, especially for CDM lamps, an interesting behaviour. The results show an explanation for the observed extinguishing of the CDM lamps after a quick step to a lower power level. The maximum allowed parallel capacitor decreases rapidly with a power step down. Remarkable is that this behaviour is only found by CDM burners, expected is that this is the result of the increased pressure

inside the arc tube compared to the MHW quartz lamp.

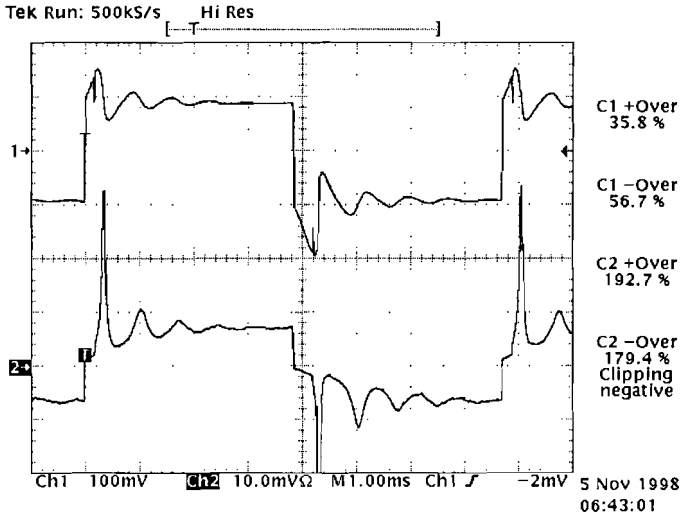

Figure 4.9: Measurement showing lamp voltage (100V/div.) on top and the lamp current (1A/div.) below.

A step down of the power level results in a strongly under-damped system. In a practical measurement (figure 4.9) a square wave lamp operation is showed. This scope view is taken directly after a step down in power. The large fluctuations in the current and the resulting fluctuations in the power level can cause extinguishing of the lamp. Measurement with an electronic MHC 070 ballast and a CDM burner. (Note: In this version of the MHC070 ballast a saturated igniter coil is used with L=12mH).

4.7 Electrode behaviour in reduced power mode

Principles of electrode heating.
The electrodes are assumed to be heated by ion bombardment during the cathode half cycle (with power input equal to the product of the ion current times cathode fall) only during starting and by electron bombardment on the anode half cycle (power input equal to the product of the total current times anode fall) during normal operation. The temperature rise of the cathode is determined from the above power inputs, the heat capacity of the cathode, and its thermal conductivity and radiative dissipation. Remark: It's important to know that the burning position affects the individual electrode temperatures, especially in vertical burning position, the upper electrode most of the time has a higher temperature compared to the electrode placed lower. During the starting phase the transition to the arc occurs when the electrode temperature reaches the point that electron emission by thermionic emission dominates over secondary emission due to ion bombardment [6].

Electrode temperature behaviour for operating from the mains systems
The average temperatures of the arc terminus (hot spot) of the cathode half cycle can be considerably different from the anode half cycle. This results in the thermal conduction away from the small hot spot area, which can cool the spot and its immediate neighbourhood in a time much less than a half cycle of the 50/60Hz mains frequency. The electrode can actually be cooled during the cathode half cycle and reheated during the anode portion of the cycle [7]. For systems operating on a higher commutation frequency it can be assumed that the temperature variations becomes smaller with increasing frequency.

Definitions of electrode operation modes
The most important parameter in electrode operation is the temperature, because it defines

the mode of operation. To describe a mode of operation, several names are used for the same phenomena in the literature.

High-field / low-field
During normal full power operation we can assume that the electrodes have an appropriate temperature for thermionic emission, the so-called low-field mode. An electrode on the border of designed performance tends to switch over from diffuse-mode (low-field) to the spot mode (high-field), obeying the minimum principle of energy [10]. It escapes into the more favourite mode for electrode emission (figure 4.10).

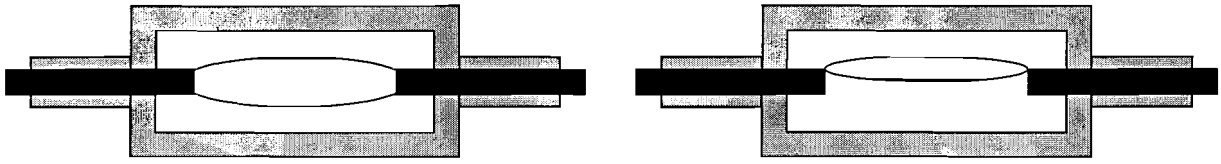

Diffuse mode
(normal stable operation
correct electrode temperature and function)

Spot mode
(dimming/starting unstable operation
insufficient electrode temperature)

Figure 4.10: Electrode behaviour

A static cathode spot of about 1e-5 to 1e-4 cm^2 where the temperature exceeds that of the rod end by several hundred degrees, enlarges electron emission. Spot generation is an effect associated with an electrode of insufficient temperature, as is the flickering effect. So a spot generation and the synchronous voltage jump on the re-ignition peak are indications of a flickering lamp [9].

Vapour arc
Its widely assumed that severe electrode erosion is due to sputtering during the glow discharge. However, the vapour arc mode is responsible for the most severe erosion. Here, the term 'vapour' means that the cathodic plasma contains electrode vapour (metal vapour and activator material vapour) but does not include the lamp filling gas.

The arc is forced to turn in a vapour mode, which is characterised by a quickly moving cathode spot, as long as the cathode is not sufficiently heated for providing the discharge current by thermionic electron emission.

The mode of arc cathode operation can be determined by the voltage noise method. The substance of this method is that the voltage noise caused by micro-explosions at the cathode is used for the detection of a quickly moving spot. In the voltage noise method, the burning voltage is investigated by a high pass filter. So, the low-frequency part of the voltage is suppressed whilst the high frequency part gives information whether the arc is in vapour arc mode or in thermionic arc mode [11,12].

Lamp re-ignition
A qualitative demonstration of a transition between the two burning modes, low-/high-field mode, is given in figure 4.11.

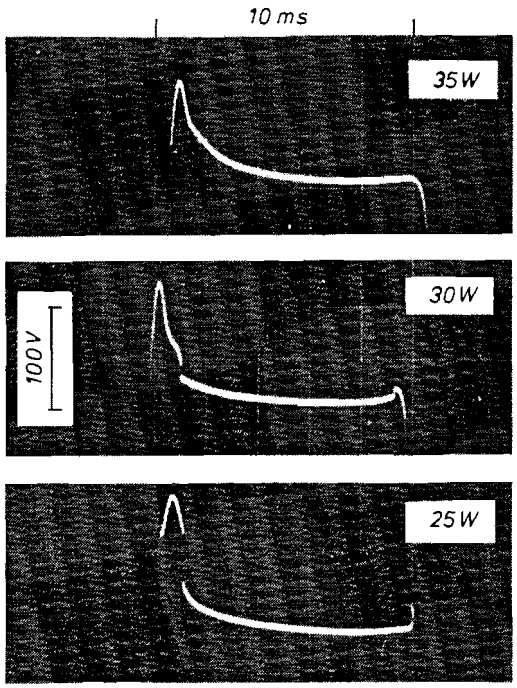

Figure 4.11: Arc voltage versus time for AC (50Hz) operated 35W lamp [10]

If the temperature of the cathode is high enough, the arc voltage will show a smooth behaviour as shown in the upper photograph (figure 4.11). The arc burns in low-field mode all of the time. If the arc power is decreased, the tip temperature is lowered. Thus, after current reversal, the arc starts in high-field mode. With increasing current the conditions of the electrode change. Higher current and higher tip temperature favour the low-field mode. Within some tents of a millisecond the arc switches to this mode. The transition shows up in the time dependence of the arc voltage as a sudden drop of the order of 10V (figure 4.11 centre). If it occurs during the re-ignition peak, it may even be as large as 50V (figure 4.11 bottom) [10].

Lamp maintenance effects

The loss of wall transparency with operation time is one of the major mechanisms that contributes to lamp lumen decrement over life. Two distinct types of wall darkening occur in metal halide lamps: temporary wall transmission loss during start-up due to mercury deposition on the wall and permanent wall darkening due to tungsten deposition on the wall. The tungsten deposition comprises two components: that resulting from sputtering at starting and that resulting from evaporation during continuous operation. The permanent darkening of the arc tube is due to the decomposition of the electrode material on the wall. The starting process plays an important role in the lumen maintenance characteristics of metal halide lamps. "Smart ballasting" can affect the lamp electrical conditions. Electronic ballasting will provide additional degrees of freedom to tailor electrical waveforms during the starting process to minimise electrode sputtering [8].

Lamp flickering

In the region between about 30 to 85 cycles the sensitivity of the human eye with respect to the flicker (a modulated luminous flux of a light source), can be described as an exponentially decreasing function of frequency. At a frequency of 85 cycles and above, the human eye becomes insensitive to flickering phenomena. However, a distinctive flickering might occur if the luminous flux shows a modulation of 50 – 60 cycles, the frequency of the mains voltage. For incandescent lamps, flickering is not normally observed because the luminous flux has a frequency of 100 – 120 cycles. This doubling of the supplies frequency

is disturbed in the case of discharge lamps, at least in the region of the electrodes where the cathode and anode mode lead to a different brightness of the arc related to the two phases of the arc cycle. If not only a small area near the electrodes but the whole arc shows variations of brightness with a frequency of 50- 60 cycles, a disturbing flicker results. This is always the case if the time of re-ignition is different for each electrode. Because the lamp current and voltage differs for both half cycles, a net DC fraction of the lamp current results.

Measurements shows: flickering decreases with decreasing rod radius. The key to the solution is an appropriate electrode temperature. Thermionic emission must exist over a broad area of the electrode front surface, i.e. the so called low-field mode of operation has to prevail [9].

Measurements of lamp electrode behaviour

In the first measurement we zoom in on the lamp voltage between the commutation intervals, to observe the electrical properties of the electrode behaviour. The voltage is measured before the commutator, to get the rectified burner voltage. In the second measurement the voltage and the current are measured directly after a commutation, to investigate the reaction on the commutation process.

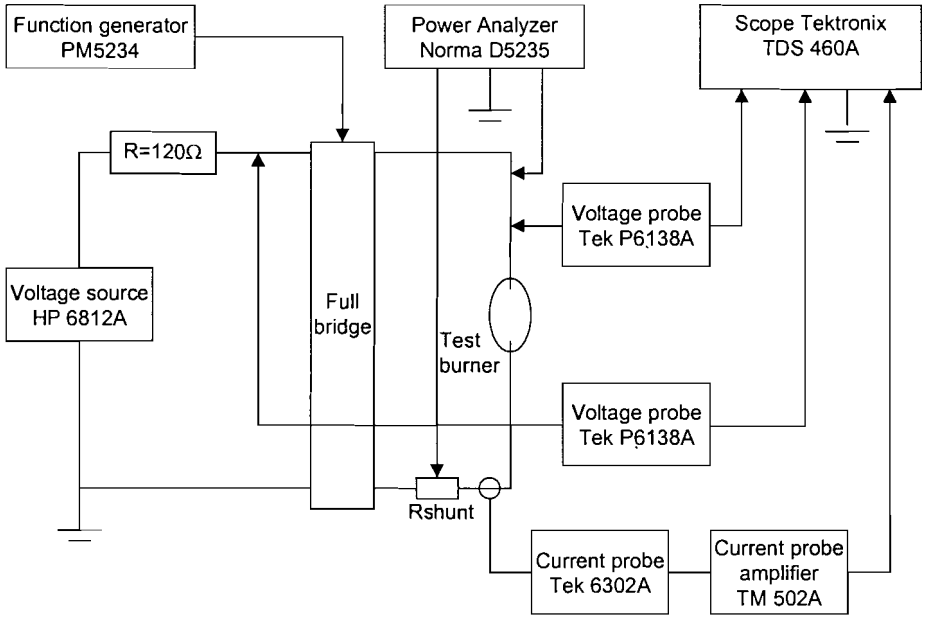

Figure 4.12: Measurement set-up

The measurement set-up is shown in figure 4.12. Scales of the resulting scope plots are: lamp voltage 1V/div and time scale 2msec./div.

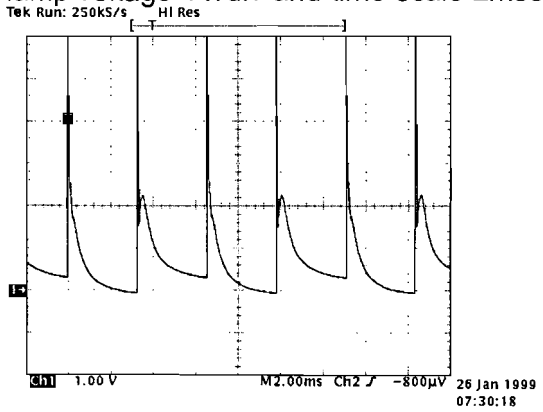

Figure 4.13(a): CDM-T 70W/83 P_{la} = 73W

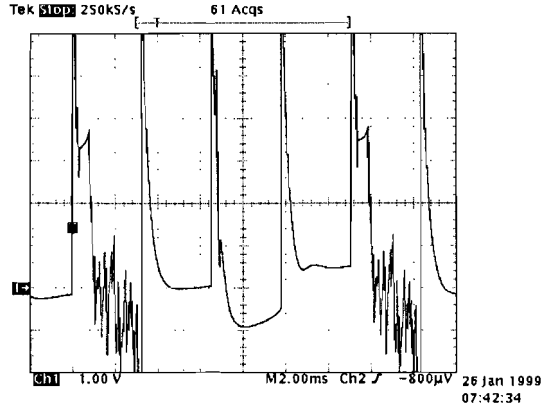

Figure 4.13(b): CDM-T 70W/83 P_{la} = 35W

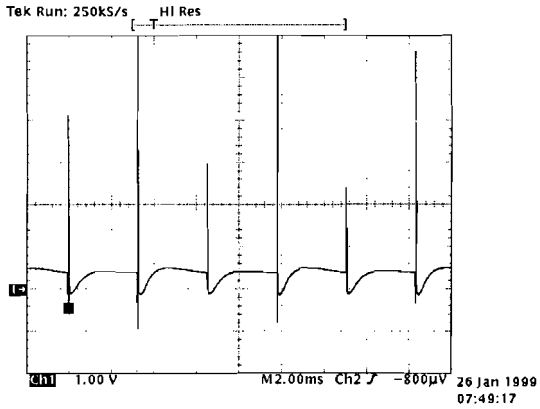

Figure 4.14(a): MHW-TD 70W P_{la} = 73W

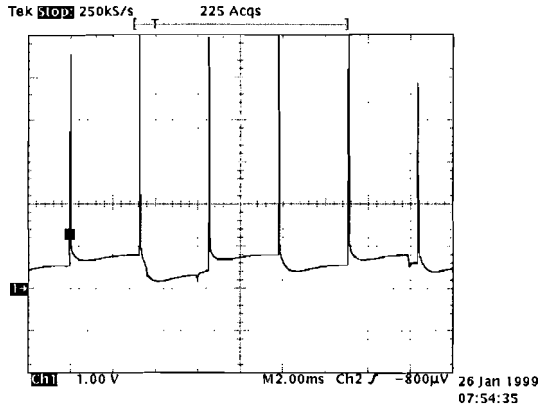

Figure 4.14(b): MHW-TD 70W P_{la} = 35W

Normal power operation with the CDM burner (figure 4.13(a)) shows a small decrease in voltage during the commutation interval and a little difference between the burning voltage for both half cycles. For reduced power operation (figure 4.13(b)), we see a large difference in the burning voltage every half cycle. One electrode has serious problems and switches over from thermionic mode of operation to a spot mode sometimes a vapour mode this is indicated by the high frequency component superposed on the burning voltage. The amount of light flickering is related to the differences in burning voltage between the commutations (a low frequency component).
To compare the results of the CDM burner the same measurement is done with a MHW burner in figure 4.14. For normal power operation the scope picture shows a smooth burning voltage. For reduced power operation there is a little difference between both half cycles, but the electrodes for this lamp have no problems for this power level.

In the second electrode measurement the lamp voltage and current are measured (see figure 4.12) with the measurement set-up. Now we zoom in on the commutation process to observe the behaviour of the lamp directly after the current reversal. In the resulting plots three lines are projected, on top the lamp voltage (100V/div.), in the middle the instantaneous lamp power and below the lamp current (1A/div.). The time scale is always 10µsec/div.

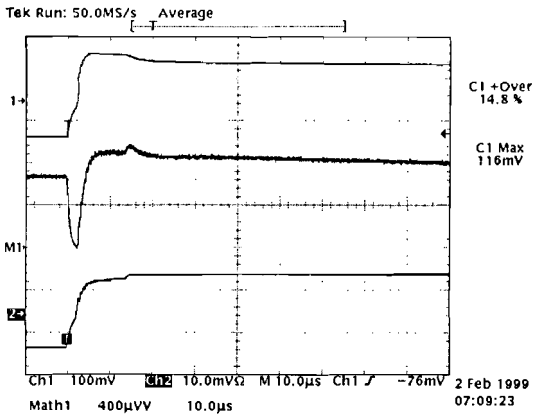

Figure 4.15(a): CDM-T 70W/83 P_{la} = 73W

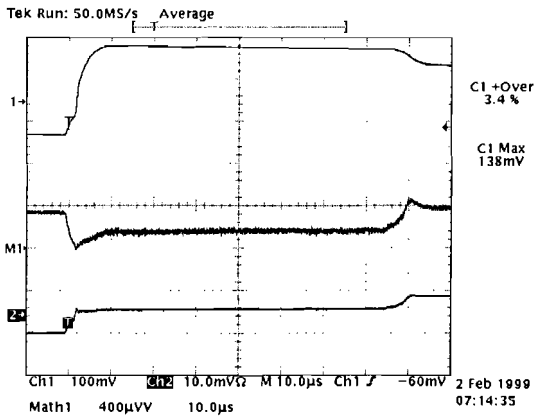

Figure 4.15(b): CDM-T 70W/83 P_{la} = 35W

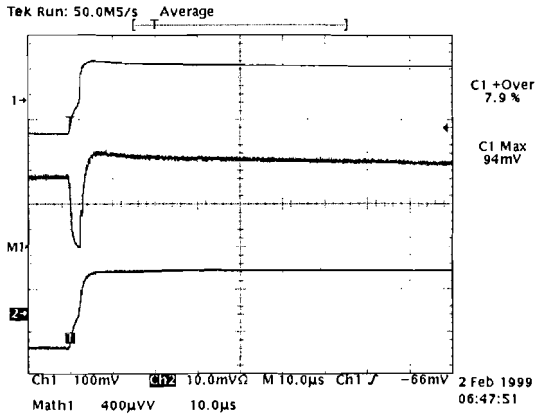

Figure 4.16(a): MHW-TD 70W P_{la} = 73W

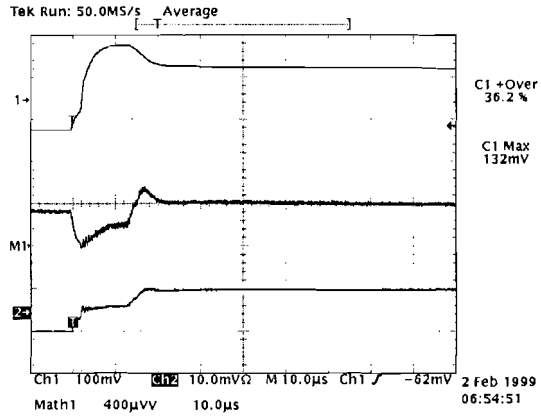

Figure 4.16(b): MHW-TD 70W P_{la} = 35W

Full power operation with the CDM burner figure 4.15(a), shows a very fast commutation process. The voltage shows a small re-ignition peak after the commutation and the power level also. In dimmed situation (figure 4.15(b)), after commutation the lamp voltage shifts to a high value and the current stays very low, also the power level. For a period of about 80µsec, this situation holds then the lamp current, voltage and the power return to their normal values for this reduced power operation mode. Exactly the same measurement is done with a MHW burner, and especially for the reduced power mode the differences are compared with the CDM burner (figure 4.16). The MHW burner has obviously less problems with commutation by low power operation.

The time of low current and high voltage after the commutation is a reliable parameter to define the border of stable low power operation. If the border is reached the "current low time" or "voltage high time" is highly related with the supplied power level. If the time become too long the lamp extinguishes immediately. In practice it seems to be that 80µsec. (for CDM and MHW lamps) is the border value for stable operation, as shown in figure 4.15(b).

Discussion results

The high frequency components mentioned in the literature can be easily observed and used to determine the vapour mode of operation of the electrodes. The observed low frequency fluctuations caused by the burning voltage differences between the commutations can be related with the static spot mode. The high frequency component can be related with lamp maintenance and the low frequency component with light flickering. But both parameters don't give reliable information if the border of low power operation is reached. Practical measurements show lamps with a smooth electrical behaviour between the commutation intervals in low power operation but extinguishing a minute there after. Only with the "current low/ voltage high time" parameter can this stability border be easily observed. Of course also the lamp re-ignition must be observed. It should never exceed the open voltage because the lamp would extinguish.

A good dimmable lamp must have an appropriate electrode temperature for low power operation. Thermionic emission must exist over a broad area of the electrode front surface and the so-called low-field mode has to prevail. The volt-second area of the re-ignition peak must be minimised to avoid arc tube blackening.

Note: The observed electric lamp behavior is related to lamp physical aspects based on literature articles discribing other types of discharge and not being validated by practical measurements for the CDM 70W burner. Further research is absolutely needed to prove this physical relations.

5. Lamp modelling

5.1 Identification

Modelling is the art of creating a mathematical description of e.g., physical, chemical or electrotechnical phenomena which appear in reality. For many purposes, among them analysis and design, we want to be able to describe a process in an understandable way. This means that we want to describe some aspects of a real-world object, in an abstract way. We have to decide which characteristics to take in account, and which properties to ignore. It is the essence of the art of modelling to select only those characteristics, among the many available, which are necessary and sufficiently describe the process accurately enough according to the objectives of the modeller.

Sometimes it is possible to derive a model by deduction only, based on the underlying, physical laws and known parameters. Such a model is called a white-box model. In other situations almost no prior information is available, and the model has to be derived from the measured data of the input and output signals, without any information concerning the internal structure and internal relations. These models are called black-box models. It's advisable to use as much prior information as possible. Most of the time we have to handle problems laying between those extremes, called grey box models (figure 5.1).

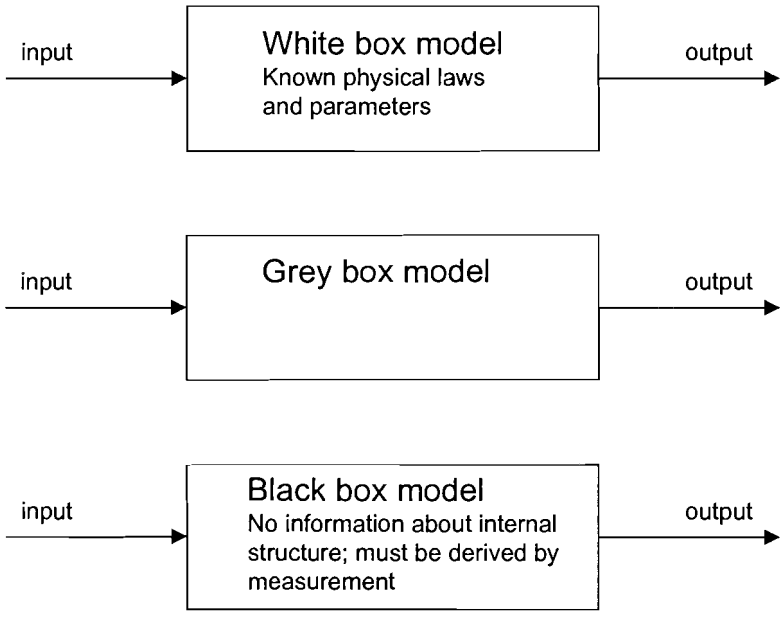

Figure 5.1: Types of models

5.2 Lamp model

The electrical behaviour of a high-pressure lamp (CDM-T 70W/830) will be described by means of a grey box model based on the lamp physics. The applied equations are simplified by lumping physical constants together to create new constants. Then identification techniques are used to find proper values for most of these constants, other are directly related to lamp physics and can be filled in.

Firstly an introduction in the lamp physics and derived lamp model [15] is given.
A discharge plasma is an electrically conducting medium with the presence of approximately equal numbers of free electrons and ions in the gas. The electrons, being accelerated by the electric field, gain energy, they collide with each other or with the gas atoms, which results in

transfer of energy between electrons and electrons, or electrons and atoms. When an electron collides with an atom, it can take some energy from or transfer some to the atom. According to the Maxwell-Boltzmann distribution, the majority of the electrons carry a small amouth of energy, which is partly transferred to the atoms and result in heating them up (elastic collisions). However, a small percentage of the electrons, acquiring enough kinetic energy, can make inelastic collisions with the atoms, which ionise them to upper energy states from which the atoms radiate.

Local Thermodynamic Equilibrium (LTE) can be defined as a state of the plasma in which all distribution functions, with exception of the radiation energy, are given by Boltzmann distributions. This means that the plasma stationary state can be described by the laws of the thermodynamic equilibrium, but energy is lost by radiation. In these systems, equilibrium is possible due to high frequency of collisions between electrons and other species. A consequence is that the electron temperature and the gas temperature of the system are approximately the same. We can now compute the concentration of atoms in a particular excited state according to Boltzmann law:

$$n_k = n_o \frac{g_k}{g_o} e^{-\frac{eV_k}{kT}} \tag{14}$$

where n_k = concentration excited atoms
n_o = concentration of atoms in the ground state
g_o, g_k = statistical weights
e = elementary charge
V_k = volts above ground level
k = Boltzmann constant
T = absolute electron-gas temperature (of the arc)

The concentration of electrons n_e can determined from Saha's [14] equation:

$$\frac{n_i n_e}{n_o} = \left(\frac{2(2\pi m_e)^{\frac{3}{2}}}{h^3} T^{\frac{3}{2}} \right) \frac{U_i(T)}{U_o(T)} e^{-\frac{eV_i}{kT}} \tag{15}$$

with n_i = concentration ions
n_e = concentration electrons
m_e = electron mass
h = constant Planck
$U_i(T)$, $U_o(T)$ = statistical weights
V_i = ionisation potential

5.2.1 Energy balance

The main source of energy supplied to the lamp is the electrical energy, which is dissipated through the lamp electrodes and the arc discharge. In the latter, energy can escape by means of radiation, thermal conduction of the wall of the discharge tube, diffusion of electrons, ions and excited atoms, and convection. Losses by diffusion of particles and by convection are small compared to losses by thermal conduction and radiation; therefore, they can be neglected [14]. Consequently, the energy balance equation is given by

$$P_{in} = P_{rad} + P_{cond} + P_{th} \tag{16}$$

with P_{in} = electrical input power
P_{rad} = radiated power

P_{cond} = conducted power
P_{th} = electrode power lost through thermal radiation

Note that inclusion of the electrode power into the energy balance equation implies that the anode and cathode falls are not treated as separate entries, but appear implicitly in the model. This means that the lamp voltage generated from the model will represent the combination of the electrode drop and the voltage across the arc discharge. Remark: For the electrodes is assumed a constant thermionic mode of operation for all power levels.

Conservation of power at the outer mantle near to the wall can be realised by three factors. First, the conducted power escapes the plasma and heats the wall. Also, part of the radiated power is absorbed by the atoms in this region. Lastly heat can escape the discharge tube in form of thermal radiation P_{out}. Consequently, at steady state this results in

$$P_{out} = P_{cond} + a_2 P_{rad} \tag{17}$$

where P_{out} = total thermal power
a_2 = absorption coefficient wall

Thermal model high pressure lamp
The high pressure lamp is modelled with a two step temperature profile, all quantities being considered as cylindrically symmetrical about the axis of the tube. The discharge tube is restricted into two regions: the arc discharge with a constant temperature profile T, and the outer mantle also with a constant temperature profile T_w. The consequence of the above assumptions is that one loses information about the temperature profile of the discharge tube, since it is simplified to two distinct temperatures, T and T_w. The lamp temperatures T and T_w are the most important variables, since they control the lamp dynamics.

5.2.2 Dynamics

If the input power P_{in} is instantaneously changed, the momentary imbalance of the input and output power in the energy balance equation should cause fluctuation in the arc temperature T, before a new equilibrium is reached. This dynamic response is modelled with a first order system as follows

$$\frac{dT}{dt} = M_1\left(P_{in} - P_{rad}(T,T_w) - P_{cond}(T,T_w) - P_{th}\right) \tag{18}$$

where M_1 = constant, controls the dynamics of the arc temperature
T = average arc temperature
T_w = average wall temperature

Dynamics of the outer mantle temperature due the thermal conducted and radiated energy is also modelled by a first order dynamical system as follows

$$\frac{dT_w}{dt} = M_2\left(P_{cond}(T,T_w) + a_2 P_{rad}(T,T_w) - P_{out}(T_w)\right) \tag{19}$$

with M_2 , a constant, which controls the dynamics of the wall temperature

So the total system can be described by a set of two algebraic non-linear equations, that is formed by the combination of formula (18) and (19), leading to

$$\begin{cases} \dfrac{dT}{dt} = M_1\left(P_{in} - P_{rad}(T, T_w) - P_{cond}(T, T_w) - P_{th}\right) \\ \dfrac{dT_w}{dt} = M_2\left(P_{cond}(T, T_w) + a_2 P_{rad}(T, T_w) - P_{out}(T_w)\right) \end{cases} \tag{20}$$

5.2.3 Definition of variables

The radiated power P_{rad} is related to the Boltzmann law. Radiation is due to the transition of the excited outer valence electron orbiting the mercury atom from a higher level of energy state to a lower level of energy state. The total radiation of a metal halide lamp is a combined spectrum of mercury and metal additives radiation. The radiated power caused by the mercury atoms, which is simplified by taking a constant value (b) for the energy level, can be described by

$$P_{rad} = n_o(T,T_w)\sum_m \frac{g_m}{g_o}\sum_n A_{mn} eV_{mn} e^{-\frac{eV_m}{kT}} = n_o(T,T_w)\cdot b \cdot e^{-\frac{eV_m}{kT}} \tag{21}$$

with n_o = concentration of atoms in the ground state
g_o, g_m = statistical weights
A_{mn} = probability transition state m to n
eV_{mn} = photon energy
e = elementary charge
b = constant for the energy level
V_m = volts above ground level
k = Boltzmann constant
T = average arc temperature

At normal operating condition, the amount of mercury inside the arc tube is fully volatised. However, decreasing the electrical input power will decrease the cold spot temperature, and the mercury gas may start to condense when the cold-spot temperature approaches the threshold temperature T_{sat} of mercury. Under this circumstance, the concentration of the mercury gas decreases. The cold spot temperature can be assumed to be the wall temperature. According the ideal gas law follows that n_o is given by

$$n_o(T,T_w) = \frac{P(T_w)\cdot V}{RT} \approx \frac{e^{\frac{-\alpha_p}{f(T_w)}}}{T} \tag{22}$$

with P = arc tube gas pressure
V = arc tube volume
R = gas constant
α_p = pressure constant
$f(T_w)$ = function cold spot temperature

$$f(T_w) = \begin{cases} T_{sat} & if \quad T_w > T_{sat} \\ T_w & if \quad T_w \le T_{sat} \end{cases} \tag{23}$$

where T_{sat} is the saturation temperature of the mercury.

Equation 22 has been simplified by knowing that the pressure is an exponential function of the cold spot temperature T_w when mercury is not fully volatised, and approaches a constant otherwise.

The total radiated power for metal halide lamps, which consists of the combined spectrum of mercury and metal additives, is given by

$$P_{rad} = \frac{b_1}{T} e^{\frac{-\alpha_1}{f(T_w)} - \frac{eV_{Hg}}{kT}} + \frac{b_2}{T} e^{\frac{-\alpha_2}{T_w} - \frac{eV_{METAL}}{kT}} \quad (24)$$

where b_1 = constant for the mercury energy level
b_2 = constant for the metal additives energy level
α_1 = pressure constant for the mercury component
α_2 = pressure constant for the metal additives
e = elementary charge
V_{HG} = excitation level mercury
V_{METAL} = average excitation level for all the metal additives
T = average arc temperature
T_w = average wall temperature

The power loss by thermal conduction is determined by

$$P_{cond} = -L2\pi\lambda(T)\frac{\Delta T}{\Delta r} \approx L2\pi\lambda(T - T_w) = a_1(T - T_w) \quad (25)$$

where L = length of the discharge
$\lambda(T)$ = coefficient of thermal conduction of the vapour
a_1 = constant for the thermal conductivity of the vapour

Note that the temperature gradient with respect to a small radial direction is $(\Delta T/\Delta r) < 0$. $\lambda(T)$ can be approximated as constant because T doesn't vary much with the electrical input power.

Thermal radiation loss from the electrodes, P_{th}, is a linear function of T^4_{el}, where T_{el} is the average electrode temperature. Since T_{el} is approximated constant over time, one can assume that P_{th} is constant to the first order approximation of the dynamics. The total thermal power can be approximated as

$$P_{out} = a_3 T_w^4 \quad (26)$$

where a_3 is proportionality constant between the output power and the wall temperature.

Saha's law can be used to approximate the lamp resistance yielding

$$n_e^2 \propto n_a T^{3/2} e^{-\frac{eV_i}{2kT}} \Rightarrow n_e \propto T^{3/2}\left(n_{Hg} e^{-\frac{eV_{iHG}}{2kT}} + n_m e^{-\frac{eV_{im}}{2kT}}\right) \quad (27)$$

with n_e =concentration of the electrons in the plasma. This is approximately equal to the number of ions ($n_i \cong n_e$).
n_a =concentration atoms which is approximately equal to the concentration atoms in the ground state
n_{HG} =concentration mercury atoms
n_m =concentration metal halide atoms
V_{iHG} =ionisation potential of mercury
V_{im} =ionisation potential of the various metal halides

With metal additives added to the discharge, the electron mobility μ is proportional to

$$\mu \propto T^{-1/2}\left(n_{Hg}Q_{Hg} + n_m Q_m\right)^{-1} \quad (28)$$

where Q_{HG} = collision cross section of the mercury
Q_m = average collisions cross section of the metal halides

The current density j is proportional with

$$j = e\mu n_e E \tag{29}$$

with E = electric field
μ = electron mobility
n_e = concentration of the electrons in the plasma.
e = elementary charge

Substituting the concentration of the electrons n_e (equation 27) and the electron mobility μ (equation 28) into the current density formula yields:

$$j_{lamp} \propto E T^{1/4}\left(n_{HG}Q_{HG} + n_m Q_m\right)^{-1}\sqrt{n_{HG}e^{-\frac{eV_{iHG}}{kT}} + n_m e^{-\frac{eV_{im}}{kT}}} \tag{30}$$

It follows that the lamp resistance can be approximated by

$$R \propto T^{-1/4}\left(n_{HG}Q_{HG} + n_m Q_m\right)\left(n_{HG}e^{-\frac{eV_{iHG}}{kT}} + n_m e^{-\frac{eV_{im}}{kT}}\right)^{-1/2} \tag{31}$$

For further simplification one can assume that Q_{HG} and Q_m are equal, and by applying the ideal gas law (equation 22) this results in

$$R(T,T_w) = \frac{a_4 T^{3/4}\left(e^{\frac{-\alpha_1}{f(T_w)}} + e^{\frac{-\alpha_2}{T_w}}\right)}{\sqrt{e^{\frac{-\alpha_1}{f(T_w)}-\frac{eV_{iHG}}{kT}} + e^{\frac{-\alpha_2}{T_w}-\frac{eV_{im}}{kT}}}} \tag{32}$$

where a_4 is a proportionality constant of the lamp resistance

Concluding, we have in equation (20),(24),(25),(26) and (32) a set of parameters (displayed in table 5.1), where some must identified and others are constants related directly with the lamp physics that can be filled in.

Table 5.1: Main lamp parameters

Lamp parameters for steady state identification	
a_1	Constant for the thermal conductivity of the vapour
a_2	Absorption coefficient wall
a_3	Proportionality constant between the output power and the wall temperature
a_4	Proportionality constant lamp resistance
b_1	Constant for the mercury energy level
b_2	Constant for the metal additives energy level
α_1	Pressure constant for the mercury component
α_2	Pressure constant for the metal additives
P_{th}	Constant for electrode power loss
Lamp parameters for dynamical identification	
M_1	Constant, controls the dynamics of the arc temperature
M_2	Constant, controls the dynamics of the wall temperature
Lamp parameters which can be filled in	
V_{HG}	Excitation level mercury

V_{METAL}	Average excitation level for all the metal additives
V_{iHG}	Ionisation potential of mercury
V_{im}	Ionisation potential of the various metal halides
T_{sat}	Saturation temperature mercury

5.3 Parameter extraction

The model structure is discussed in the previous section. Now the parameter extraction must be done. It's important to note that only the lamp voltage and current are needed. One can devise the identification procedure into separated stages.

1. Steady state identification (9 unknown parameters).
2. Dynamic identification: Fast dynamics (parameter M1)
3. Dynamic identification: Slow dynamics (parameter M2)

The identification procedure for this grey box model can be spit up in three sections. This possible because in the lamp model, the main part can be identified with a steady state data set (without dynamical effects). Further it is known that the lamp dynamics can modelled by means of two time constants. One is in order of milli-seconds and the other is in the sec. range. So the dynamic identification procedure can separated into two independent parts. Concluding the identification procedure consists of three parts. The advantage of this method are the reduced data sets for every identification. To identify a black box model one enormous data set is needed to excite all modes of the model structure. Also a grey box modelling is expected to yield better accuracy over a larger range of lamp operation than black-box modelling.

5.3.1 Steady-state identification

For the parameter extraction the steady state lamp voltage and current are needed, for several power levels. If the lamp is allowed to reach the steady-state operation, the operating condition will converge to an equilibrium state at which the lamp temperature T, and the wall temperature T_w become constant. This implies dT/dt=0 and dTw/dt=0. Consequently in formula 20 the dynamical parameters M1 and M2 disappear. It follows that this equation then reduce to a set of non-linear equations

$$\begin{cases} P_{in} - P_{rad}(T, T_w) - P_{cond}(T, T_w) - P_{th} = 0 \\ P_{cond}(T, T_w) + a_2 P_{rad}(T, T_w) - P_{out}(T_w) = 0 \end{cases} \tag{33}$$

First the vectors P_{in} and R must be calculated. For a given P_{in} the lamp temperatures T and T_w can be solved using a least square fit procedure. The next step is to calculate the lamp resistance, which can be done by substituting the lamp temperatures in equation 32. The total calculation is shown in figure 5.2.

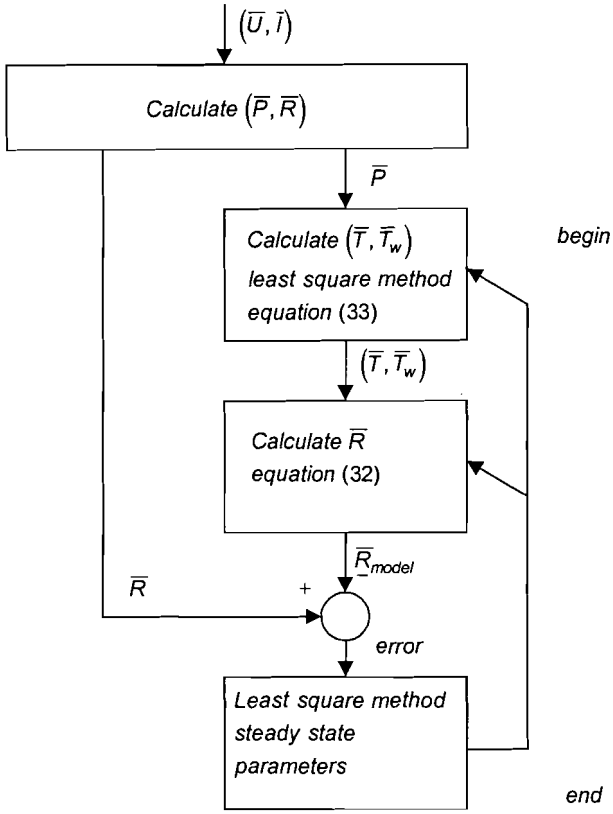

Figure 5.2: Steady-state identification procedure

Now the computed resistance vector R_{model} and the actual measured resistance vector R corresponding with the given P_{in} vector can be compared, resulting in an error vector. To minimise the error vector by adjusting the unknown parameters, is done with a least square method.

Practical implementation of the algorithm
The algorithm is implemented in Matlab, using the optim toolbox facilities. For all the minimalization problems a least square tool is used. Selected is the Gauss-Newton method in combination with a cubic interpolation line search method. If the standard mixed polynomial line search method is used, algorithm instability may occur. As mentioned before, the first step in the identification procedure is to compute the two temperatures used in the model (T,T_w). These temperatures must be calculated for every measured steady state point. The next step is to calculate the resistance (vector) as output value of the simulation model. Finally the error vector can be computed, and the real identification procedure of the unknown steady-state parameters can start.

After every iteration of the minimalization, the algorithm adjusts the unknown parameters towards convergence to a minimum error. However, this multi-dimensional search, may encounter many local minima, preventing convergence to the global minimum. In fact, it is seen quite often that the identification will lead to a local minimum instead of the global minimum, if the initial guesses for the unknown parameters are not selected properly. To overcome this problem a constrained optimalization is used.

Experimental set-up
The experimental set-up for determining the steady state parameters is illustrated in fig 5.3. The energy is supplied by a voltage source, with an additional output filter to minimise the output ripple. To achieve stability a series resistor is used to offset the negative impedance characteristic of the lamp. To provide an alternating current, a full bridge is implemented.

The switching frequency is set to 100Hz, which is very close to the normal operating frequency of square wave electronic ballast circuits. This frequency is chosen in contrast with the experimental set-up in rapport [17] to avoid acoustic resonances. During initial measurements with square wave operation above 20kHz, instabilities occurred in the CDM-T 70W burner.

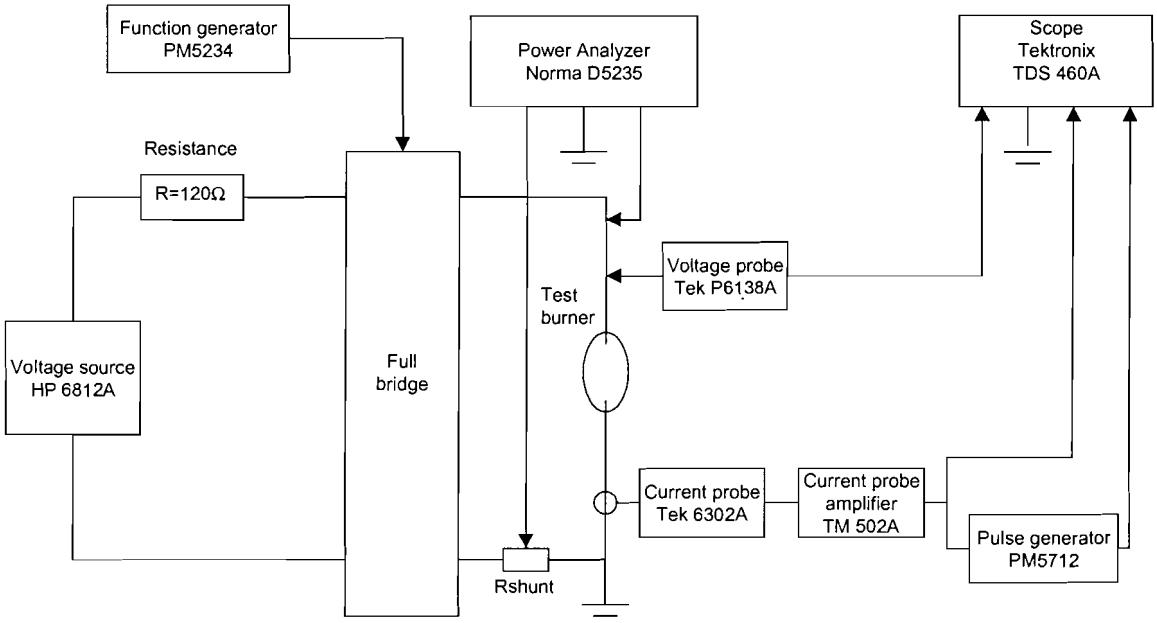

Figure 5.3: Experimental set-up for steady state identification

By varying the input voltage, one can control the steady state lamp power thereby. Also, since the lamp voltage and currents at various power levels can be measured experimentally, the lamp power and the lamp resistance can be obtained accordingly. The supply voltage is decreased with discrete steps using a waiting period of two minutes before measuring to ensure that the lamp has reached the quasi steady state. The supply voltage is kept decreasing and the steady state lamp voltage and current are recorded until the lamp extinguished. To get a sufficient resolution for the parameter extraction, more than 30 steady state points are needed.

For every power level in quasi steady state V_{rms} and I_{rms} must be determined. It follows that the lamp voltage and current waveform are almost square waves. By knowing this, it is allowed to take one sample during a period. For this purpose, a delay generator is used to take a sample in the middle of the positive square wave part. The delay generator is triggered by the commutation process. By taking about 100 samples and averaging a very accurate sample for the voltage and current can be determined. It should be noticed that, by doing this, information of the re-ignition peak is lost, but for the steady state identification only the steady state resistive value is the point of interest. Dynamical effects are taken in account in other parts of the total identification process. Further more, in contrast to full power operation the value of the re-ignition peak for low power is not only based on plasma effects. Electrode effects begin to play a very important role. But remember that only the thermionic mode of electrode operation is taken into account in the lamp model. So measuring re-ignition peaks for very low power mode (electrodes operating not in thermionic mode) results in a remarkable mismatch in the measured data.

Modelling steady state CDM-T 70W/830

A new CDM-T 70W/830 lamp is selected for modelling because this type will be used for

dimming purposes in the future. Some initial knowledge regarding the lamp characteristics is required beforehand: the ionisation potentials and the average excitation potentials of the various elements in the discharge, and the threshold saturation temperature of mercury. In addition to mercury, the 70W CDM lamp is known to contain sodium iodide, dysprosium, and thallium. Their ionisation potentials and the excitation potentials of the strongest resonance lines are given in table 5.2. For simplification of the model the ionisation potentials of the various metal halides are averaged to a single potential, the same averaging action is applied to the excitation potential.

Table 5.2

	Ionisation potential [V]	Average value ionisation potential [V]	Excitation potential of the strongest resonance lines [V]	Average value excitation potential [V]
Mercury	10.4	10.4	7.8	7.8
Sodium Iodide	5.1	6.0	4.57 and 3.27	4.0
Dysprosium	6.0		2.91	
Thallium	6.0		4.14	

The identification procedure results in the following steady state parameters in combination with filled-in parameters for the CDM-T 70W/830 burner shown in table 5.3.

Table 5.3

Parameter identified	CDM-T 70W/830
a_1	0.0036
a_2	0.1675
a_3	7.2135e-12
a_4	1626.8
a_5	1.4121
b_1	4.3916e15
b_2	7.6500e14
$\alpha 1$	10002
$\alpha 2$	15996
Parameter filled in	
V1	7.8
V2	4.0
Vi1	10.4
Vi2	6.0
T_{sat}	1030

To verify the accuracy of the identification, the resistance versus power characteristic is generated using the identified model compared against the measured data (figure 5.4). The circle marks are measurements and the continuous line shows the modelling result. Its clear that there is a very good agreement between the measured data and the model fit for the lamp.

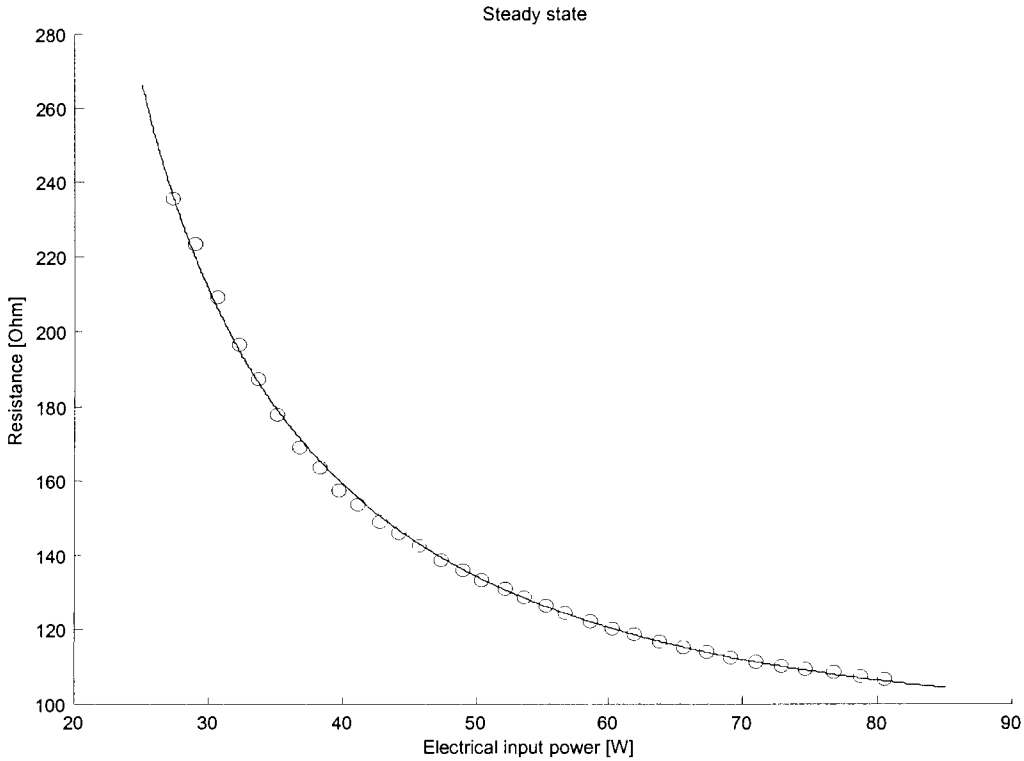

Figure 5.4: Steady state identification result

In order to make sure that the determined parameters yield a model that makes physical sense, the plasma temperatures T, wall temperature T_w and the radiated power P_{rad} (absorption excluded) are calculated for different power levels shown in figure 5.5. As the lamp power is increased, T_w increases whereas T increases and start to decrease when the lamp power exceeds the 55W power level. The decrease in the arc temperature at high power results from the vaporisation of the excess metal halides due to the increase in the cold spot temperature, which makes the arc cooler. Also figure 5.5(c) indicates an important property of the lamp: The radiated power is proportional to the input electrical power.

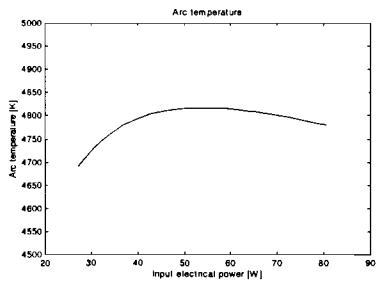

Figure 5.5(a): Arc temp.

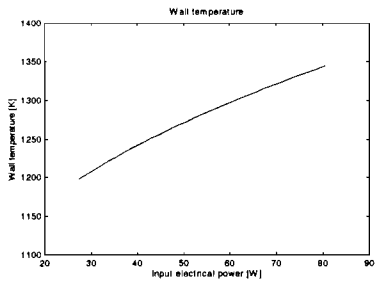

Figure 5.5(b): Wall temp.

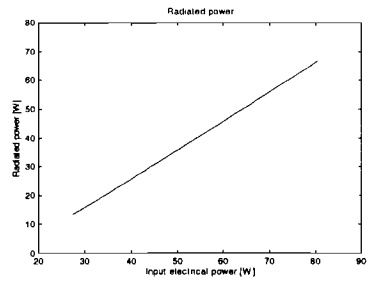

Figure 5.5(c): Radiated power

5.3.2 Dynamics identification

Once the steady state parameters are identified the parameters M1 and M2, related to the system dynamics, can be determined. Its possible to break the dynamics identification process into separated extraction procedures for M1 and M2. Indeed it is known that the time constant of the wall temperature T_w is in the seconds range and is much slower than the time constant of the discharge temperature T. It follows that under fast perturbation T_w is

essentially constant, whereas under slow perturbations T must already reach the quasi-steady state.

Fast dynamics parameter M1

In order to determine M1 a fast dynamic perturbation must be injected into the system to excite the modes that control the state variable T. Since T_w is a slow state variable, T_w can be considered constant during the perturbation process. The lamp transfer function formula (20) now becomes

$$\begin{cases} \dfrac{dT}{dt} = M_1\left(P_{in} - P_{rad}(T, T_w) - P_{cond}(T, T_w) - P_{th}\right) \\ P_{cond}(T, T_w) + a_2 P_{rad}(T, T_w) - P_{out}(T_w) = 0 \end{cases} \tag{34}$$

because the slow dynamics parameter M2 disappears, and M1 still appears. For the identification the second state equation in formula 34 is neglected. It follows that the first state equation in formula 34 is equivalently represented in the block diagram (figure 5.6). Notice that M_1 appears only in the unknown block.

During the fast dynamic perturbation, the lamp voltage and current are measured and a set of $\{P_{in}, R\}$ can be computed subsequently. The constant wall temperature T_w can be solved using equation 33 with $P_{average}$ being the average power of the fast dynamic perturbation. Further the arc temperature T can be calculated with the lamp resistance equation (32).

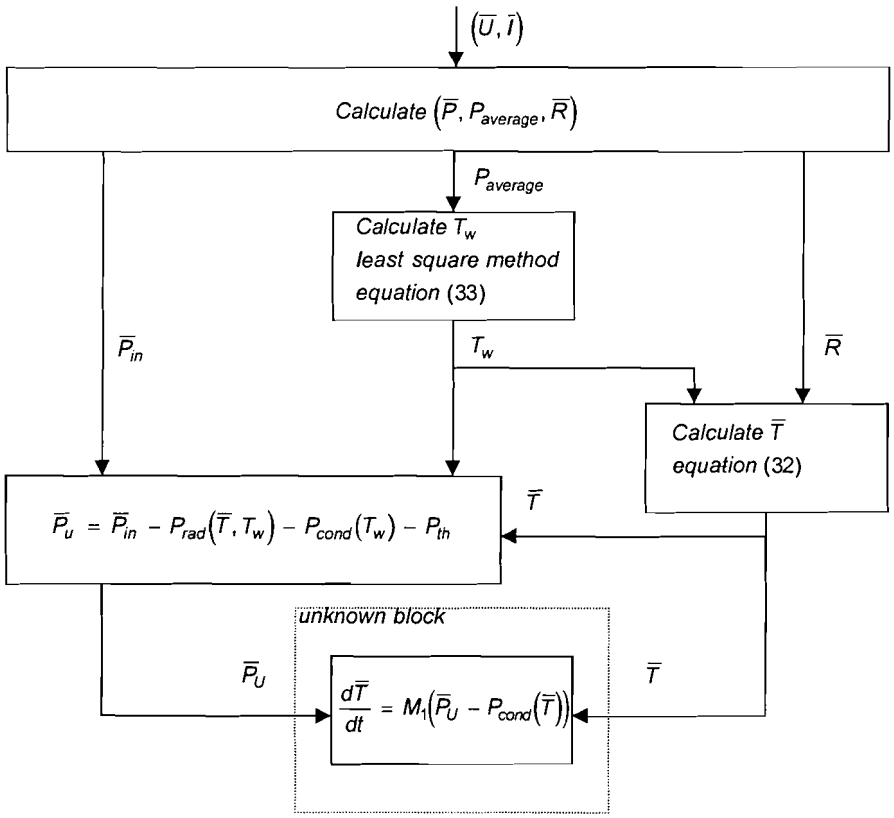

Figure 5.6: Identification parameter M1

Once $\{P_u, T\}$ is determined, the next step is to identify the unknown system, and extract the parameter M1. Since system is a continuous–time first order linear model, it can be transformed into an equivalent first order Auto Regressive Moving Average (ARMA) model (discrete model) using the bilinear transformation as showed in figure 5.7 (see appendix 4).

A discrete model is needed to identify the system on discrete sample moments.
The function in the unknown block can be written as

$$\frac{dT}{dt} = M_1\left(\overline{P}_u - P_{cond}\left(\overline{T}\right)\right) = M_1\left(\overline{P}_u - a_1\overline{T}\right) \tag{35}$$

by using equation 25.

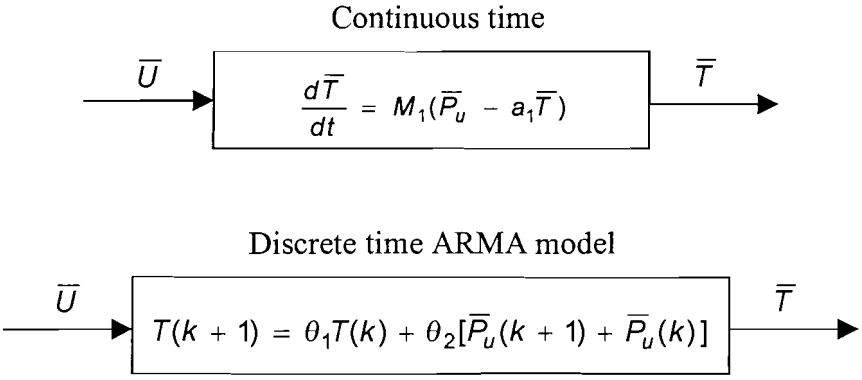

Figure 5.7: Equivalent ARMA model

In the equation of the ARMA model the two unknown parameters $[\theta_1,\theta_2]$ are identified with a least square method using MATLAB.

$$\begin{cases} \theta_1 = \dfrac{K - M_1 a_1}{K + M_1 a_1} \\ \theta_2 = \dfrac{M_1}{K + M_1 a_1} \end{cases} \qquad K = \frac{2}{T_s} \tag{36}$$

Once the parameters $[\theta_1,\theta_2]$ are found M1 can be solved by using

$$M_1 = \frac{f_s\theta_2}{1 - a_1\theta_1} \tag{37}$$

Experimental set-up + Results
As pointed out earlier, fast perturbation must be injected into the system to excite the plasma temperature response, which is controlled by M1. This is done in the same experimental set-up as showed in figure 5.3, but now with a switched resistor parallel with the voltage source and the ballast resistor. The switching resistor is practically implemented as a series circuit consist of a power resistor and a mosfet controlled with a square wave generator. Chosen is for a single perturbation frequency because only the exponential behaviour after a step in the power is of interest. The perturbation frequency is set to 750Hz to measure a sufficient part of the exponential behaviour after a step in the supplied power to the lamp.
Two thousand data points of the lamp power and resistance are recorded with a sampling rate f_s = 2MHz, and shown in figure 5.8(a and b). Further the calculated vectors P_U and T (plasma temperature) are plotted in figure 5.8(c) and 5.8(d). Figure 5.8(c) shows the characteristic exponential behaviour after a power change like the small signal analysis as described in section 4.6. Figure 5.8(d) shows the arc temperature versus time, the speed of the temperature change in time is reversed proportional with the identified fast dynamics parameter M1.

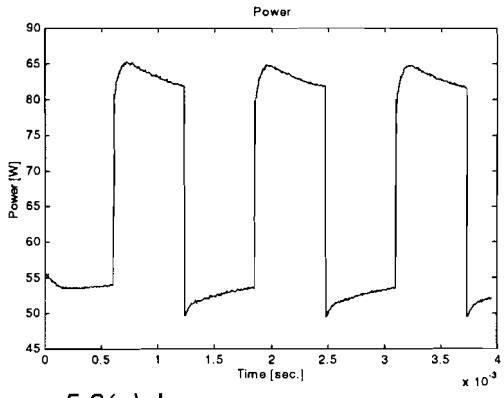

Figure 5.8(a): Lamp power

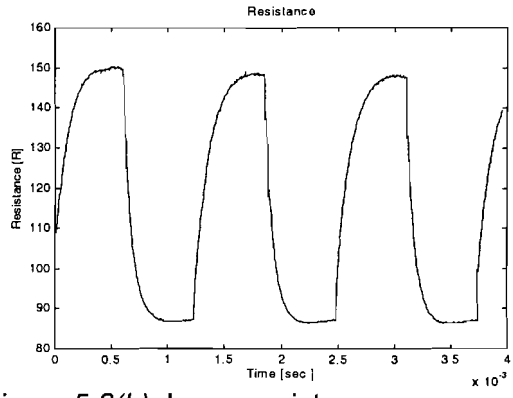

Figure 5.8(b): Lamp resistance

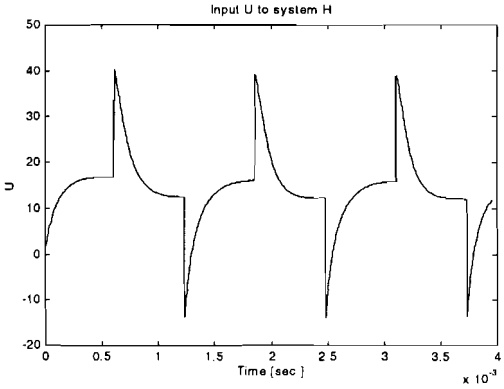

Figure 5.8(c): Calculated vector P_U

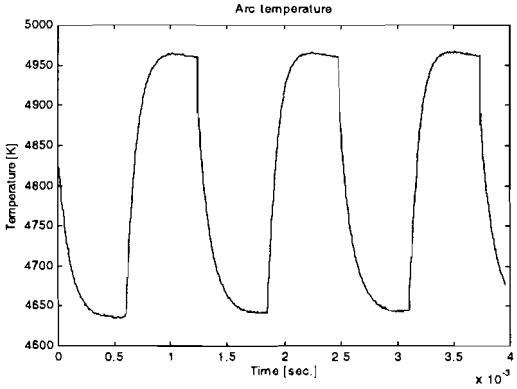

Figure 5.8(d): Calculated vector T

Finally, the identification result for the parameter M1 is showed in table 5.4.

Table 5.4

Parameter identified	CDM-T 70W/830
M1	1.5016e5

To verify the accuracy of the identified parameter M1. The calculated vector T is compared with the temperature vector computed with the identified block containing parameter M_1, both for the same set of P_u. The resulting temperatures are plotted in one figure (5.9). The continuous line is computed from the measurement data and the dashed line is approximated from the identified system. There is a very good fit between the two temperatures, indicating that the identification is very accurate.

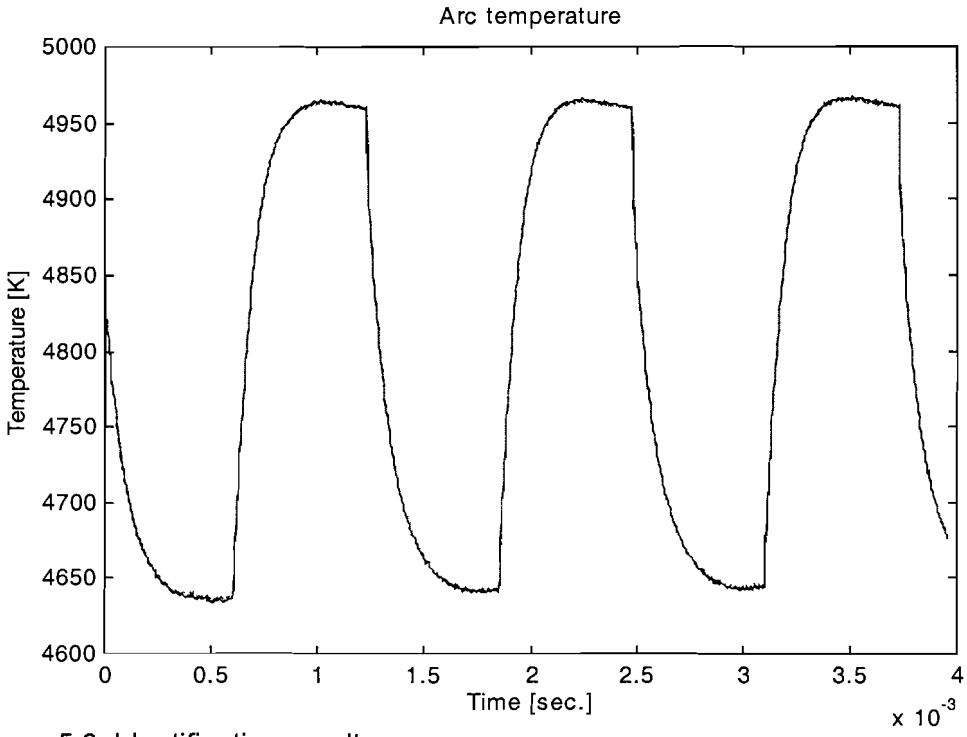

Figure 5.9: Identification result

Slow dynamics parameter M2

Parameter M2 controls the time constant of the wall temperature T_w. Knowing that the run-up period of the lamp is controlled by the wall temperature, the run-up behaviour can be used to approximate the parameter M2.

As mentioned earlier, the discharge temperature T reaches quasi-steady state under very slow perturbation, since the time constant of T is in the milli-second range. Thus, when the lamp is slowly perturbed, the lamp model reduces to the following transfer function

$$\begin{cases} P_{in} - P_{rad}(T, T_w) - P_{cond}(T, T_w) - P_{th} = 0 \\ \dfrac{dT_w}{dt} = M2 \cdot \left(P_{cond}(T, T_w) + a_2 P_{rad}(T, T_w) - P_{out}(T_w)\right) \end{cases} \tag{38}$$

The first state equation of formula (37) can be written as

$$P_{rad}(T, T_w) = P_{in} - P_{cond}(T, T_w) - P_{th} \tag{39}$$

Substituting equation (39) in the second part of state equation (38) yields

$$\frac{dT_w}{dt} = M_2\left((1 - a_2)Pcond(T, T_w) + a_2(P_{in} - P_{th}) - Pout(T_w)\right) \tag{40}$$

Consequentially, under slow perturbation, the lamp model can be equivalently represented by the block diagram shown in figure 5.9. The $\{P_{in},R\}$ vectors are calculated as result of the run-up measurements and they are the start values for the further calculations. Now the lamp temperatures T (plasma temperature) and T_w (wall temperature) for every element of the resistance vector can be computed. If also the internal vector P_u is calculated the identification of the unknown block with the parameter M2 can start.

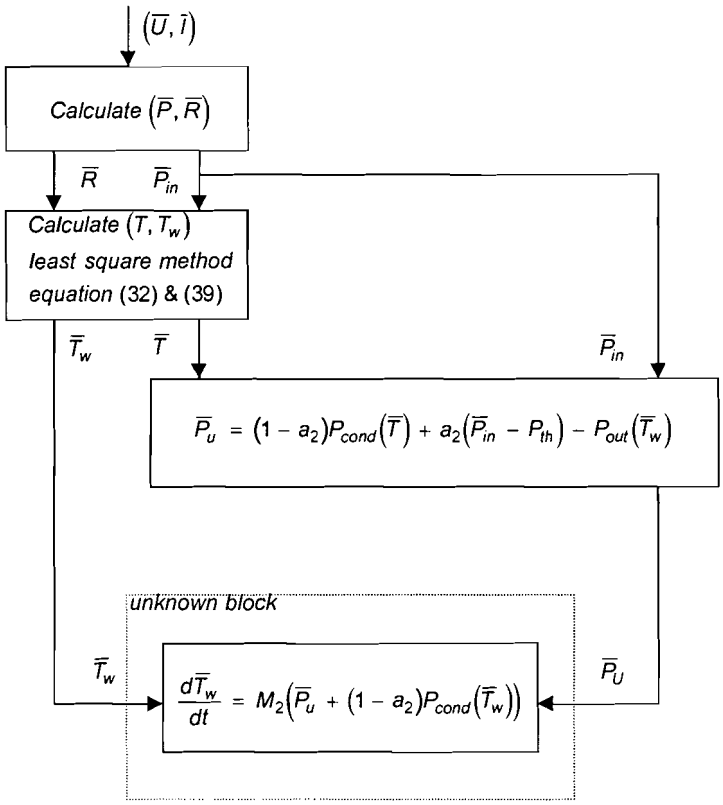

Figure 5.10: Identification slow dynamics

The function in the unknown block in figure 5.10 can be written as

$$\frac{d\bar{T}_w}{dt} = M_2\left(\bar{P}_u + (1 - a_2)P_{cond}(\bar{T}_w)\right) = M_2\left(\bar{P}_u - (1 - a_2)a_1\bar{T}_w\right) \tag{41}$$

by using equation 25.

The continuous time first order linear model can be transformed into an equivalent ARMA model using the bilinear transformation shown in figure 5.10 (see appendix 4). A discrete model is needed to identify the system on discrete sample moments.

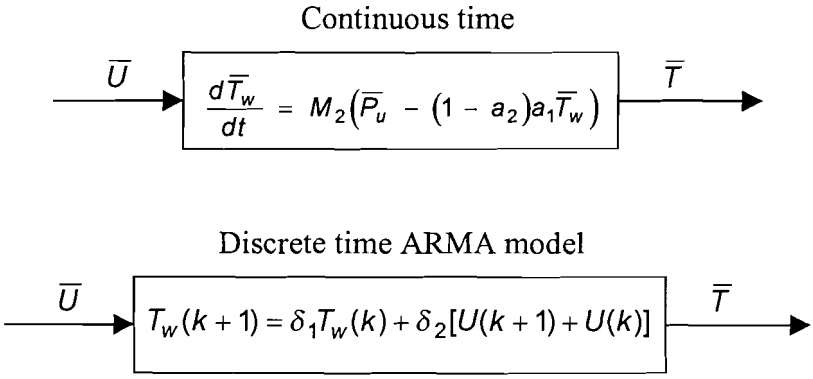

Figure 5.11: Transformation to an ARMA model

In the equation of the ARMA model the two unknown parameters $[\delta_1, \delta_2]$ are identified with a least square method using MATLAB.

$$\begin{cases} \delta_1 = \dfrac{K - M_2(1-a_2)a_1}{K + M_2(1-a_2)a_1} \\ \delta_2 = \dfrac{M_2}{K + M_2(1-a_2)a_1} \end{cases} \qquad K = \frac{2}{T_s} \tag{42}$$

Once the parameters $[\delta_1, \delta_2]$ are found M1 can be solved by using

$$M_2 = \frac{f_s \delta_2}{1 - a_1 \delta_1} \tag{43}$$

Experimental set-up + Results

The experimental set-up for measuring the run-up period of the lamp is the same as the one used for the steady state identification. The voltage source is set at a specified voltage to get a correct nominal power operation after the run-up period (in combination with the used resistor). The acquisition of the lamp voltage and current starts 5 seconds after the ignition of the lamp. In the run-up voltage and resistance (figure 5.12(a & b)) direct after the start an exponential increase with time is observed. This is characteristic for the mercury vaporisation phase. In this phase the pressure is an exponential function of the cold spot temperature (see equation 22). After the mercury vaporisation phase, the change of the lamp voltage slows down, indicating that all the mercury must have completely volatised and that the lamp is approaching the steady-state equilibrium condition. In fact, since LTE starts at the very early stage of the run-up period the model should be valid for most of the run-up phase. Figure 5.12(d) shows the wall temperature versus time, the speed of the temperature change in time is reversed proportional with the identified slow dynamics parameter M2.

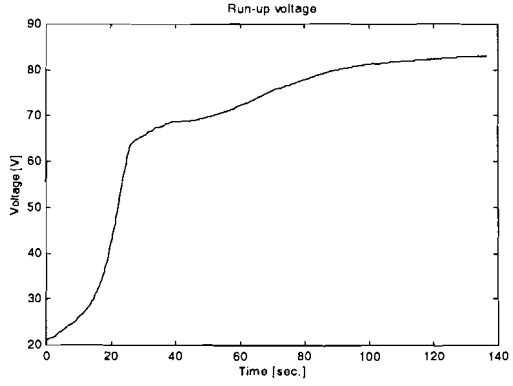

Figure 5.12(a): Run-up voltage

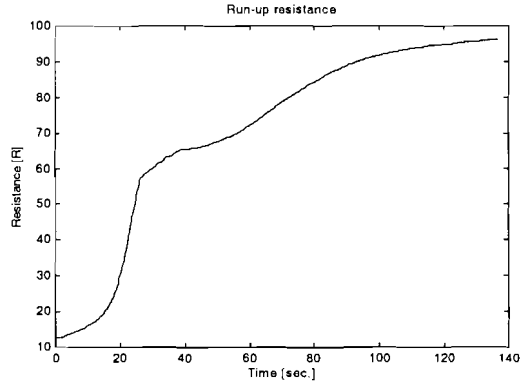

Figure 5.12(b): Resistance

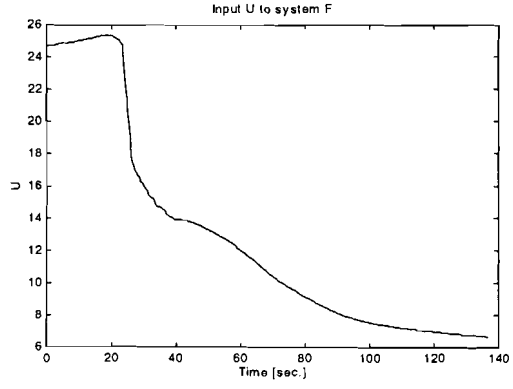

Figure 5.12(c): Calculated vector P_U

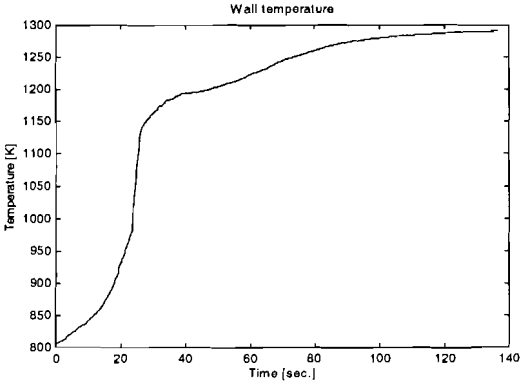

Figure 5.12(d): Calculated wall temperature

Finally the identification results for the parameter M1 showed in table 5.5.

Table 5.5

Parameter identified	CDM-T 70W/830
M2	1.4293

To verify the accuracy of the identified parameter M2. The calculated vector T_w is compared with the temperature vector computed with the identified block containing parameter M_2, both for the same set of P_u. The resulting temperatures are plotted in one figure (5.13). The continuous line is computed from the measurement data and the dashed line is approximated from the identified system. There is a very good fit between the two temperatures, indicating that the identification is very accurate.

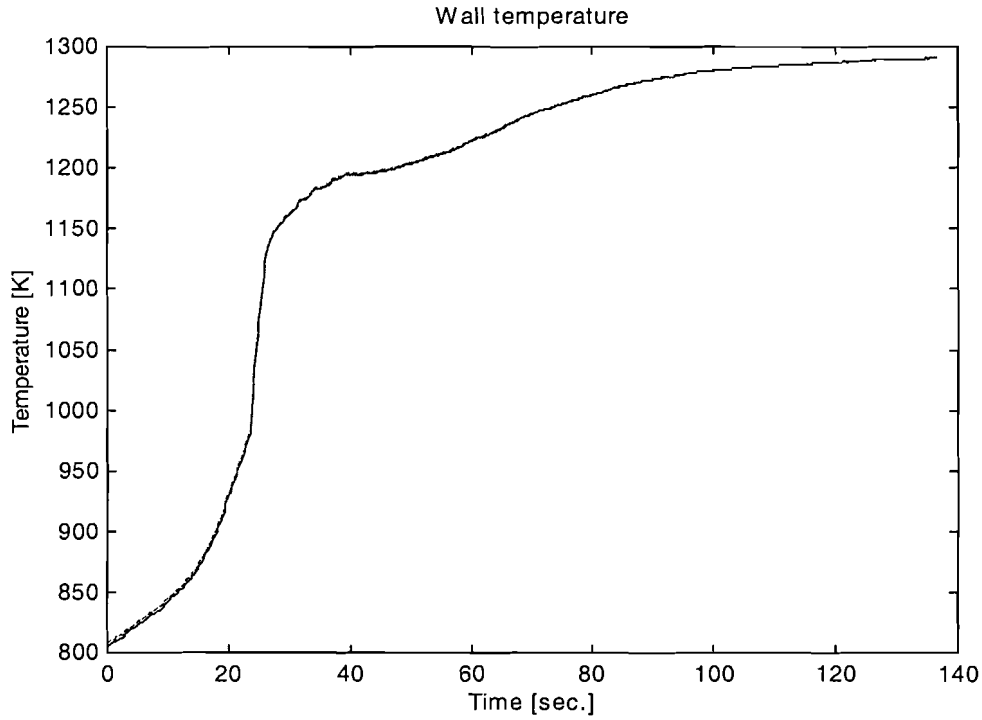

Figure 5.13: Identification result

5.4 Verification lamp model

In this section the identified lamp model is compared with the practical situation. Is there a good fit between the results of a computer simulation and the measured values? For the verification is chosen for a 50Hz sinusoidal conventional ballast situation. The used type magnetic ballast (BMH 70L 302 I TS) is for CDM/MH 70W. To avoid saturation effects in the current peak, four ballasts are connected in a series parallel circuit. In Simulink an ideal coil model in series with the lamp model (section 6.2) is implemented. For several power levels the measured voltage and current are compared with the simulated voltage and current.

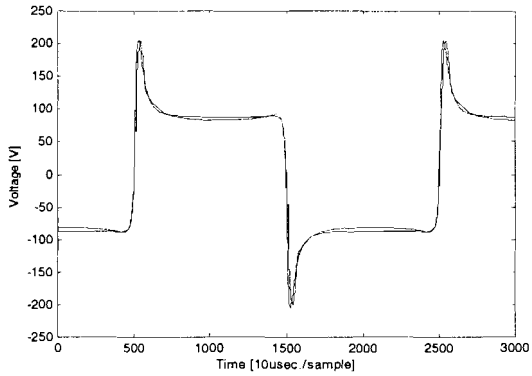

Figure 5.14(a): Lamp voltage P_{la}=73W (M1=1.5e5)

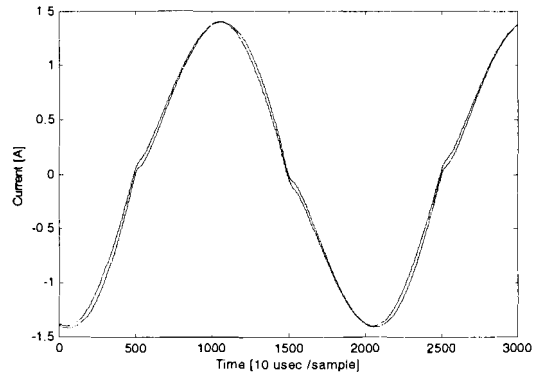

Figure 5.14(b): Lamp current P_{la}=73W (M1=1.5e5)

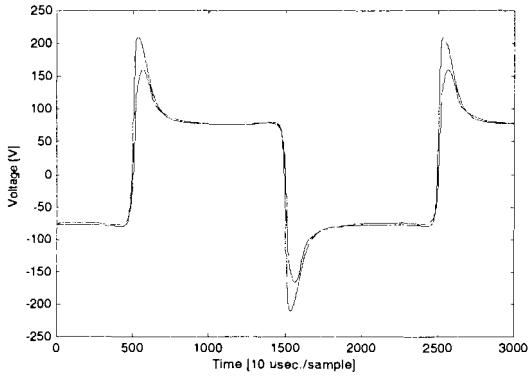

Figure 5.15(a): Lamp voltage P_{la}=50W (M1=1.5e5)

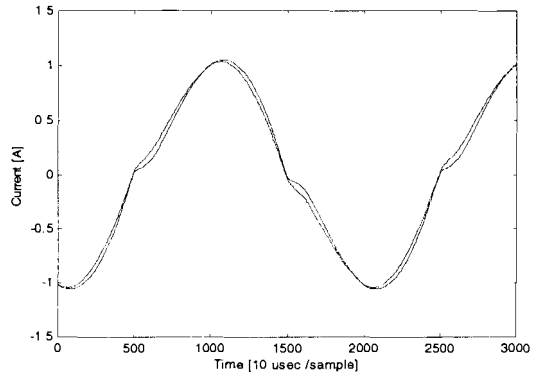

Figure 5.15(b): Lamp current P_{la}=50W (M1=1.5e5)

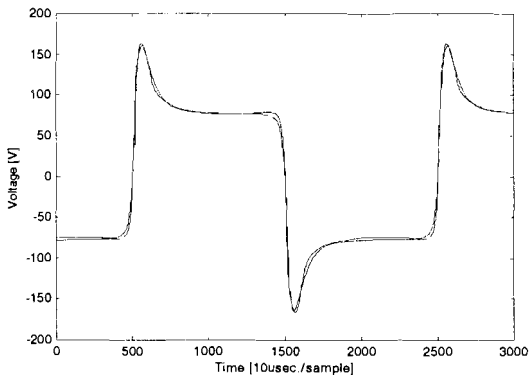

Figure 5.16(a): Lamp voltage P_{la}=50W (M1=0.7e5)

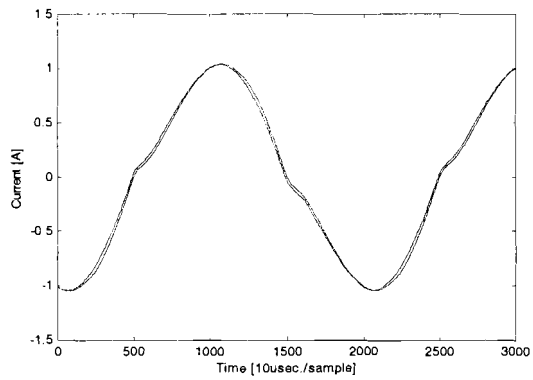

Figure 5.16(b): Lamp current P_{la}=50W (M1=0.7e5)

For full power (figure 5.14) there is good agreement between the simulation and the measurement. The dynamical height and width of the re-ignition peaks fits together, also the static value of the square wave plateau has a good fit. Apparently, the parameters in the lamp model, which were identified with totally different signals, gives a good result also for 50Hz excitation. This means the lamp model is able to predict the voltage behaviour for different current forms. Let's continue with the verification for reduced power operation P_{la}=50W (figure 5.15). The simulated re-ignition peaks are now too large compared with the reality. But with an adapted fast dynamics parameter M1 a good fit is possible (figure 5.16). It seems that a constant fast dynamics parameter is not a good choice for different power levels. It's interesting to know how the relation is between the parameter M1 and the used power level. In order to determine this behaviour a power level between the already

simulated power levels is needed. So also for 60W an adapted fast dynamics parameter M1 is defined. In figure 4.17 the power level is displayed against M1. It seems to be that there is a linear relation. By knowing this it is possible to improve the lamp model by implementing this linear relation between the fast dynamics parameter M1 (resiproke time constant) and the used power level. Concluding with the improved lamp model it's possible to give an accurate simulation of the voltage and current for several power levels. But for very low power levels the prediction goes wrong, when the electrodes reach the border of thermionic operation. Because in the lamp model is assumed thermoinic electrode mode for all power levels.

The behaviour of the lamp simulation model is also presented in other forms to compare the results with other lamp simulation models [18]. Beside the voltage and current plots for full power the dynamic voltage/current characteristic is shown in figure 4.18, it has the typical shape of a duckbill. Further the lamp conductance and resistance are given in respectively figure 4.19 and 4.20.

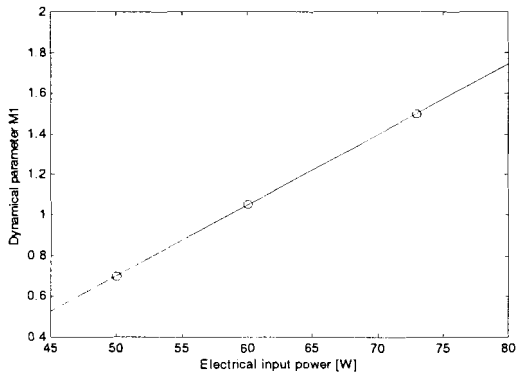

Figure 4.17: Relation power and M1

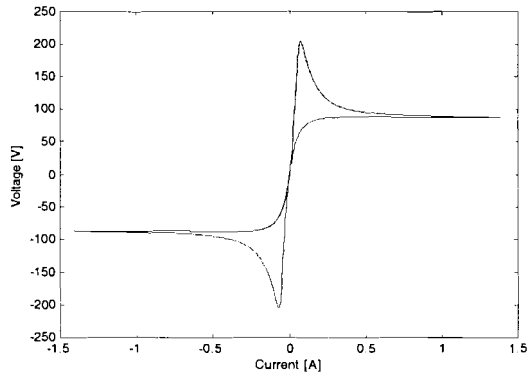

Figure 4.18: IU plot simulation Pla=73W

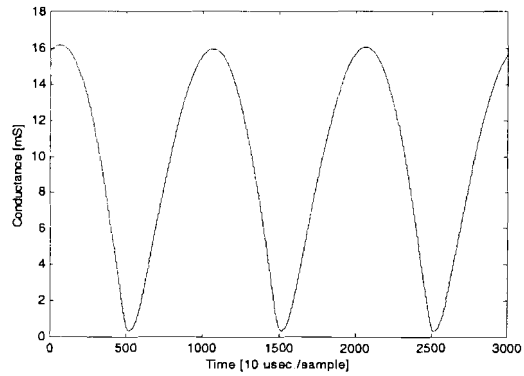

Figure 4.19: Lamp conductance Pla=73W

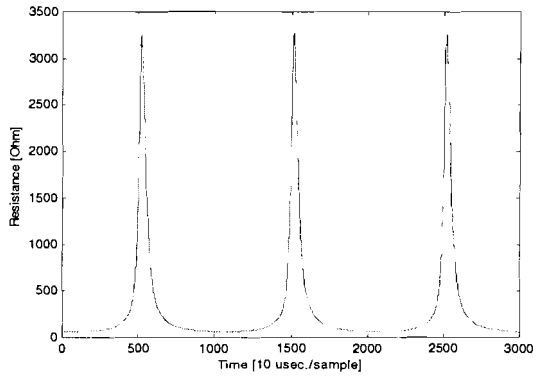

Figure 4.20: Lamp resistance Pla=73W

6. Lamp ballast interaction

6.1 Interaction between lamp and the electronic ballast

The direct interaction between the burner and the circuit (figure 6.1) can be split up in three parts:

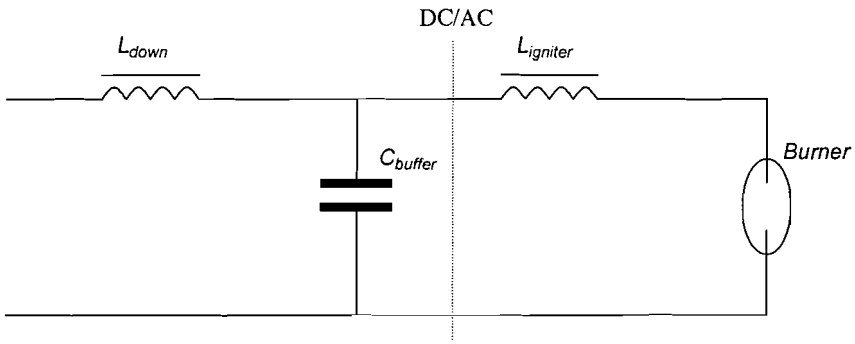

Figure 6.1: Interaction ballast – burner

Plasma interference
The interaction between the burner and the buffer capacitor causes an electrical instability after a commutation or other disturbance. The series igniter coil reduces the damping of the circuit, so resulting current fluctuations becomes larger.

Commutation slows down
The igniter coil delays the current reversal. In particular during low power operation this can result in re-ignition problems, caused by the lamp cooling down during the slow commutation process. The buffer capacitor also slows down the lamp commutation through a slow voltage rise towards the required re-ignition value.

Filter
The critical discontinuous down converter produces triangle shaped pulses with a high frequency which can cause acoustic resonances in the burner. To avoid these problems the current ripple on the lamp must be kept below 10% [13]. The buffer capacitor in combination with the igniter coil must fullfill these requirements. The igniter coil can not be chosen freely, the inductance is based on the energy requirements for the ignition pulse.

6.2 Simulink model of the lamp

Simulink is chosen for implementation of the lamp model and the electronic ballast. Because it is build on top of Matlab, the Simulink user has direct access to the Matlab tools. The first model presented is the lamp model.

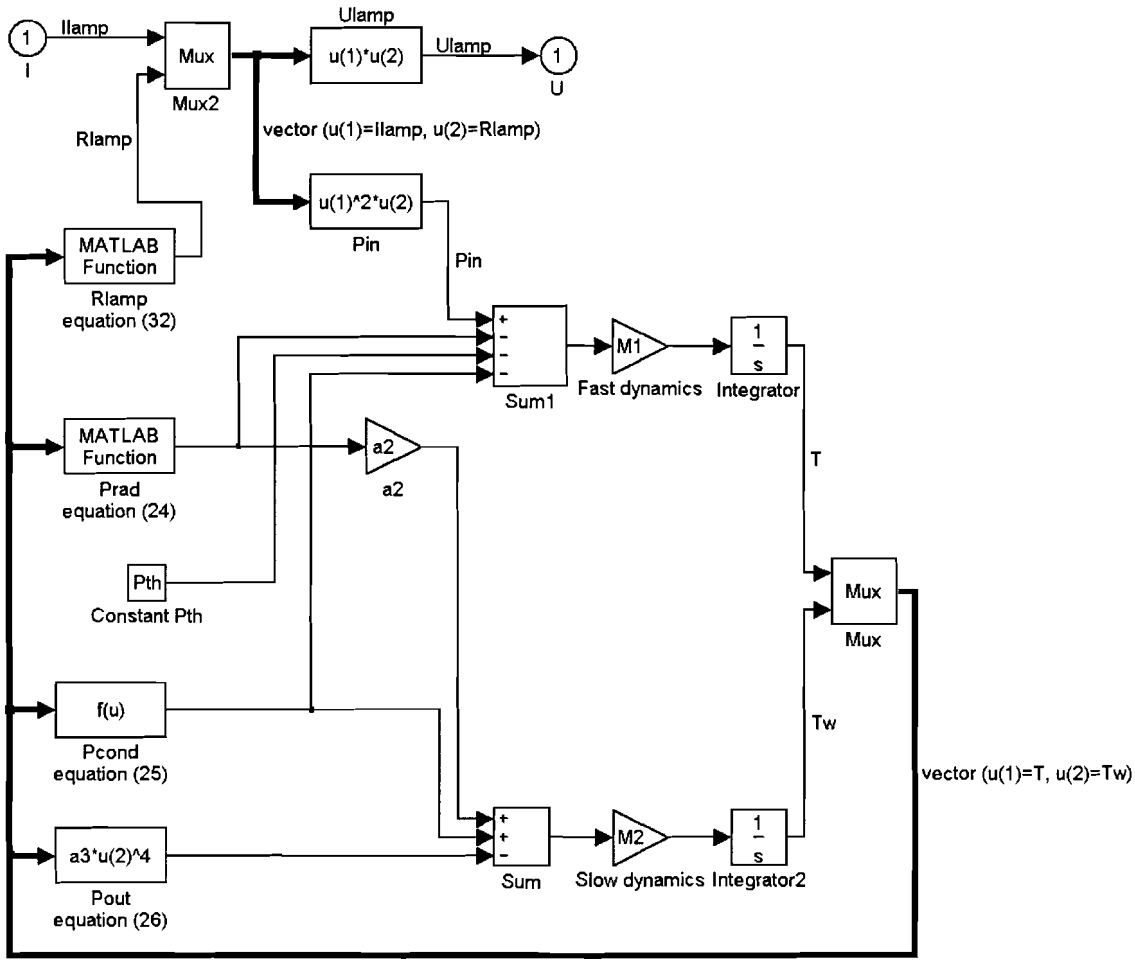

Figure 6.2: Simulink lamp model

In the lamp model (figure 6.2) the power formulas as derived in chapter 5 are positioned on the left side, containing the identified steady state and filled in parameters. On the right side are the lamp dynamics implemented, by means of two integrators, one for the fast and one for the slow dynamics. The output values of the integrators for the fast and slow dynamics are, respectively, the arc and the wall temperature. The dynamic behaviour parameters (M_1 & M_2) define the time constants of the integration actions, and so the speed of variation in the two temperatures. With the instantaneous temperatures the lamp resistance is calculated as output, and the instantaneous electrical power is the input for the model. The last step is the transformation of the lamp resistance and the electrical input power into the lamp voltage and current. The lamp current is the input magnitude and the lamp voltage is the resulting magnitude.

6.3 Down converter Simulink model

Operating a CDM burner on an electronic ballast, the indirect interaction of the down converter with the lamp is very important for the resulting dynamical behaviour. We assume that the input voltage of the down converter, the pre-conditioner voltage, doesn't change during transients. So the dynamics of the pre-conditioner section are neglected in this investigation. To be sure of accurate results in fast power transients, the switching behaviour of the critical discontinuous down converter is not averaged but real-time simulated.

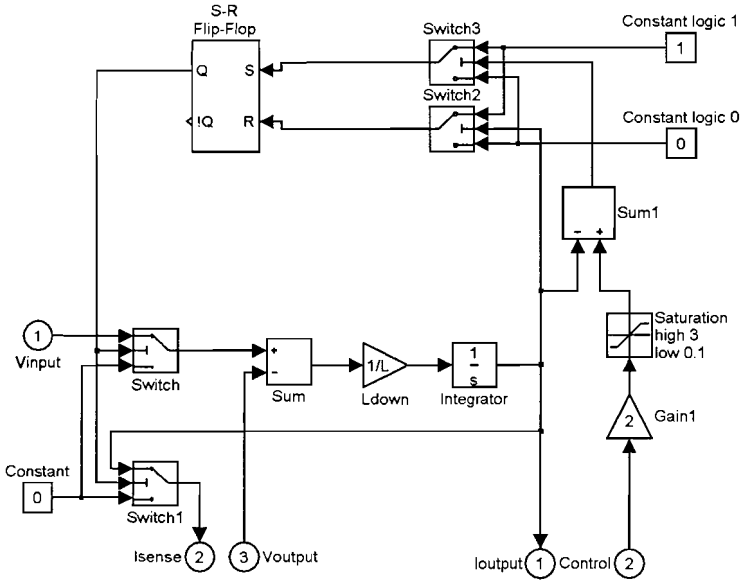

Figure 6.3(a): Simulink down converter model

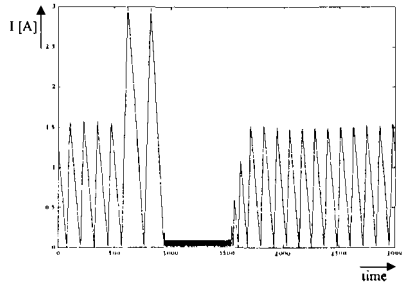

Figure 6.3(b): Output current

The down converter model (figure 6.3(a)) simulates a converter operating at critical discontinuous current mode. This is implemented with a S-R flip-flop which switches the virtual down coil between the input and output voltage difference, and the output voltage (freewheel diode effect). The inductance is modelled in a straightforward way:

$$u_L = L\frac{di_L}{dt} \Rightarrow Laplace \Rightarrow i_L = \frac{u_L}{Ls} \tag{44}$$

The critical discontinuous converter is controlled by means of the current top value. In order to control the average value of the current on the input side, the internal peak value is multiplied two fold. The maximum and minimum current are limited like in the practical situation by a saturation function. For extern control facilities, an input current sense is implemented. The output current of the down converter is displayed in figure 6.3(b) during a power transient. It becomes clear that for high output currents the switch frequency drops and for low current the frequency rises.

6.4 Total interaction model

First a overview of the original situation as used in the square wave MHC070 ballast is given figure 6.4. The pre-conditioner is shown in a dotted line style to stress there is no dynamical influence of this part in the lamp ballast interaction.

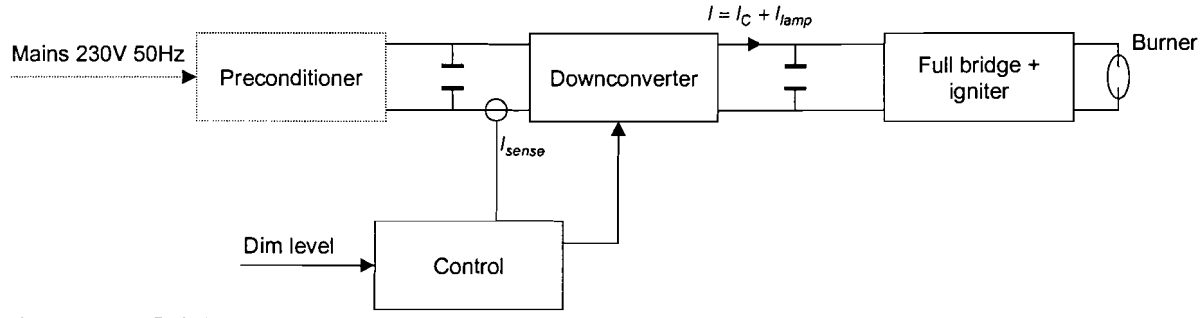

Figure 6.4: Original control

The lamp model and the down converter model have been already introduced. Now the

remaining components and the control must be defined to get a realistic copy of the burner and the ballast in the simulation model.

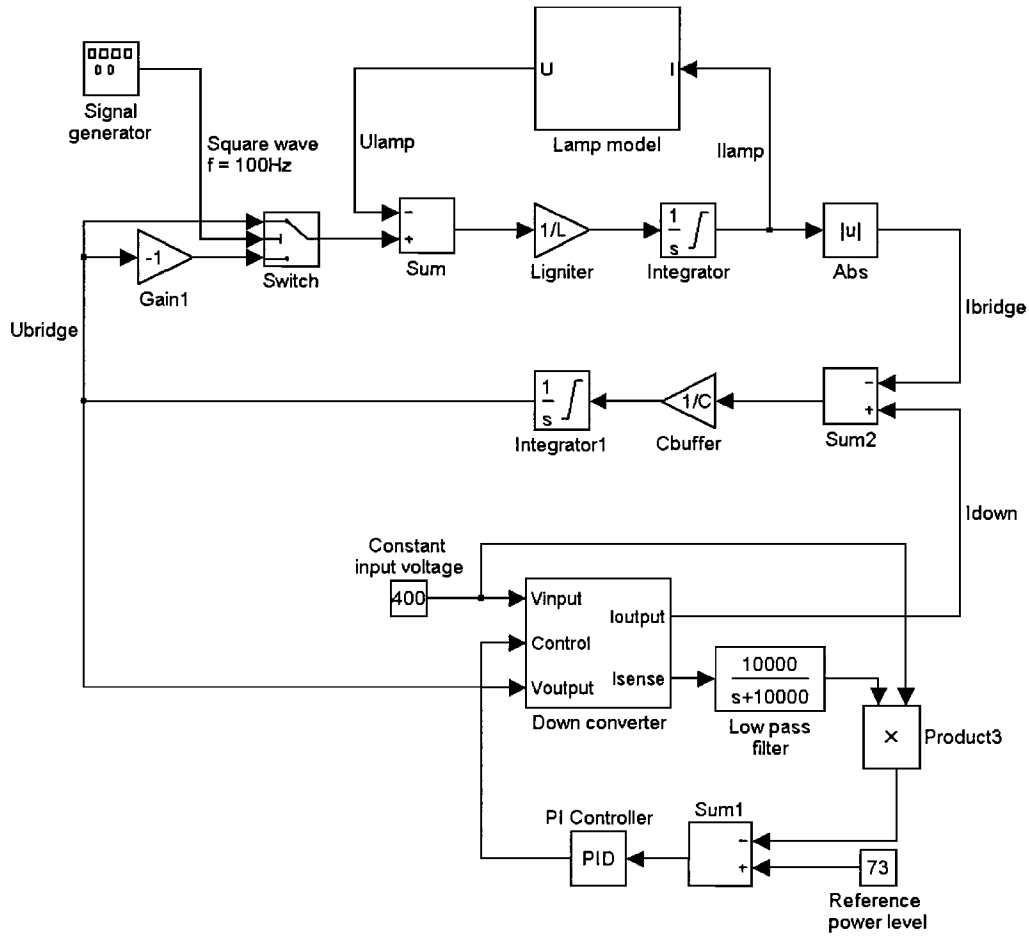

Figure 6.5: Simulink interaction model with down converter input power measurement

On top of figure 6.5, we see the lamp model connected in series with the virtual igniter coil (formula 44). They are driven by a square wave voltage controlled by a function generator as implementation for the full bridge. The resulting alternating current is rectified by means of an absolute value block. As in the practical situation, on the input side of the bridge a buffer capacitor is connected in parallel. The capacitor is implemented by means of simple integration action as follows:

$$i_C = C\frac{du_C}{dt} \Rightarrow Laplace \Rightarrow u_C = \frac{i_C}{Cs} \qquad (45)$$

Finally the current delivered by the down converter model is controlled by a PI regulator block. The input magnitude for the control unit is the input current of the down converter. This current is proportional with the input power of the down converter, it is assumed that input voltage of the down converter is constant.

Control loop simulation model

To implement the dynamics of the control in the simulation model, the real control loop in the MHC070 electronic ballast must be examined first (see appendix 3). All elements of the control loop are shown in table 6.1.

Table 6.1: Control loop MHC070

Element in loop	Gain [magnitude]	Pole / zero [frequency]
Current shunt	0.75	
Passive low pass filter	1	ω_{pole} = 10000 rad/sec.
Current amplifier	18	
Resistive divider	0.76	
Error amplifier	1	ω_{pole} = 0 rad/sec. / ω_{zero} = 213 rad/sec.
Multiplier	2.5	
Total gain	≈ 26	

In the simulation model the control loop is build up as follows. The measured input current of the down converter passes a first order low pass filter with $\omega_{turnover}$ = 10000 rad/sec. Then the error signal is calculated by means of the reference signal minus the measured current. The error signal is the input for the PI regulator. The PI controller contains a pole in the origin, a zero set by the turnover frequency ω = I/P, and an amplification factor P which follows the conventional description as

$$P + \frac{I}{s} = \frac{P\left(s + \frac{I}{P}\right)}{s} \tag{46}$$

The parameter P is set at 13 times as given from Table 6.1, (remember that in the down converter simulation model the peak current input is multiplied two times). The parameter I is set at I = ω*P = 213*13=2769 rad/sec. with accordance with Table 6.1.

6.5 Verification

In order to prove the accuracy of the total simulation model a verification measurement is needed. In the practical set-up, the CDM 70W reference burner is connected with a MHC070 electronic ballast. The resulting lamp voltage and current are recorded with a Tektronix TDS460A oscilloscope. The measurement is taken for full power (P_{la}=73W), at steady state operation. In the simulation model the down converter is also set at a power level of 73W.

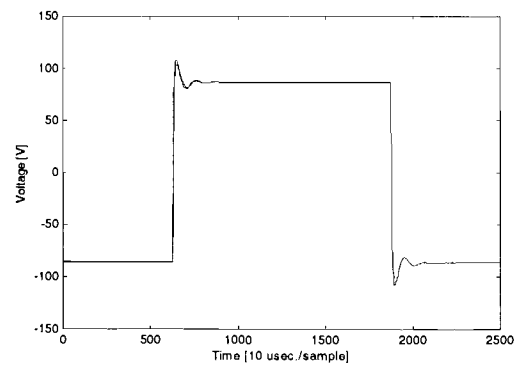

Figure 6.6(a): Reference measurement P_{la}=73W (voltage)

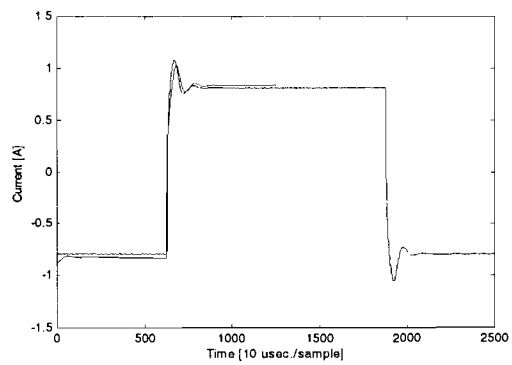

Figure 6.6(b): Reference measurement P_{la}=73W (current)

Finally, the measured voltage and current are loaded in Matlab, and plotted in the same figure with the simulation results. Note that the practical measurement contains 2500

samples, and the simulation results contains 1250 samples. The results for the voltage (figure 6.6a) showed a very good fit. The size of the re-ignition peak and the damping are modelled very well. The current shows (figure 6.6b) a little difference in the steady state amplitude, caused by a difference in the absolute power level between the practical situation and the simulation. In practice, the NORMA power analyser D5235 takes the whole wave in account for the power calculation. The re-ignition peak has influence on the power level, this is in contradiction with the power level in the simulation model.

For reduced power levels, the simulation model can also predict accurately, when we implement in the lamp model a linear relation between the fast time constant M_1 and the used power level (see section 5.4). But it is important to know that the electrode losses are part of the calculations in the model. And it is expected that the electrodes work always in thermionic mode. So on the border of the electrode function the prediction of the model isn't very accurate any more.

6.6 Improving HID lamp dimming

To improve the dimming the following actions can be taken:

1. Switched capacitor
2. Control improvement
3. Lamp behaviour feedback
4. Pulse operation

6.6.1 Switched capacitor

Chapter 4 showed plasma instabilities caused by the interaction between the lamp and the parallel capacitor. The instabilities occur especially during low power operation. Since the down converter shifts to higher operation frequency for lower power operation, the used capacitor can be reduced, without exceeding the 10% current ripple claim [13]. As a result, of the smaller capacitor, the stability margin becomes larger.

This idea was tested in a practical situation for the MHC070 electronic gear to prove the results of the larger stability margin. Depending on the used power level, the parallel capacitor is changed in discrete steps by means of mosfets (figure 6.7). The mosfets are controlled by comparators adjusted on specified power levels (table 6.2).

Table 6.2

Lamp power level [W]	Resulting parallel capacitor value [μF]
P = 73 – 55	C=0.947
P = 55 – 45	C=0.267
P = 45 – 35	C=0.047

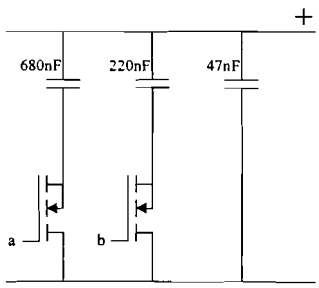

Figure 6.7: Switched capacitor

The results with this switched capacitor are good. The increased stability margin, which was predicted in theory, showed in a practical situation also an increased lamp stability. The burner doesn't extinguish when the power was lowered stepwise from 100% to 50%.

6.6.2 Control improvement

To achieve stability in critical situations, like a power step down, and to optimise the commutation process, a new control is proposed. We assume that the simulation results with the new control are close to reality, as showed by the verification of the original control (section 6.4).

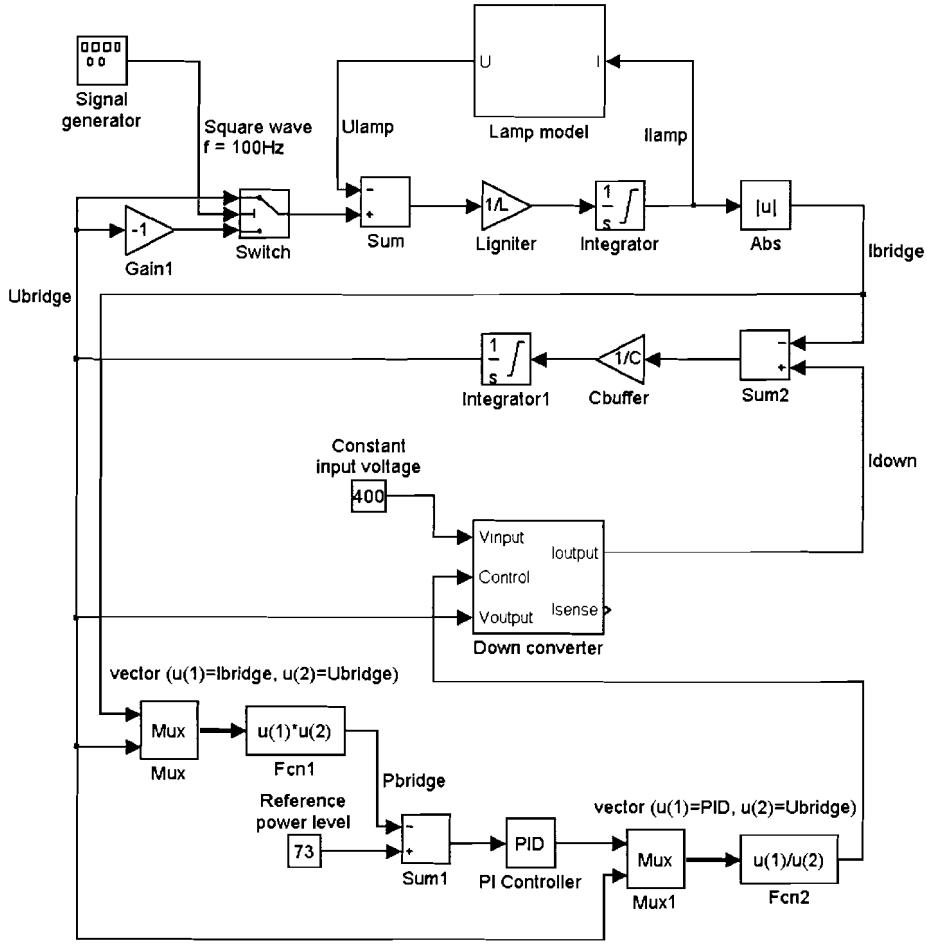

Figure 6.8: Simulink interaction model with bridge power measurement

The proposed new control is shown in figure 6.8. Now the current sense of the down converter is not used any more as input for the control unit. The power is calculated through multiplication of the voltage and the current before the bridge and after the buffer capacitor. For long term power control there is no difference between the two measurement methods, but for transients like commutation effects there are large differences.

New control loop design

The bridge voltage and current are multiplied and compared with the reference, resulting in a error signal. This error signal is the input for the PI controller (formula 46). The parameter P is now set at 15 and the parameter I at I = ω*P=200*15 = 3000 rad/sec. (ω_{zero}=200 rad/sec.). Note that a very high loop gain will lead to sub-harmonic oscillations in the critical discontinuous down current. The controlled output power is divided with the voltage to get

the controlled current value.

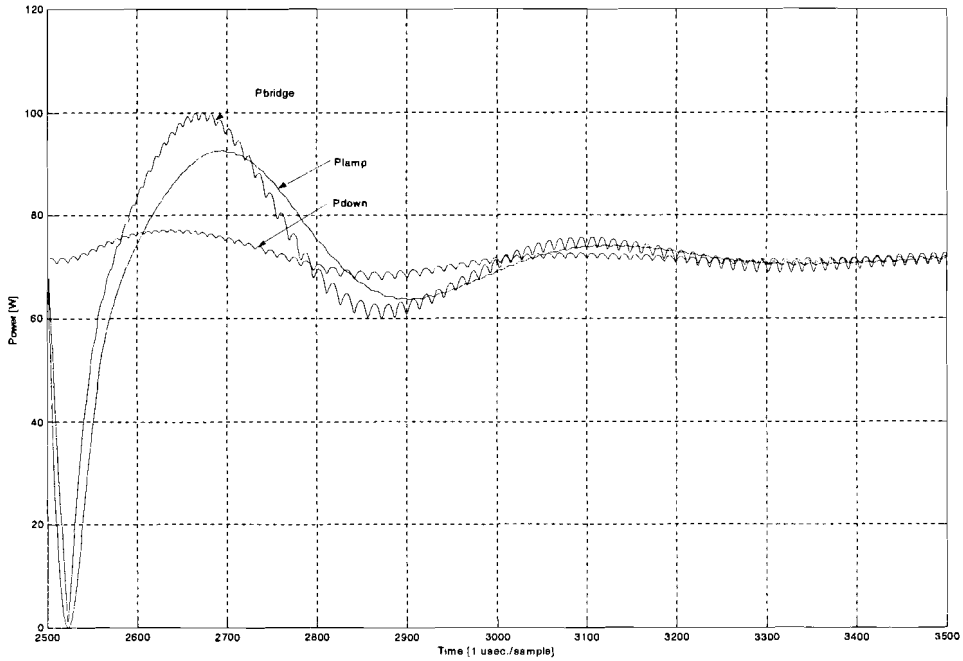

Figure 6.9: Power plot with original MHC070 control (P_{down} input power sense)

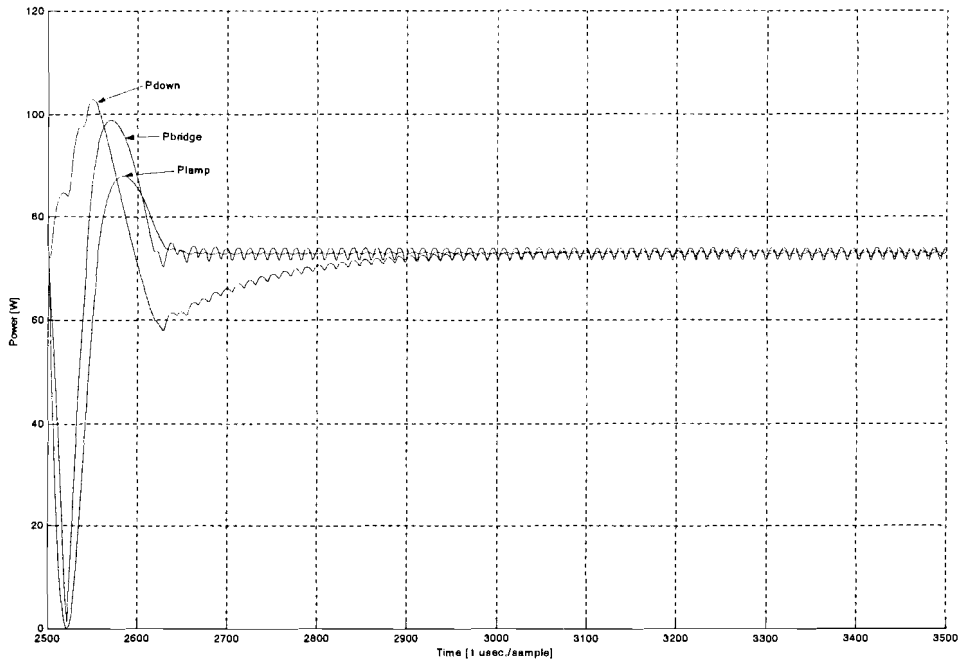

Figure 6.10: Power plot with new control (P_{bridge} sense)

In the power plots three different power levels shown as follows:

P_{lamp} = U_{lamp}*I_{lamp} (see figure 6.8)

P_{brige} = U_{bridge}*I_{bridge} (see figure 6.8)

P_{down} = I_{sense}*$U_{constant}$ input voltage (see figure 6.5)

To highlight the differences between the original and the new control we zoom in on the commutation process. The commutation process is a cyclic disturbance in power, and excites the instabilities in the system. In figure 6.9 the commutation process for full power with the original control is displayed. In figure 6.10 the results with the new control are presented also for full power operation. A first view shows a faster commutation process, with an increased damping. The commutation time with the original control equals 92 μsec, and the commutation time with the new control equals 56 μsec. Another important point is that the negative overshoot in the lamp power has disappeared. Especially for low power operation this is very important, as presented in chapter 4. The explanation for the decreased commutation time is that the down converter delivers maximum current during the current reversal. Especially in reduced power mode this results in a very fast commutation. The switching behaviour of the down converter can be easily observed in the ripple of the P_{down} and P_{bridge} line (figure 6.9 & 6.10). Remark: the ripple on P_{down} is extra filtered to get a clear picture; in practice the ripple is larger. The filter turnover frequency is chosen sufficient high to be sure of a neglectible influence on the dynamics.

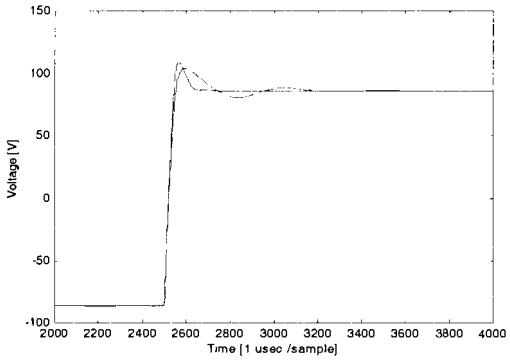

Figure 6.11(a): Voltage for original and new control

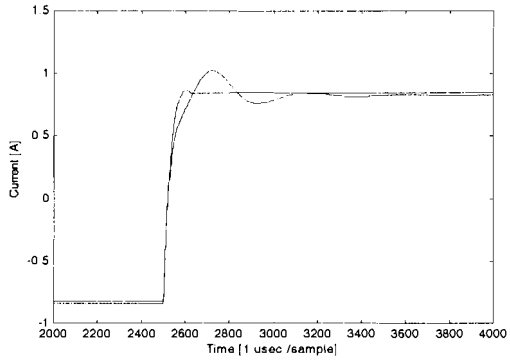

Figure 6.11(b): Current for original and new control

The voltage and current waveforms for the original control compared with the new control are presented in, respectively, figure 6.11a and 6.11b. The same story as for power: A faster commutation with a increased damping. Note the current overshoot has become very small. The voltage overshoot is a lamp related behaviour.

As a final stability test the buffer capacitor value is increased towards the critical value derived with the stability criterion in section 4.4.

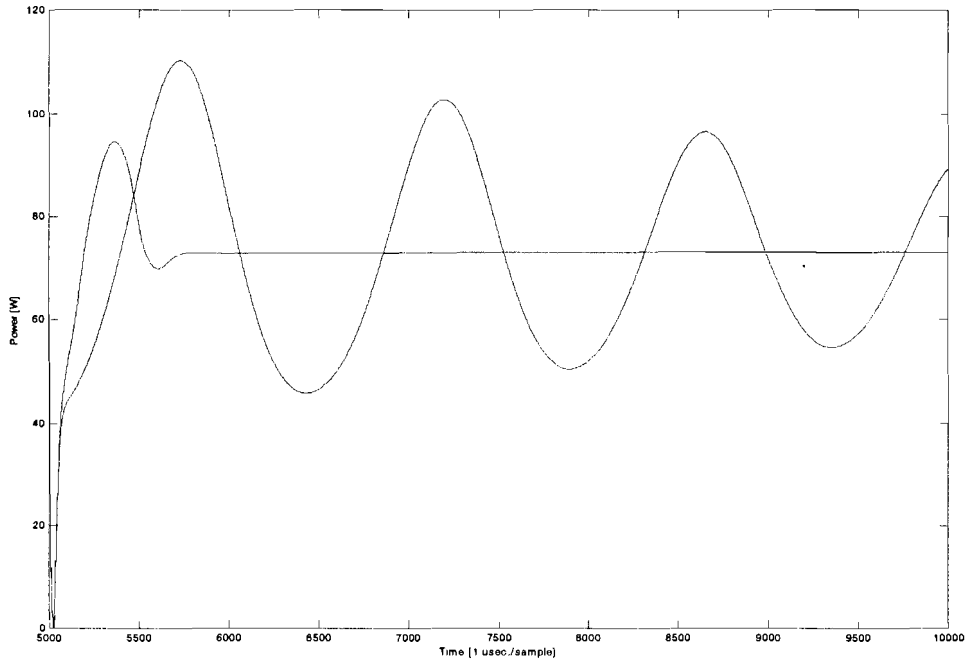

Figure 6.12: Simulation with original and new control in combination with C=8.2 μF parallel.

In figure 6.12 the resulting power plots for both controls are shown, the line with the large fluctuations is for the original control and the line with the fast damping for the new control. When the critical capacitor value is applied with a open control loop a undamped oscillation will result. When the original control loop is closed a oscillation with small damping effect becomes visible. The situation where the new control loop is applied gives a total different result. The damping is increased enormously. This means that the applied critical capacitor value, is not as critical as before the new control is applied. The new control can achieved stability for fast lamps in combination with relatively large capacitors.

6.6.3 Lamp behaviour feedback

Plasma and electrode effects investigated in chapter four can be used to observe the dimming border, related to extinguishing of the lamp or other unwanted effects like flickering and maintenance decreasing. In table 6.3 four signals are presented useful for lamp behaviour feedback. The first three signals can be found in section 4.7.

Table 6.3

	Feedback signal	Border value	Lamp effect
1	Current low / voltage high time after commutation	80 μsec.	Extinguishing
2	Voltage low frequent fluctuations	2 Volt	Flickering
3	Voltage high frequent fluctuations	Occur	Maintenance
4	Maximum lamp voltage versus open voltage buck converter	Safety margin 50 Volt	Extinguishing

6.6.4 Pulse operation

If a current pulse is given to the lamp before commutation, a more reliable re-ignition during the commutation itself follow [21]. This idea is based on the fact that heating the anode a

little before commutation will lead to a sufficient heated cathode after the current reversal. Remember that the cathode emits the electrons.

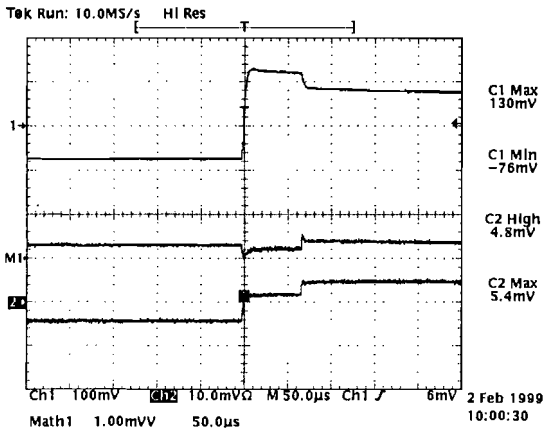

Figure(a): P_{lamp} = 35W

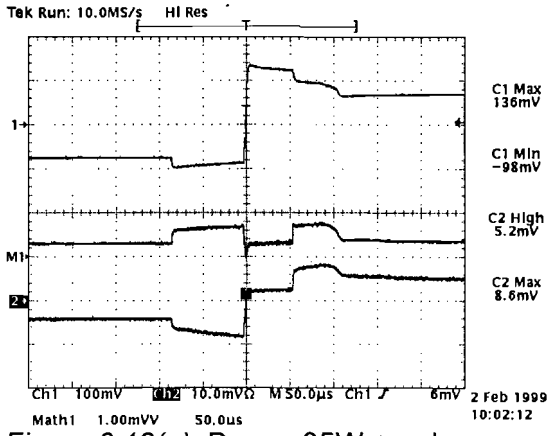

Figure 6.13(a): P_{lamp} = 35W + pulse

Upper trace: lamp voltage 100V/div., middle trace: lamp power 100W/div, bottom trace: lamp current 1A/div. Time scale 50µsec./div.

Operation with a pulse around the commutation is examined. The used measurement set-up is given in figure 4.4. The switched series resistor is now dimensioned to give a current pulse equals $I_{nominal}$ in reduced power operation. In figure 6.13(a) the commutation process for a CDM burner operating on 35W is given. The situation with pulse, shows a little decrease in commutation time, given in figure 6.13(b).

This pulse operation results in more power during commutation and less power between the commutations, for the same average power level. On the border of stable low power operation, the current level between the commutations become very low and can result in unstable behaviour.

Practical measurements shows a little decrease in commutation time, for current pulses in reduced power mode with a maximum size 1,5x the nominal power level. There has been no tests with very large pulses of several times P_{nom}, because it is not clear what the maintenance effect is of such large pulses applied in continuous reduced power mode.

Concluding: Pulse operation can not extend the border of stable low power operation. For this type of HID lamp (CDM070) it seems that the time constant of the electrodes is too large to heat up sufficiently by means of a short pulse. The average electrode temperature, depending on the average applied power level, still imposes the border of stability.

7. Conclusions & Recommendations

7.1 Conclusions

- Metal halide lamps are able to replace incandescent halogen lamps, especially when ballast features like dimming become available. The investigation described in this rapport showed that it is possible to achieve stable operation for a CDM070 burner within the 50% to 100% power range.
- When a lamp is operated on a low frequency alternating sinusoidal or a non ideal square wave current, the lamp must re-ignite after every change in current polarity. During the polarity change the current level is low and even momentarily zero, which results in a decrease in the plasma temperature with, as consequence, an increase of the lamp resistance. This results in a re-ignition peak in the voltage when the current begin to flow after the polarity change. To minimise the voltage peak, the current commutation must be as fast as possible.
- The calculated dynamical critical capacitor behaviour shows, especially for CDM lamps, an interesting behaviour. The results give an explanation for the observed extinguishing of the CDM lamps after a quick step to a lower power level. The maximum allowed parallel capacitor decreases rapidly with a power step down. Remarkable is that this behaviour is only found for CDM burners. Expected is that this is the result of the increased pressure inside the arc tube compared to the classical high pressure mercury lamp.
- The high frequency components mentioned in the literature can be easily observed and used to determine the vapour mode of operation of the electrodes. The observed low frequency fluctuations caused by the burning voltage differences between the commutations that can be related to the static spot mode. The high frequency component can be related with lamp maintenance and the low frequency component with light flickering. But both parameters don't give reliable information if the border of low power operation is reached. Only with the "current low/ voltage high time" parameter can this stability border be easily observed. Of course also the lamp re-ignition must be observed. It should never exceed the open voltage because the lamp would extinguish.
- The verification of the lamp model, for a 50Hz conventional ballast full power situation, gives a good fit. For reduced power mode with a constant fast dynamics parameter the prediction of the re-ignition peaks is wrong. An improved lamp model, which implements a linear relation between the fast dynamics parameter M1 and the used power level, gives an accurate prediction also for low power operation.
- The plasma instabilities can be reduced by applying a switched parallel capacitor. During low power operation smaller capacitor should be used. As a result the stability margin becomes larger.
- The results with the new control for full power operation, show a faster commutation process with an increased damping. Another important point is that the negative overshoot in the lamp power disappears. Especially for low power operation this is very important as presented in chapter 4. The reason for the decreased commutation time is that the down converter delivers maximal current during the current reversal. Especially in reduced power mode, this results in a very fast commutation. And even if the critical capacitor value is applied, the new control can hold the situation stable, contrary to the original control.
- Pulse operation cannot extend the border of stable low power operation. For this type of HID lamp (CDM070) it seems that the time constant of the electrodes is to large to heat up sufficient by means of a short pulse. The average electrode temperature, depending on the average applied power level, still determine the border of stability.

7.2 Recommendations

A good dimmable lamp must have an appropriate electrode temperature for low power operation. Thermionic emission must exist over a broad area of the electrode front surface and the so-called low-field mode has to prevail. The volt-second area of the re-ignition peak must be minimised to avoid arc tube blackening.

To guarantee stable operation during dimming for several lamp types and in all stages of ageing, the lamp behaviour must be feedbacked to the power control unit. The four signals introduced in section 6.6.3 must be observed simultaneously. If one of the signals reaches the adjusted border value, the minimum dimming level is also reached. A proposal for a µ-processor power control unit is shown in figure 7.1. The power control unit delivers the reference signal for the down converter control loop.

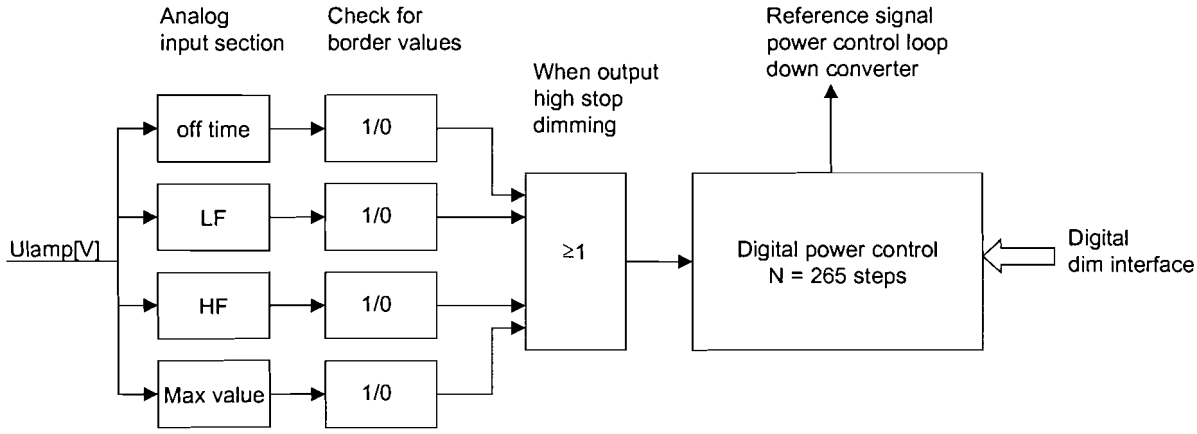

Figure 7.1: Implementation lamp behaviour feedback

In figure 7.2 a closer view on the proposed new ballast situation with new control and additional feedback of the lamp behaviour is given.

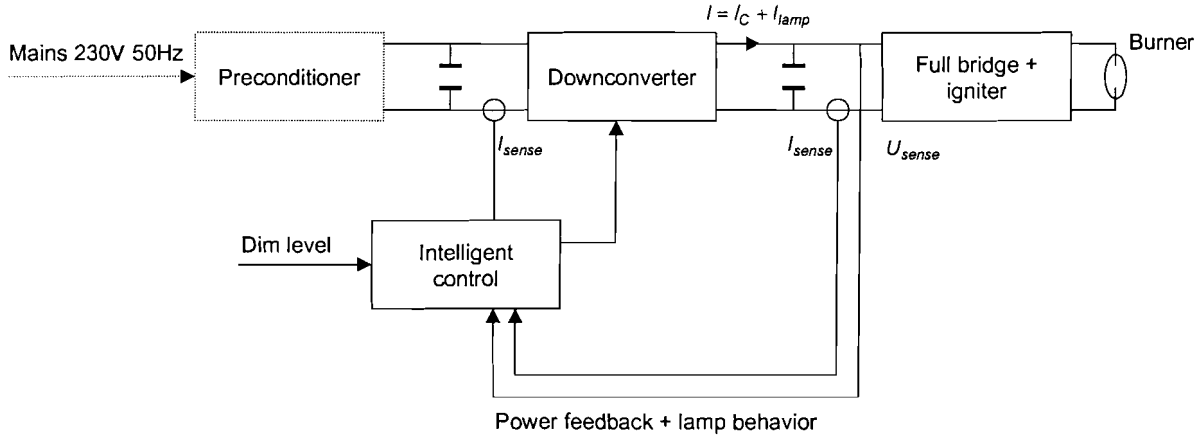

Figure 7.2: New control + additional feedback

The voltage and current values are measured before the bridge and after the capacitor. (Note: I_{sense} before the down converter is still required to control the critical discontinuous switching process). The voltage and current are used to calculate the instantaneous power level and to observe the lamp behaviour. The new power control yields plasma stability independent of the used lamp and its changes over time. The electrode behaviour is distillated out of the voltage signal to set the minimum dimming level, depending on the used

lamp and ageing. Remember, new lamps perform much better than old ones, so the minimum dimming level for stable and flicker-free light increases with the life time.

8. References

[1] Ris, H.R.
NATRIUM-XENON-LAMPE MIT UMSCHALTBARE FARBETEMPERATUR
Licht no.2 (1994) p.123-126

[2] Smith, D. and H.Zhu
PROPERTIES OF HIGH INTENSITY DISCHARGE LAMPS OPERATING ON REDUCED POWER LIGHTING SYSTEMS
Journal of the illuminating engineering society vol.22 summer (1993) p.27-39

[3] Gibson, R.G.
DIMMING OF METAL HALIDE LAMPS
Journal of the illuminating engineering society vol.23 summer (1994) p.19-25

[4] Keijser, R.
DIMMING OF CERAMIC METAL HALIDE LAMPS
Proceedings 8th International Symposium on Science & Technology of Light Sources. Germany, p. 226-227, 1998. Ed. by G.Babucke

[5] Seinen, P.
HIGH INTENSITY DISCHARGE LAMPS WITH CERAMIC ENVELOPS
Proceedings 7th International Symposium on Science & Technology of Light Sources. Kyoto, p.?, 1995.

[6] Waymouth, J.F.
THE GLOW TO THERMIONIC ARC TRANSITION
Journal of the illuminating engineering society vol.16 summer (1987) p.166-180

[7] Springer, R.H. and W.H.Lake
THERMAL BALANCES OF HID ELECTRODES
Journal of the illuminating engineering society vol.13 April (1984) p. 304-307

[8] Gregor, P.D. and Y.M.Li, A.B.Budinger, W.W.Byszewski
ARC TUBE TRANSPARENCY LOSS DUE TO STARTING OF HID LAMPS
Journal of the illuminating engineering society vol.25 summer (1996) p.150-159

[9] Fromm, D.C. and A.Hohlfeld
REDUCED FLICKERING OF METAL HALIDE LAMPS BY OPTIMIZED ELECTRODE DESIGN
Journal of the illuminating engineering society vol.22 summer (1993) p.69-76

[10] Fischer, E.
MODELLING OF LOW-POWER HIGH-PRESSURE DISCHARGE LAMPS
Philips journal of research vol.42 (1987) no.1 p.58-85

[11] Anders, A.
ELECTRODE BEHAVIOUR OF PULSED HIGH-PRESSURE SODIUM LAMPS
Lighting research & Technology vol.23 (1991) no.1 p.81-84

[12] Anders, A. and B.Juttner
CATHODE MODE TRANSITION IN HIGH-PRESSURE DISCHARGE LAMPS AT START-UP
Lighting research & Technology vol.22 (1990) no.2 p.111-115

[13] Faehnrich, H.J. and E.Rasch
ELECTRONIC BALLASTS FOR METAL HALIDE LAMPS
Journal of the illuminating engineering society vol.17 summer (1988) p.131-140

[14] Waymouth, J.F.
ELECTRIC DISCHARGE LAMPS HIGH-PRESSURE MERCURY LAMPS
Cambridge: MIT press, 1971

[15] Huynh, P. and A.H.Bergman
ELECTRICAL MODELLING OF HIGH PRESSURE DISCHARGE LAMPS
Philips research USA. Braircliff Manor, New York (1996)
Internal rapport TR-96-033

[16] Kimmels, A.
OPERATION OF HIGH-VOLTAGE MASTERFLUC BURNERS ON MODIFIED MHC DRIVERS
Central Development Lighting, Eindhoven (1997)
Internal raport DLEE 1010/97

[17] Bergman, A.H.
A LABVIEW SYSTEM SET-UP FOR HID LAMP RELATED EXPERIMENTS
Philips research USA. Braircliff Manor, New York (1997)
Internal report TR-97-009

[18] Giese, H.
ELECTRICAL MODELLING OF HID LAMPS PART2: REVIEW OF ELECTRICAL MODELS FOR DISCHARGE LAMPS
Philips GmbH. Forschungslaboratorien, Germany (1998)
Internal Laborberichte Nr.????/98 (Preliminary version)

[19] Deurloo, O.
MHC070 DESCIPTION OF LAMPDRIVER (MS1 STATUS)
Central Development Lighting, Eindhoven (1997)
Internal rapport DLEE 1021/97

[20] Kool, B.S. de
DIMMING OF HID LAMPS
Central Development Lighting, Eindhoven (1996)
Internal trainee report LAMPS II 4002/96

[21] Kern, R.
VORRICHTUNG ZUM BETREIBEN EINER GASENTLADUNGSLAMP
Applicant: Robert Bosch GmbH. 70442 Stuttgart, Germany
European Patent Office, 1998
Patent EP 0 791 282 B1 (23.09.1995)

[22] Jack, A.G. and M.Koedam
ENERGY BALANCES FOR SOME HIGH PRESSURE GAS DISCHARGE LAMPS
Journal of the illuminating engineering society vol.3 July (1974) p.323-329

[23] Comandatatore, G. and U.Moriconi
DESIGNING A HIGH POWER FACTOR SWITCHING PREREGULATOR WITH THE L6560A TRANSITION MODE I.C.
SGS-THOMSON Microelectronics, Italy 1997
Application note AN667/1297

9. Appendix

Appendix 1: Light related terms

Colour rendering

The colour rendering properties of light sources are used to define their colour effect. They are expressed in groups of the "general colour rendering index" Ra. The colour rendering index is a measure of the correspondence between a surface colour and its appearance under the relevant reference source. To determine the Ra values of light sources, eight defined test colours that are predominant in the environment are illuminated with the reference light source (with an Ra of 100) and the light source under test. The smaller or larger the deviation in the colour rendering of the illuminated test colour, the better or worse the colour rendering property of the tested light source. A light source with an Ra of 100 makes all the colours appear perfectly as they do under the reference light source. The lower the Ra value, the worse the surface colours of the illuminated objects are rendered. Example: Tungsten-halogen lamps have a colour rendering index Ra >99, so they offer ideal colour rendering properties.

Colour temperature

The light colour of a lamp is expressed as colour temperature. The unit of measurement is the kelvin (K). The kelvin scale starts at absolute zero (0 K = -273° C). The colour temperature of a light source is defined in comparison with a "black body radiator". If a "black radiator" is heated, the colour of the radiation emitted by it will run through a scale from dark red, red, orange, yellow, white to light blue. The higher the temperature of this "black body radiator" the whiter the colour. An incandescent lamp with a warm white light, for example, has a colour temperature of 2800 K, whereas a daylight fluorescent lamp has a colour temperature of 5000 K. The relevant standard divides the light colour of lamps into three groups: daylight white, intermediate white and warm white. Despite having the same light colour, lamps may have very different colour rendering properties owing to the spectral composition of their light.

Generation of light

Lamps generate light either by thermal radiation (incandescent lamps) or by gas discharge (discharge lamps). Their radiant energy is either directly visible or is converted into visible light by fluorescent material.

Illuminance

Illuminance indicates the luminous flux from a light source falling on a unit area of a surface. The unit of measurement is the lux (lx). An illuminance of 1 lx occurs when a luminous flux of 1 lm is evenly distributed over an area of 1 square metre (figure 9.1).

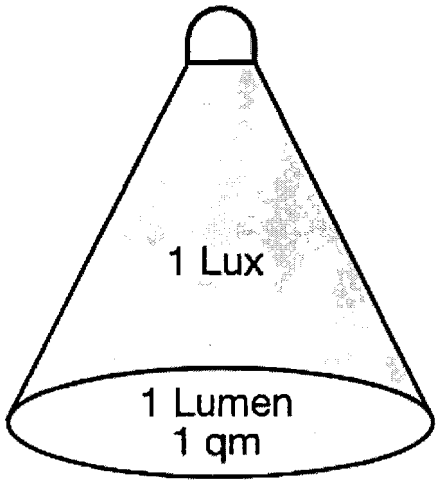

Figure 9.1: Illuminance

Incandescent lamps

Incandescent lamps are thermal radiators. They consist in principle of a tungsten filament in a glass bulb. The bulb contains a vacuum, an inert gas/nitrogen mixture or just an inert gas. Current is passed through the tungsten filament causing it to reach temperatures of up to 3000°C and emit light. When current flows through the filament, the electrons hit the tungsten atoms in the tungsten wire. The energy transferred to the atoms is given off as heat and light.

Light

Light is taken to mean the electromagnetic radiation that the human eye perceives as brightness, in other words that part of the spectrum that can be seen. This is a radiation with a wavelength between 380 and 780 nm [nanometre], a tiny fraction of the known spectrum of electromagnetic radiation.

Luminance

Luminance, measured in candela per unit area (cd/m²), is a measure of the brightness of an illuminated or self-luminous area to the human eye (figure 9.2). For lamps, cd/cm² is a more useful unit.

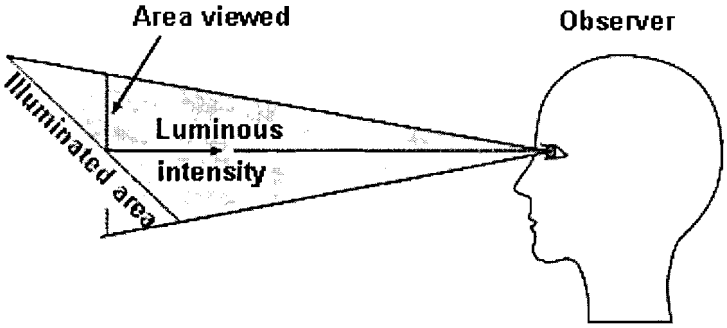

Figure 9.2: Luminance

Luminous efficacy

Luminous efficacy indicates the efficiency with which the electrical power consumed is converted into light. It is measured in lumens per watt (lm/W). The luminous efficacy of an incandescent lamp is approx. 14 lm/W, whereas that of a compact electronic fluorescent lamp is approx. 60 lm/W.

Luminous flux

Luminous flux is the light output of a lamp. It is measured in lumens (lm). A 100 W incandescent lamp has a luminous flux of around 1380 lm; a 20 W compact electronic fluorescent lamp has a luminous flux of about 1200 lm.

Luminous intensity

Luminous intensity is the part of the luminous flux radiated in a particular direction (figure 9.3). The unit of measurement is the candela (cd).

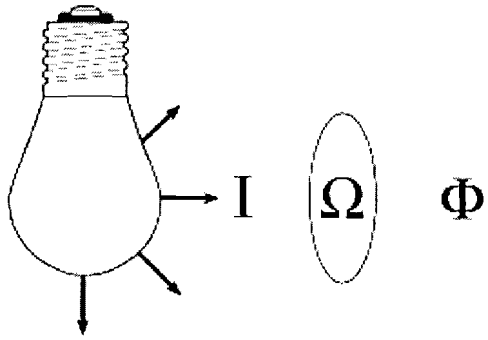

Luminous intensity I is a measure of the lumnious flux Φ emitted in solid angle Ω.

Figure 9.3: Luminous intensity

Luminous intensity distribution

The spatial distribution of the luminous intensity of a reflector lamp or luminaire is defined by the luminous intensity distribution surface. It can be shown for different planes in polar diagrams (luminous intensity distribution curves). To make comparisons easier, luminous intensities relate to units of 1000 lm for the lamps operated in the luminaire and are expressed as cd/klm (= candelas per kilolumen). The shape of a luminous intensity distribution curve indicates whether the luminaire (or reflector lamp) is a deep, wide, symmetrical or asymmetrical radiator.

Appendix 2: **Extended table plasma behaviour** (small signal analysis)

Table: 9.1

CDM-T 70W				
	Power [W]	τ [µsec.]	-r [V/A]	C_{crit} [µF]
Steady state	70	85	9,65	8,8
	60	100	9,69	10,3
	50	155	18,02	8,6
Dynamic	70 – 60	90	14,33	6,28
	70 – 50	122	21,07	5,79
	60 – 70	95	7,95	11,95
	50 - 70	125	6,23	20
MHW-TD 70W				
	Power [W]	τ [µsec.]	-r [V/A]	C_{crit} [µF]
Steady state	70	190	4,6	41,3
	60	170	13,9	12,23
	50	240	14	17
Dynamic	70 – 60	230	9,26	24,8
	70 – 50	190	4,28	44,4
	60 – 70	190	7,76	24,48
	50 – 70	180	3,79	47,5
SON 70W				
	Power [W]	τ [µsec.]	-r [V/A]	C_{crit} [µF]
Steady state	70	190	20,0	9,48
	60	140	12,5	11,2
	50	220	15,18	14,59
Dynamic	70 – 60	214	16,2	13,2
	70 – 50	270	17,3	15,6
	60 – 70	195	10,6	18,3
	50 – 70	275	11,9	23,1

Appendix 3: Derivation control loop MHC070

The control loop of the MHC 070 is given simplified in figure 9.4

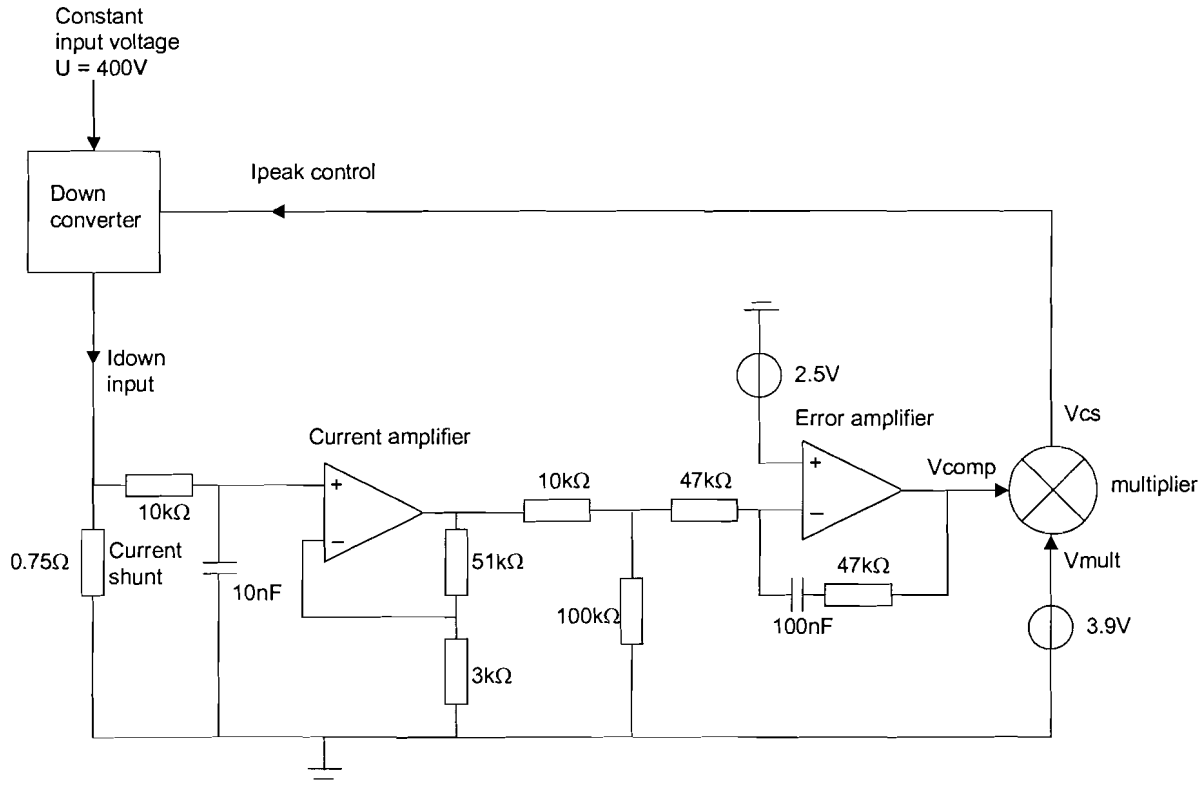

Figure 9.4: Control loop MHC070

Derivation of the used elements in the control loop as given in figure 9.4 from the left side to the right side.

The transfer for R_{shunt} gives

$$\frac{U_{shunt}}{I_{down}} = R_{shunt} = 0.75\,{}^{V}\!/_{A} \tag{47}$$

The passive low pass filter has a pole on

$$\omega_{pole} = \frac{1}{RC} = \frac{1}{10k \cdot 10n} = 10000\,{}^{rad}\!/_{sec.} \tag{48}$$

The gain of the current amplifier equals

$$Gain = 1 + \frac{R_1}{R_2} = 1 + \frac{51k}{3k} = 18 \tag{49}$$

The attenuation of the resistor divider equals

$$100k \;//\; 47k \approx 32k \Rightarrow \frac{R_2}{R_1 + R_2} = \frac{32k}{10k + 32k} \approx 0.76 \tag{50}$$

The error amplifier transfer is given by

$$Gain = \frac{R_2}{R_1} = 1$$
$$\omega_{pole} = 0\ {}^{rad}/_{sec.} \quad and \quad \omega_{zero} = \frac{1}{RC} = \frac{1}{47k \cdot 100n} \approx 213\ {}^{rad}/_{sec.} \tag{51}$$

The multiplier characteristics [23] are given in figure 9.5

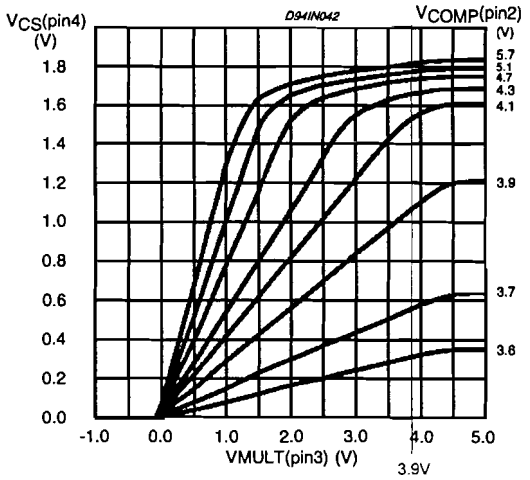

Figure 9.5: Multiplier characteristics

U_{cs} approximately equals for full power operation:

$$Ucs = Ipeak * Rshunt = 2 * 0.85A * 0.75\Omega \approx 1.3V \tag{52}$$

Note: By knowing $I_{peak} = 2*I_{down}$ and $I_{down} \approx 0.85A$ for full power operation.

V_{mult} is connected to a voltage source which equals 3.9V. Investigation of the gain in the region of the estimated U_{cs} lead to

$$multiplier\ gain = \frac{\left(\frac{Vcs_1}{Vcs_2}\right)}{\left(\frac{Vcomp_1}{Vcomp_2}\right)} = \frac{\left(\frac{4.1}{3.9}\right)}{\left(\frac{1.55}{1.05}\right)} \approx 2.5 \tag{53}$$

Finally an overview of the elements in the control loop is given in table 9.2.

Table 9.2: Control loop MHC070

Element in loop	Gain [magnitude]	Pole / zero [frequency]
Current shunt	0.75	
Passive low pass filter	1	ω_{pole} = 10000 rad/sec.
Current amplifier	18	
Resistive divider	0.76	
Error amplifier	1	ω_{pole} = 0 rad/sec. / ω_{zero} = 213 rad/sec.
Multiplier	2.5	
Total gain	≈ 26	

Appendix 4: ARMA model

The standard ARMA (auto regressive moving average) model is given by

$$y_t = \sum_{l=1}^{n} a_l y_{t-l} + \sum_{l=0}^{n} b_l u_{t-l} \tag{54}$$

The "$a_j y_{t-1}$" portion of this is the auto regressive part and the "$b_k u_{t-k}$" portion is the moving average part.

A first order ARMA model with input u, and output y, is given by

$$y(t+1) = ay(t) + b[u(t+1) + u(t)] \tag{55}$$

Then it is desirable to estimate the unknown parameters [a,b] based on the measured data {u,y} in such way that the indentified ARMA model can mimic the response from the measured data. Substituting N sampled data points of the set {u,y} in equation 55 yields

$$Y = W\theta + E \tag{56}$$

where

$$Y = \begin{bmatrix} y(1) \\ y(2) \\ \vdots \\ y(N) \end{bmatrix}, \; W = \begin{bmatrix} y(0) & u(1) + u(0) \\ y(1) & u(2) + u(1) \\ \vdots & \\ y(N-1) & u(N) + u(N-1) \end{bmatrix}, \; \theta = [a\ b]^T, \; E = \textit{error vector}$$

Let S denote the sum square error,

$$S = E^T E = (Y^T - \theta^T W^T)(Y - W\theta) \tag{57}$$

Then, θ needs to be indentified such that S is minimised (least square-fit creterion)

Appendix 5: MHC070 electronic gear

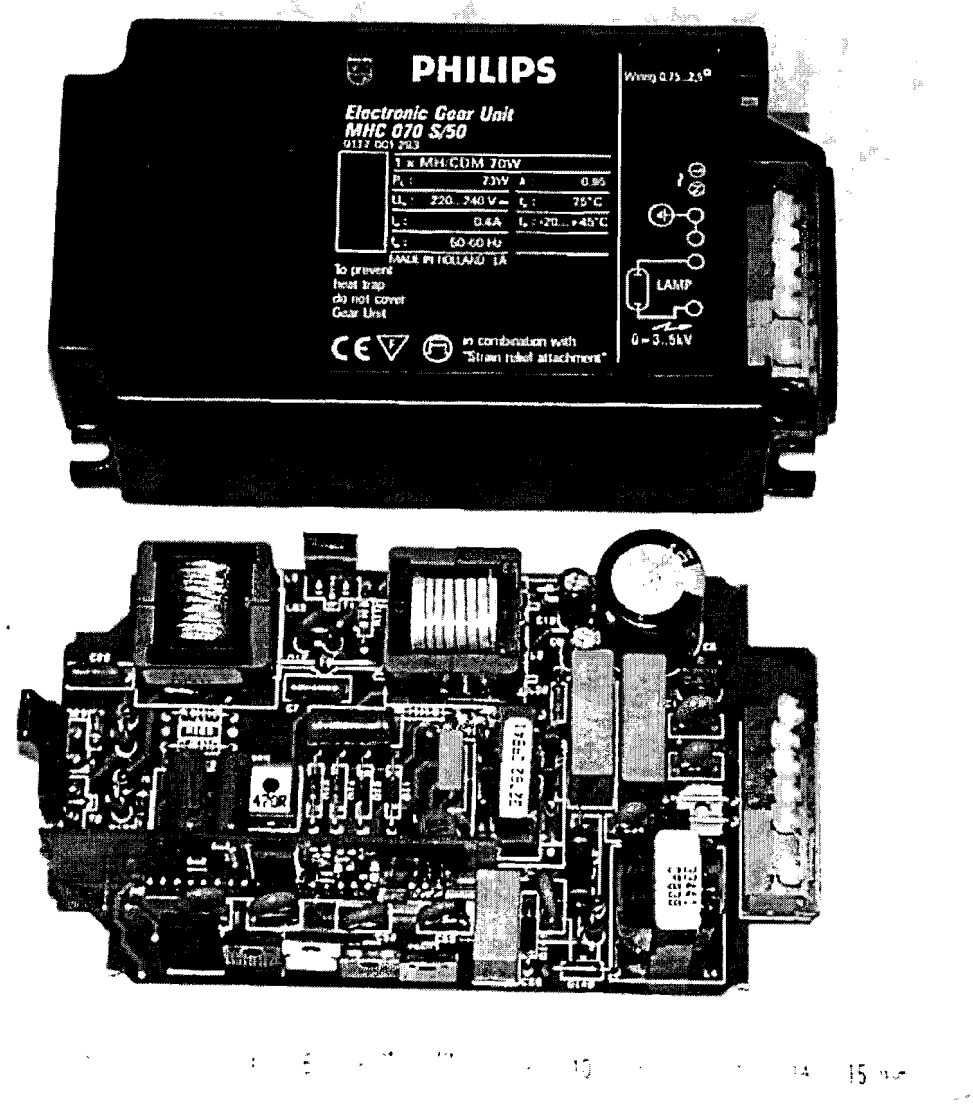

Figure 9.4: Picture MHC070